I ON PARAMETRIC OSCILLATIONS
IN ELECTRONIC CIRCUITS

AND

II A GRAPHICAL ANALYSIS FOR
NON-LINEAR SYSTEMS.

Thesis
submitted by

PEI-SU HSIA

B.Sc.
(Central University of China)

For the degree of

Ph. D.

University of Edinburgh
May, 1950.

C O N T E N T S.

INTRODUCTION

When a parameter of an electric circuit is periodically varied, the circuit behaviour is quite different from that when the parameters are all constants. Circuits with varying parameters have played important rôles in radio, e.g., in frequency-modulation and super-regeneration. Besides these practical cases, the parametric-oscillation phenomenon has attracted increasing attention in recent years. Self-oscillation may be obtained in positively-damped circuits having a parameter varied at a suitable frequency, particularly at approximately twice the natural frequency of the circuit. This phenomenon is termed parametric excitation.

Parametric excitation was investigated in 1883 by Lord Rayleigh [1]. He repeated Melde's classic experiment in which one end of a horizontal thread was fixed and the other end attached to the prong of a vertically-mounted tuning-fork: the thread vibrated with a frequency one-half that of the fork. The system was represented in terms of the Mathieu equation and solved by Hill's method of infinite determinant.

About thirty years later, C.V. Raman [2] performed similar but more extensive experiments. He found that the thread vibrated when the frequency of its

free oscillations was nearly equal to any integral multiple of half the frequency of the fork. He also attached the two ends of the thread to two tuning-forks with different frequencies f_1 and f_2, and observed that the thread vibrated at frequencies $\frac{1}{2}(rf_1 \pm sf_2)$, where r and s were positive integers.

In 1931, H. Winter-Günther[3] obtained parametric excitations by varying the inductance of a tuned circuit. Two stator and three rotor phases of a 3-phase alternator were all connected in series for inductance modulation. The frequency of oscillations was one-half that of the variation of the inductance. Winter-Günther also treated this problem mathematically.

From 1934 to 1936, W.L. Barrow[4] and his collaborators solved the Mathieu equation on a differential analyzer, and also produced electric parametric oscillations by using a three-phase selsyn transformer. They studied forced oscillations with a sinusoidal electro-motive force when the capacitance was varied by commutating two fixed condensers. They found that the amplitude of forced oscillations was dependent on the phase-angle between the variation of the capacitor and the applied voltage. They also observed that resonance occurred when the frequency of the applied e.m.f. was $\frac{n}{m}$ times that of the

variation of the parameter, where m and n are integers.

In 1931, Mandelstam and Paralexi [5] started a systematic study of parametric oscillations. They built parametric voltage generators with specially designed variable inductors and capacitors. These machines were able to generate high voltages with considerable power and high efficiency.

The experiments described in all the papers mentioned above used mechanical means of varying the appropriate parameters. In this thesis consideration is given to parametric excitations produced in stationary electronic circuits, in which measurements of the various quantities can be more accurately made. The frequency of variation of the parameter is about twice the natural frequency of the circuit, and the frequency of the parametric excitation obtained is exactly one half that of the variation of the parameter. Under certain conditions, phenomena of "jump" and "hysteresis" are observed, which seem to have escaped the notice of the earlier workers. When an external e.m.f. with the frequency of the parameter-variation is applied, oscillations both with constant amplitude and frequency (half that of the external e.m.f.) and with periodically-varying amplitude and frequency are obtained.

As regards mathematical analysis, all the previous authors, except Mandelstam and Paralexi, considered the differential equations for their systems of the

form of Mathieu's equation with or without an additional damping term. However, because of the linear nature of the Mathieu equation (6), it can be shown that its solution, as time increases, either tends to infinity (unstable solution) or tends to zero if there is damping (stable solution), or remains finite in amplitude as endowed by the initial conditions (stable or neutral solution). That the oscillations at first build up and then reach a finite amplitude, which is the actual result from experiment, is outside the compass of the linear Mathieu equation. To account for this and other phenomena, considerations of non-linearity must be introduced; and this is achieved in Part I of the present thesis.

For self-excitation, the differential equations developed in this thesis are solved both analytically and topologically. The analysis is based on Poincaré's small-parameter method, in which the non-linearity and the variation of parameter are small. The condition of self-excitation, the stability of various solutions, and the phenomena of jump and hysteresis, are investigated in detail. The results of mathematical analysis are compared with those obtained from experiment. The agreement is in general good.

For forced-oscillation conditions, a different approach is made in which the line of Kryloff and Bogoliuboff is followed. A periodic solution of

modulated amplitude and frequency is obtained, which explains qualitatively the phenomena observed. As for forced oscillations of constant amplitude and frequency, they differ little from the case of self-excitation. The condition under which the same process of analysis can be applied to both these two cases is stated, but no detailed calculation regarding this type of forced oscillation is made.

Besides the analytical method, a graphical process applicable to cases where the analytical method fails, is also developed in this thesis. The graphical method, which is applicable to most second-order differential equations, is a generalization of the methods of K.J. Dejuhasz [7] and A. Preisman [8], who applied them only to linear systems, and to systems with non-linear damping, respectively.

Among problems for which analytical methods are not available are cases involving a non-linearity which is either large, or not analytic. Most of these cases can be solved graphically with varying degrees of labour. This method can also directly solve problems in which analytical expressions for the non-linear elements - which are often obtained from experimental data - are not known. It is not necessary, when the graphical method is used, to fit the experimental curves with equations.

General principles and constructions are given in Part II, which also includes some applications to

problems discussed in Part I. The process of construction of each problem is shown in detail. As a test of the accuracy of the graphical solutions worked out, comparisons are made either with experimental results, or with analytical and numerical calculations.

Thus the work set out in this thesis deals with circuit phenomena due to parametric variations, taking non-linearity into account, with or without externally applied force. The results for self-excitation are that parametric oscillations have been observed in electronic circuit, with "jump" and "hysteresis" under certain conditions, and quantitative agreement obtained between theoretical predictions and experimental results; and for forced oscillation, oscillations with modulated amplitude and frequency are observed besides those with constant amplitude and frequency, and theoretical considerations show both possibilities. In addition, a graphical analysis is developed applicable to most problems involving non-linearity.

PART I.

ON PARAMETRIC OSCILLATIONS IN ELECTRONIC CIRCUITS.

1. PRELIMINARY.

In this section the circuits considered in this investigation are described, and differential equations for them derived. In Fig. 1, V1 and V2 are two identical valves and are operated under the same conditions. L the inductance, R the resistance, C the capacitance, M the mutual inductance, and k are all constants, and e_s is an external e.m.f. If the grid currents and the effects of anode reactions are neglected, then by Kirchhoff's law, the equations for the circuit are:

$$i_{a1} + i_{a2} + i_1 + i_2 = 0, \tag{1}$$

$$L\frac{di_1}{dt} + R i_1 = \frac{1}{C}\int i_2\, dt, \tag{2}$$

and

$$v = M\frac{di_1}{dt}, \tag{3}$$

where $i_{a1} = f(v, e_s)$ is a non-linear function representing the anode current i_{a1} as a function of both the grid voltages v and e_s, and $i_{a2} = f(0, ke_s)$ has the same form as $f(v, e_s)$, which is usually expressible in the form of a double power series in v and e_s, i.e.

$$\begin{aligned} f(v, e_s) = {} & l_1 v + l_2 v^2 + l_3 v^3 + \cdots \\ & + m_1 e_s + m_2 e_s^2 + m_3 e_s^3 + \cdots \\ & + n_1 e_s v + n_2 e_s^2 v + n_3 e_s v^2 + \cdots, \end{aligned} \tag{4}$$

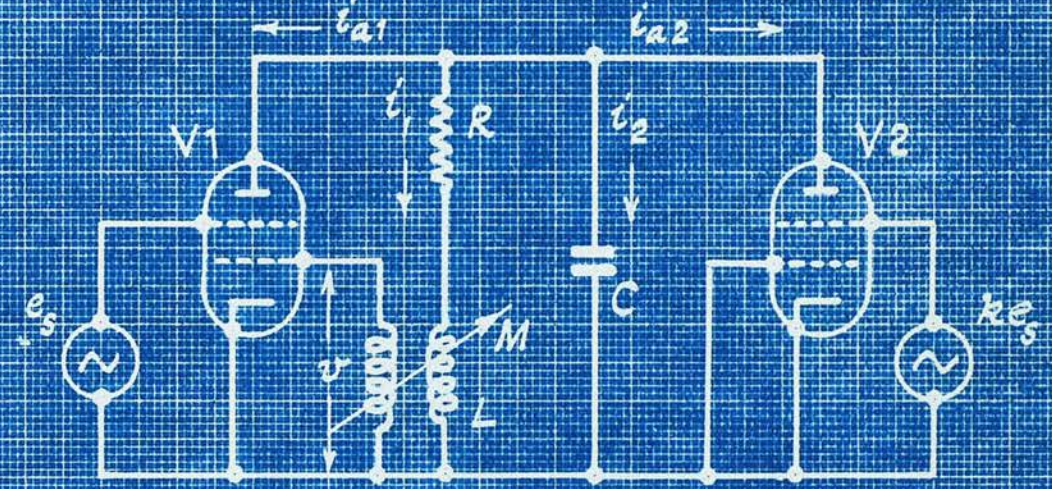

Fig. 1

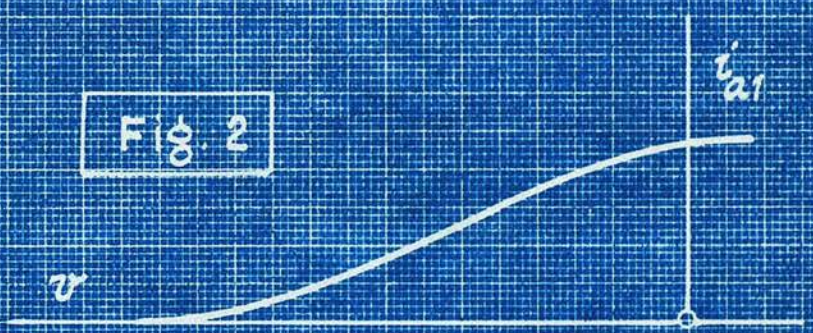

Fig. 2

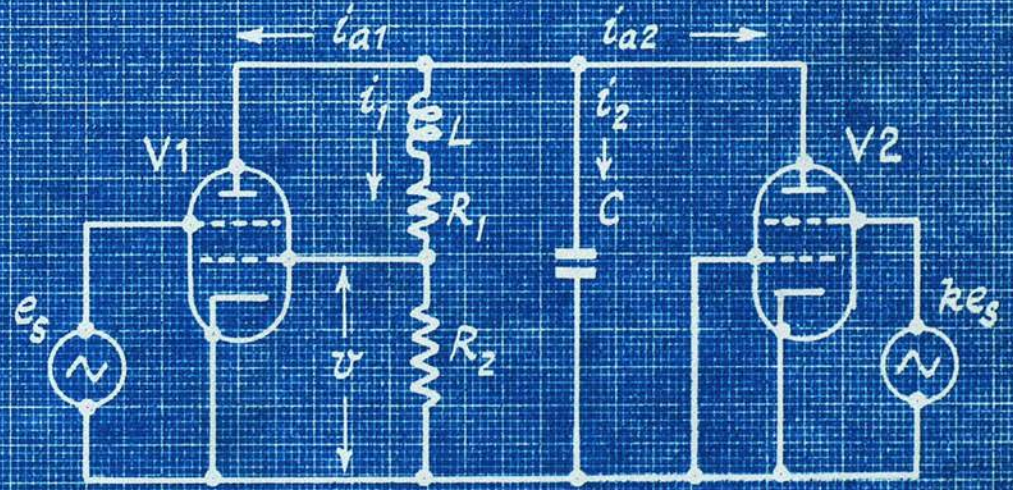

Fig. 3

where

$$l_1 = \left(\frac{\partial f}{\partial v}\right)_{v=e_s=0}, \quad l_2 = \frac{1}{2}\left(\frac{\partial^2 f}{\partial v^2}\right)_{v=e_s=0}, \quad l_3 = \frac{1}{3!}\left(\frac{\partial^3 f}{\partial v^3}\right)_{v=e_s=0}, \cdots,$$

$$m_1 = \left(\frac{\partial f}{\partial e_s}\right)_{v=e_s=0}, \quad m_2 = \frac{1}{2}\left(\frac{\partial^2 f}{\partial e_s^2}\right)_{v=e_s=0}, \quad m_3 = \frac{1}{3!}\left(\frac{\partial^3 f}{\partial e_s^3}\right)_{v=e_s=0}, \cdots,$$

$$n_1 = \left(\frac{\partial^2 f}{\partial e_s \partial v}\right)_{v=e_s=0}, \quad n_2 = \frac{1}{2}\left(\frac{\partial^3 f}{\partial v \partial e_s^2}\right)_{v=e_s=0}, \quad n_3 = \frac{1}{2}\left(\frac{\partial^3 f}{\partial v^2 \partial e_s}\right)_{v=e_s=0}, \cdots.$$

As, in practice, $f(v, e_s)$ is an unknown function, the l's, m's, and n's have to be determined from the characteristic curves of the valve, obtained by measurement. The m's can be found from the i_{a1}/e_s characteristic with $v=0$: in our case, the grid to which e_s is applied is operated within the linear part of the i_{a1}/e_s curve, so that $m_2, m_3, \ldots$ can be neglected. The n's are determined from families of i_{a1}/v and i_{a1}/e_s characteristics around $e_s = v = 0$: n_1 is the slope of the curve $\left(\frac{\partial f}{\partial e_s}\right)_{e_s=0} \Big/ v$ at $v=0$, or of the curve $\left(\frac{\partial f}{\partial v}\right)_{v=0} \Big/ e_s$ at $e_s=0$; n_2 is one half the slope of the curve $\left(\frac{\partial^2 f}{\partial e_s \partial v}\right)_{v=0} \Big/ e_s$ at $e_s=0$, or of the curve $\left(\frac{\partial^2 f}{\partial e_s^2}\right)_{e_s=0} \Big/ v$ at $v=0$; and so on. In the present case, $n_2, n_3, \ldots\ldots$ are negligibly small. Finally, the l's are obtained from the i_{a1}/v characteristic while $e_s=0$: a typical form of the i_{a1}/v relation is shown in Fig. 2. If the first grid is biased at a point near the inflection point of the curve, it is found that, by analyzing the curve to fit eq. (4):

(a) the values of $l_1, l_5, \ldots\ldots$ are positive,

(b) those of $l_3, l_7, \ldots\ldots$ are negative,

(c) the inequalities

$$|l_2| \ll |l_1|, \quad |l_4| \ll |l_3|, \quad |l_6| \ll |l_5|, \cdots,$$

and $|l_1| >> |l_3| >> |l_5| \cdots$ hold.

In view of these inequalities (c), the first few terms in eq. (4) are sufficient to represent the characteristic. In this way, eq. (4) therefore becomes, if $e_s = \lambda_0 \sin 2\omega t$, λ_0 and ω being constants,

$$f(v, e_s) = i_{a1} = m_1 \lambda_0 \sin 2\omega t + n_1 \lambda_0 v \sin 2\omega t + l_1 v + l_2 v^2 + l_3 v^3 + \cdots . \quad (5)$$

As i_{a2} has the same expression as i_{a1}, except that $v = 0$, and e_s (or λ_0) is changed into ke_s (or $k\lambda_0$), we have

$$i_{a2} = k m_1 \lambda_0 \sin 2\omega t, \quad (6)$$

Substituting eqs. (5) and (6) into eq. (1), and differentiating with respect to t, we obtain

$$n_1 \lambda_0 \left(\sin 2\omega t \frac{dv}{dt} + 2\omega v \cos 2\omega t\right) + 2(1+k) m_1 \lambda_0 \omega \cos 2\omega t + \left(l_1 + 2 l_2 v + 3 l_3 v^2 + \cdots\right) \frac{dv}{dt} + \frac{di_1}{dt} + \frac{di_2}{dt} = 0, \quad (7)$$

Inserting eq. (3) into eq. (2) and differentiating twice, gives:

$$\frac{di_2}{dt} = \frac{LC}{M} \frac{d^2 v}{dt^2} + \frac{RC}{M} \frac{dv}{dt}. \quad (8)$$

Putting eqs. (3) and (8) into eq. (7), yields

$$LC \frac{d^2 v}{dt^2} + RC \frac{dv}{dt} + v + M\left[2(1+k)\omega m_1 \lambda_0 \cos 2\omega t + n_1 \lambda_0 \left(\sin 2\omega t \frac{dv}{dt} + 2\omega v \cos 2\omega t\right) + \left(l_1 + 2 l_2 v + 3 l_3 v^2 + \cdots\right) \frac{dv}{dt}\right] = 0, \quad (9)$$

In eq. (9), the term of highest power in v must be positive, for otherwise the system would possess a negative resistance for large values of v, which is physically impossible. In the present case, the mutual inductance M, is made negative, and l_3 is negative as shown previously, so that the expression $3 l_3 M v^2 \frac{dv}{dt}$ is positive and is taken as the term of highest power in v in eq. (9). The term $2 l_2 M v \frac{dv}{dt}$ may be positive under some operating conditions, but we do not choose this as the highest power in the non-linearity, as $2 l_2$ may be smaller than $3 l_3$ and also for the reason, explained in Section 2.1, that even powers of non-linearity have no effect on the zeroth-order solutions of self-excitation.

Let

$$\left.\begin{aligned} \tau &= \omega t, \\ \sigma_1 &= \frac{1}{LC\omega^2}, \\ \epsilon r_1 &= \frac{R}{\omega L} + \frac{M l_1}{\omega L C}, \\ \epsilon r_2 &= \frac{2 l_2 M}{\omega L C}, \\ \epsilon r_3 &= \frac{3 l_3 M}{\omega L C}, \\ \epsilon q_1 &= -\frac{n_1 \lambda_0 M}{LC\omega}, \end{aligned}\right\} \quad (10)$$

and

$$\lambda_1 = -\frac{2(1+k)\lambda_0 m_1 M}{LC\omega},$$

where ϵ is a constant. Then eq. (9) becomes

$$\frac{d^2v}{d\tau^2} + \left[\sigma_1 - 2\epsilon q_1 \cos 2\tau\right] v = \lambda_1 \cos 2\tau + \epsilon\left[q_1 \sin 2\tau - \left(r_1 + r_2 v + r_3 v^2\right)\right]\frac{dv}{d\tau}. \quad (11)$$

In Fig. 3, V1 and V2 are again two identical valves operated under the same conditions. With the same assumptions as before, the equations of the circuit are:

$$i_{a1} + i_{a2} + i_1 + i_2 = 0,$$

$$L\frac{di_1}{dt} + (R_1 + R_2)i_1 = \frac{1}{C}\int i_2 dt,$$

$$v = R_2 i_1,$$

where $i_{a1} = f(v, e_s) = m_1 e_s + n_1 e_s v + l_1 v + l_2 v^2 + l_3 v^3 + \cdots,$

and $i_{a2} = f(0, ke_s) = km_1 e_s$. Letting $e_s = \lambda_0 \cos 2\omega t$ and eliminating the variables i_{a1}, i_{a2}, i_1 and i_2 from these equations, then

$$LC\frac{d^2v}{dt^2} + (R_1 + R_2)C\frac{dv}{dt} + v + R_2\left[(1+k)m_1\lambda_0\cos 2\omega t + n_1\lambda_0 v\cos 2\omega t + l_1 v + l_2 v^2 + l_3 v^3 + l_4 v^4 + l_5 v^5 + \cdots\right] = 0. \quad (12)$$

Since the term of highest power of the non-linearity must be positive, and since the term $R_2 l_3 v^3$ is negative, the fifth power of v has to be taken into consideration. Now l_5 is positive as shown before, so that the term $R_2 l_5 v^5$ forms the highest power of v in this case. Let

$$\left.\begin{aligned} \tau &= \omega t, \\ \sigma_2 &= \frac{1 + R_2 l_1}{LC\omega^2}, \\ \epsilon q_2 &= -\frac{n_1\lambda_0 R_2}{2LC\omega^2}, \\ \lambda_2 &= -\frac{(1+k)R_2 m_1 \lambda_0}{LC\omega^2}, \\ \epsilon\gamma &= \frac{R_1 + R_2}{\omega L}, \end{aligned}\right\} \quad (13)$$

and $\epsilon p_n = \frac{R_2}{LC\omega^2} l_n$, $(n = 2, 3, 4, 5)$.

Then equation (12) changes to

$$\frac{d^2v}{d\tau^2}+\left[\sigma_2-2\epsilon q_2\cos 2\tau\right]v=\lambda_2\cos 2\tau-\epsilon\left[r\frac{dv}{d\tau}+\sum_{n=2}^{5}p_n v^n\right]. \qquad (14)$$

It should be noticed that eqs. (11) and (14), which are derived from physical systems, have the form of the Mathieu equation but with additional non-linear terms. In the case $k=-1$, then λ_1 and λ_2 vanish and the equations are free from external force. If there are periodic solutions which represent electric oscillations in the circuits, the circuits are self-excited.

In the subsequent mathematical analysis, we shall consider a more general equation which contains eqs. (11) and (14) as special cases.

2. MATHEMATICAL ANALYSIS.

The main object of this section is to deal mathematically with a general non-linear differential equation of the type

$$\ddot{v} + 2\Psi_1(\tau)\dot{v} + \left[\sigma - \Psi_2(\tau)\right]v = E(\tau) + \epsilon D(v,\dot{v}), \tag{15}$$

which comprises the equations derived in Section 1. In this equation, the dots denote differentiations with respect to τ ; $\Psi_1(\tau)$, $\Psi_2(\tau)$ and $E(\tau)$ are periodic functions of τ not involving constant terms; $\Psi_2(\tau)$ has period π ; $D(v,\dot{v})$ is an analytical function of v and $\dot{v}$, and does not contain a constant term or linear terms of v ; σ and ϵ are positive constants; and ϵ is small. Eq. (15) represents a non-linear system with periodically varying damping and restoring forces and with an externally applied periodic force.

By introducing a new variable $x(\tau)$ defined by

$$v(\tau) = e^{-\int^{\tau}\Psi_1(\tau)d\tau}x(\tau), \tag{16}$$

the second term on the left of eq. (15) can be eliminated.

Thus

$$\ddot{x} + \left[\sigma - 2q_0\Psi(\tau)\right]x = F(\tau) + \epsilon G(x,\dot{x}), \tag{17}$$

where

$$\left.\begin{aligned} 2q_0\Psi(\tau) &= \Psi_2(\tau) + \Psi_1^2(\tau) + \dot{\Psi}_1(\tau), \\ F(\tau) &= E(\tau)e^{\int^{\tau}\Psi_1(\tau)d\tau}, \\ G(x,\dot{x}) &= D(v,\dot{v})e^{\int^{\tau}\Psi_1(\tau)d\tau}, \end{aligned}\right\} \tag{18}$$

and q_0 is a constant.

As ϵ is small, then to a first approximation the terms involving ϵ may be neglected. The solutions of the equation

$$\ddot{x} + [\sigma - 2q_0 \Psi(\tau)]x = F(\tau) \qquad (19)$$

are called the generating solutions of equation (17). There are two cases of eq. (19) to be considered: (a) When $\Psi(\tau)$ is an even function of τ, eq. (19) is of the form of Hill's equation; and (b) when terms of higher harmonics in $\Psi(\tau)$ (i.e. terms of $\sin 4\tau$, $\cos 4\tau$, $\sin 6\tau$, $\cdots$) are small, eq. (19) reduces, as a first approximation, to Mathieu's equation. Both cases have the same form of solution (6), namely

$$x = A_1 x_1(\tau) + A_2 x_2(\tau) - \frac{1}{c^2}\left[x_1(\tau)\int^{\tau} x_2(u) F(u)\,du - x_2(\tau)\int^{\tau} x_1(u) F(u)\,du\right], \qquad (20)$$

where

$$\left.\begin{aligned} x_1(\tau) &= e^{\mu\tau}\phi(\tau), \\ x_2(\tau) &= x_1(-\tau) = e^{-\mu\tau}\phi(-\tau), \\ c^2 &= x_1(0)\dot{x}_2(0) - x_2(0)\dot{x}_1(0) = \text{constant}, \end{aligned}\right\} \qquad (21)$$

$\phi(\tau)$ is a periodic function of τ representable in terms of a Fourier series. The coefficients in this Fourier series and also μ are definite functions of σ, q_0 and the constants in $\Psi(\tau)$, and A_1 and A_2 are arbitrary constants. When μ is real, x tends to infinity with τ, and the solution is therefore unstable. When μ is imaginary, x is bounded as τ

approaches infinity, but the frequencies of the terms in $\Phi(\tau)$ are changed, and the solution is thus stable.

In further discussions we shall consider two cases separately: self-excitation ($F(\tau)=0$), and forced oscillation ($F(\tau)\neq 0$).

(a) Self-Excitation. It is evident that for this case the solution of eq. (17) must be unstable (μ real) when $\epsilon=0$. The presence of the non-linearity ($\epsilon\neq 0$) controls the amplitude of the solution to a finite value. From physical grounds, one would expect that the exact solution consists of a factor of the nature of an unstable solution of Hill's equation, multiplied by a damping factor which becomes effective only when x is considerably large, so that the final oscillations attain a finite amplitude other than zero. However, such a general solution has not been found. In the present thesis attention is confined to the case of small q_0, and σ nearly equal to 1, and the main task is to seek approximations close to the final steady oscillations, and to discuss their stability.

$$\left.\begin{aligned} &\text{Let} \quad q_0 = \epsilon q, \\ &\text{and} \quad \sigma = 1+\epsilon p, \end{aligned}\right\} \qquad (21a)$$

eq. (17), with $F(\tau)=0$, becomes

$$\ddot{x} + x = \epsilon H\left[x, \dot{x}, \Psi(\tau)\right],$$

where $$H\left[x, \dot{x}, \Psi(\tau)\right] = G(x,\dot{x}) - px + 2q\,\Psi(\tau)x.$$

Here we choose simple harmonic motion as the ~~general~~-

generating solution which resembles closely the final oscillations as observed in the experiments described in Section 3.

(b) Forced Oscillation. When $\epsilon = o$, μ can be either real or imaginary. For the case of real μ , a process of analysis like that used in the case of self-excitation can be applied, provided that (21a) is satisfied. If μ is imaginary, so that $\mu = j\gamma$, we shall adopt formally eq. (20) as the solution of eq. (17) but with the arbitrary constants A_1 and A_2 in eq. (20) as functions of τ and the non-linearity. In this case, q_o and σ are not limited to values specified by (21a), but subject to another condition:

$\gamma << 1$.

2.1 Self Excitation.

2.1.1 Periodic Solutions.

Consider the equation

$$\ddot{V} + V = \epsilon H\left[V, \dot{V}, \Psi(\tau)\right], \tag{22}$$

where ϵ is a small positive constant, $\Psi(\tau)$ is a periodic function of τ, $H\left[V, \dot{V}, \Psi(\tau)\right]$ is an analytical function of V, $\dot{V}$, and $\Psi(\tau)$, and $H\left[V, \dot{V}, \Psi(\tau)\right]_{V=\dot{V}=0} = 0$. When $\epsilon = 0$, eq. (22) represents a simple harmonic oscillator, and its solution is

$$\left.\begin{aligned} V_0 &= a_0 \cos\tau + b_0 \sin\tau, \\ \dot{V}_0 &= -a_0 \sin\tau + b_0 \cos\tau. \end{aligned}\right\} \tag{23}$$

Eq. (23) is the generating solution of eq. (22). At $\tau = 0$, $V_0(0) = a_0$ and $\dot{V}_0(0) = b_0$. When $\epsilon \neq 0$, but small, we assume, at $\tau = 0$,

$$\left.\begin{aligned} V(0) &= a = V_0(0) + \alpha = a_0 + \alpha, \\ \dot{V}(0) &= b = \dot{V}_0(0) + \beta = b_0 + \beta, \end{aligned}\right\} \tag{24}$$

where α and β are functions of ϵ, and both tend to zero with ϵ. According to Poincaré's expansion theorem (5), the solution of eq. (22) can be written in the form of a power series in ϵ, α and β, i.e.

$$V = V_0 + \alpha B_1 + \beta B_2 + \epsilon C_0 + \alpha\epsilon C_1 + \beta\epsilon C_2 + \epsilon^2 C_3 + \cdots, \tag{25}$$

where V_0, B's and C's are functions of τ, and the series on the right hand side of eq. (25) converges provided that $|\alpha|$, $|\beta|$, and ϵ are sufficiently small. Differentiating eq. (25) yields

$$\dot{V} = \dot{V}_0 + \alpha\dot{B}_1 + \beta\dot{B}_2 + \epsilon\dot{C}_0 + \alpha\epsilon\dot{C}_1 + \beta\epsilon\dot{C}_2 + \epsilon^2\dot{C}_3 + \cdots, \tag{26}$$

$$\ddot{V} = \ddot{V}_0 + \alpha\ddot{B}_1 + \beta\ddot{B}_2 + \epsilon\ddot{C}_0 + \alpha\epsilon\ddot{C}_1 + \beta\epsilon\ddot{C}_2 + \epsilon^2\ddot{C}_3 + \cdots, \tag{27}$$

Expanding $H[v, \dot{v}, \Psi(\tau)]$ as a Taylor's series around v_0 and $\dot{v}_0$ gives:

$$H[v, \dot{v}, \Psi(\tau)] = H[v_0, \dot{v}_0\ \Psi(\tau)] + (v-v_0)H_v[v_0, \dot{v}_0, \Psi(\tau)] + (\dot{v}-\dot{v}_0)H_{\dot{v}}[v_0, \dot{v}_0, \Psi(\tau)] + \cdots, \quad (28)$$

where H_v and $H_{\dot{v}}$ are partial derivatives of $H[v, \dot{v}, \Psi(\tau)]$ with respect to v and $\dot{v}$ respectively. Substituting eqs. (25), (26), (27) and (28) into eq. (22), and equating the different powers of α, β, and ϵ, we find that

$$\left.\begin{aligned} &\ddot{v}_0 + v_0 = 0, \\ &\ddot{B}_m + B_m = 0, \quad (m=1, 2), \\ &\ddot{C}_n + C_n = Z_n(\tau), \quad (n=0, 1, 2, \cdots), \end{aligned}\right\} \quad (29)$$

where

$$\left.\begin{aligned} &Z_0(\tau) = H[v_0, \dot{v}_0, \Psi(\tau)], \\ &Z_1(\tau) = B_1 H_v[v_0, \dot{v}_0, \Psi(\tau)] + \dot{B}_1 H_{\dot{v}}[v_0, \dot{v}_0, \Psi(\tau)], \\ &Z_2(\tau) = B_2 H_v[v_0, \dot{v}_0, \Psi(\tau)] + \dot{B}_2 H_{\dot{v}}[v_0, \dot{v}_0, \Psi(\tau)], \\ &Z_3(\tau) = C_0 H_v[v_0, \dot{v}_0, \Psi(\tau)] + \dot{C}_0 H_{\dot{v}}[v_0, \dot{v}_0, \Psi(\tau)], \\ &------------------. \end{aligned}\right\} \quad (30)$$

The solution of the first of eq. (29) is eq. (23). When $\tau = 0$, eqs. (25) and (26) become

$$\left.\begin{aligned} &v(0) = v_0(0) + \alpha B_1(0) + \beta B_2(0) + \epsilon C_0(0) + \alpha\epsilon C_1(0) + \beta\epsilon C_2(0) + \epsilon^2 C_3(0) + \cdots, \\ &\dot{v}(0) = \dot{v}_0(0) + \alpha \dot{B}_1(0) + \beta \dot{B}_2(0) + \epsilon \dot{C}_0(0) + \alpha\epsilon \dot{C}_1(0) + \beta\epsilon \dot{C}_2(0) + \epsilon^2 \dot{C}_3(0) + \cdots \end{aligned}\right\} \quad (31)$$

Comparing eq. (31) with eq. (24), we find

$$B_1(0) = \dot{B}_2(0) = 1,$$

$$B_2(0) = \dot{B}_1(0) = C_n(0) = \dot{C}_n(0) = 0, \quad n = 0, 1, 2, \cdots.$$

With these initial conditions, the solutions of the rest of eqs. (29) are

$$\left.\begin{aligned} B_1 &= \cos\tau, \\ B_2 &= \sin\tau, \\ C_n &= \int^{\tau} Z_n(u)\sin(\tau-u)\,du, \quad n=0,1,2,\cdots. \end{aligned}\right\} \quad (32)$$

Substituting eq. (32) with $\tau = 2\pi$ into eqs. (25) and (26), gives,

$$\left.\begin{aligned} V(2\pi) &= V_0(0) + \alpha + \epsilon C_0(2\pi) + \alpha\epsilon C_1(2\pi) + \beta\epsilon C_2(2\pi) + \epsilon^2 C_3(2\pi) + \cdots, \\ \dot{V}(2\pi) &= \dot{V}_0(0) + \beta + \epsilon \dot{C}_0(2\pi) + \alpha\epsilon \dot{C}_1(2\pi) + \beta\epsilon \dot{C}_2(2\pi) + \epsilon^2 \dot{C}_3(2\pi) + \cdots, \end{aligned}\right\} \quad (33)$$

where

$$\left.\begin{aligned} C_n(2\pi) &= -\int^{2\pi} Z_n(\tau)\sin\tau\,d\tau, \\ \dot{C}_n(2\pi) &= \int^{2\pi} Z_n(\tau)\cos\tau\,d\tau, \end{aligned}\right\} \quad n=0,1,2,\cdots. \quad (34)$$

Subtracting eq. (24) from eq. (33), yields

$$\left.\begin{aligned} V(2\pi) - V(0) &= \epsilon\left[C_0(2\pi) + \alpha C_1(2\pi) + \beta C_2(2\pi) + \epsilon C_3(2\pi) + \cdots\right], \\ \dot{V}(2\pi) - \dot{V}(0) &= \epsilon\left[\dot{C}_0(2\pi) + \alpha \dot{C}_1(2\pi) + \beta \dot{C}_2(2\pi) + \epsilon \dot{C}_3(2\pi) + \cdots\right]. \end{aligned}\right\} \quad (35)$$

In view of the comments after eq. (24) about α and β, it can be assumed that

$$\left.\begin{aligned} \alpha &= \alpha_1\epsilon + \alpha_2\epsilon^2 + \alpha_3\epsilon^3 + \cdots, \\ \beta &= \beta_1\epsilon + \beta_2\epsilon^2 + \beta_3\epsilon^3 + \cdots, \end{aligned}\right\} \quad (36)$$

Where α_1, α_2, ..., β_1, β_2, ... are constants. Inserting eq. (36) into eq. (35), we obtain:

$$\left.\begin{aligned} V(2\pi) - V(0) &= \epsilon\left\{C_0(2\pi) + \epsilon\left[\alpha_1 C_1(2\pi) + \beta_1 C_2(2\pi) + C_3(2\pi)\right] + \cdots\right\}, \\ \dot{V}(2\pi) - \dot{V}(0) &= \epsilon\left\{\dot{C}_0(2\pi) + \epsilon\left[\alpha_1 \dot{C}_1(2\pi) + \beta_1 \dot{C}_2(2\pi) + \dot{C}_3(2\pi)\right] + \cdots\right\}. \end{aligned}\right\} \quad (37)$$

Now the conditions for the existence of periodic

solutions with period 2π are:

$$\left.\begin{aligned} v(2\pi) - v(0) &= 0, \\ \dot{v}(2\pi) - \dot{v}(0) &= 0. \end{aligned}\right\} \quad (38)$$

To satisfy eq. (38), the terms of different powers in ϵ of eq. (37) must vanish independently. We therefore have:

$$\left.\begin{aligned} C_0(2\pi) &= 0, \\ \dot{C}_0(2\pi) &= 0; \end{aligned}\right\} \quad (39)$$

$$\left.\begin{aligned} \alpha_1 C_1(2\pi) + \beta_1 C_2(2\pi) + C_3(2\pi) &= 0, \\ \alpha_1 \dot{C}_1(2\pi) + \beta_1 \dot{C}_2(2\pi) + \dot{C}_3(2\pi) &= 0; \end{aligned}\right\} \quad (40)$$

. . . . . .

Eqs. (39) give the values of a_0 and b_0, and eqs. (40) the values of α and β to the first order of ϵ, provided:

$$\begin{vmatrix} C_1(2\pi) & C_2(2\pi) \\ \dot{C}_1(2\pi) & \dot{C}_2(2\pi) \end{vmatrix} \neq 0.$$

To recapitulate: The periodic solution of eq. (22) with ϵ small is eq. (25). In eq. (25) v_0 is of the form of eq. (23), in which a_0 and b_0 are determined from eqs. (34) and (39); B_1, B_2, and C_n are obtained from eqs. (32); and α and β from eqs. (34) and (40) to the first order of ϵ. Higher order solutions can be obtained in a manner similar to that used for the first order solution, though with more labour. In most practical problems, the zeroth order solution (or generating solution) is sufficient.

2.1.2. Stability of Periodic Solutions.

In the preceding section, the eq. (39) from which the generating solution of eq. (22) is obtained may give several sets of solutions of a_o and b_o, and consequently eq. (22) may have several distinct solutions. The question arises as to which set of solutions or what combination of solutions we should use: the answer lies in their stability. Only stable periodic solutions have practical significance, and only one stable solution can exist at any given time for any set of parameters, save for those critical conditions under which the solutions may "jump." We now investigate the stability of the periodic solutions.

The term "stability" is used here in the sense employed by Liapounoff (5). This can be stated qualitatively as follows: A periodic solution is said to be unstable if, after a slight disturbance, it ultimately dies out, or approaches another periodic solution, or increases indefinitely; and a periodic solution is stable if it is not unstable. Following this definition, if an equation has an unstable solution with zero amplitude, this solution will either increase without limit or reach a finite amplitude. The system represented by the equation is said to be subject to self-excitation.

The stability can be examined by the perturbation method. Let the values of the periodic solution with

period 2π at an arbitrary instant (say $\tau = 0$) be $v(0) = \alpha$, and $\dot{v}(0) = b$: then the values of a solution with slightly different initial conditions $v'(0) = \alpha + \xi$, and $\dot{v}'(0) = b + \eta$ at $\tau = 2\pi$, will be of the form $v'(2\pi) = \alpha + \bar{\xi}$ and $\dot{v}'(2\pi) = b + \bar{\eta}$, where $v'(\tau)$ is the perturbed solution. It follows, therefore

$$\left.\begin{aligned} v'(2\pi) - v'(0) &= \bar{\xi} - \xi, \\ \dot{v}'(2\pi) - \dot{v}'(0) &= \bar{\eta} - \eta. \end{aligned}\right\} \quad (41)$$

With the perturbed solution, eqs. (25) and (35) retain their forms except that v, α, and β are replaced by v', $\alpha + \xi$ and $\beta + \eta$ respectively. Eq. (35) thus becomes

$$\left.\begin{aligned} v'(2\pi) - v'(0) &= \epsilon\left[C_0(2\pi) + (\alpha+\xi)C_1(2\pi) + (\beta+\eta)C_2(2\pi) + \epsilon C_3(2\pi) + \cdots\right], \\ \dot{v}'(2\pi) - \dot{v}'(0) &= \epsilon\left[\dot{C}_0(2\pi) + (\alpha+\xi)\dot{C}_1(2\pi) + (\beta+\eta)\dot{C}_2(2\pi) + \epsilon\dot{C}_3(2\pi) + \cdots\right]. \end{aligned}\right\} \quad (42)$$

With the help of eqs. (35) and (38), eq. (42) reduces to:

$$\left.\begin{aligned} v'(2\pi) - v'(0) &= \epsilon\left[\xi C_1(2\pi) + \eta C_2(2\pi) + \cdots\right], \\ \dot{v}'(2\pi) - \dot{v}'(0) &= \epsilon\left[\xi \dot{C}_1(2\pi) + \eta \dot{C}_2(2\pi) + \cdots\right]. \end{aligned}\right\} \quad (43)$$

From eqs. (41) and (43), we have,

$$\bar{\xi} = h_1\xi + h_2\eta + \cdots, \quad \bar{\eta} = h_3\xi + h_4\eta + \cdots, \quad (44)$$

where

$$\left.\begin{aligned} h_1 &= 1 + \epsilon C_1(2\pi), & h_2 &= \epsilon C_2(2\pi), \\ h_3 &= \epsilon \dot{C}_1(2\pi), & h_4 &= 1 + \epsilon \dot{C}_2(2\pi). \end{aligned}\right\} \quad (45)$$

It can be shown that the stability (9) of a periodic solution depends upon the characteristic roots of the matrix

$$\begin{bmatrix} h_1 & h_2 \\ h_3 & h_4 \end{bmatrix},$$

i.e. the roots of the equation

$$\rho^2 - (h_1 + h_4)\rho + (h_1 h_4 - h_2 h_3) = 0. \tag{46}$$

Denote the roots by ρ_1 and ρ_2. If $|\rho_1| < 1$, $|\rho_2| < 1$, the solution is completely stable. If $|\rho_1| > 1$, $|\rho_2| > 1$, the solution is completely unstable. If $\rho_1 > 1 > \rho_2 > 0$ the solution is directly stable (of "col"[10] or "saddle"[5] type). If $\rho_1 < -1 < \rho_2 < 0$, the solution is indirectly unstable. Inserting eq. (45) into eq. (46) and solving for ρ, we obtain

$$\rho = 1 + \frac{\epsilon}{2}\left\{\left[C_1(2\pi) + \dot{C}_2(2\pi)\right] \pm \sqrt{\left[C_1(2\pi) + \dot{C}_2(2\pi)\right]^2 - 4\left[C_1(2\pi)\dot{C}_2(2\pi) - C_2(2\pi)\dot{C}_1(2\pi)\right]}\right\}.$$

As a consequence of the statements above, we establish the following:

(a) For a completely stable solution,

$$C_1(2\pi) + \dot{C}_2(2\pi) < 0,$$

and

$$\begin{vmatrix} C_1(2\pi) & \dot{C}_1(2\pi) \\ C_2(2\pi) & \dot{C}_2(2\pi) \end{vmatrix} > 0$$

;

(b) For a completely unstable solution,

$$C_1(2\pi) + \dot{C}_2(2\pi) > 0,$$

and

$$\begin{vmatrix} \dot{C}_1(2\pi) & C_1(2\pi) \\ C_2(2\pi) & \dot{C}_2(2\pi) \end{vmatrix} > 0$$

;

(c) For a directly unstable solution,

$$\begin{vmatrix} C_1(2\pi) & \dot{C}_1(2\pi) \\ C_2(2\pi) & \dot{C}_2(2\pi) \end{vmatrix} < 0,$$

and $C_1(2\pi) + \dot{C}_2(2\pi)$ can be either positive or negative;

(d) There is no indirectly unstable solution.

2.1.3. Special Cases.

In order to illustrate the foregoing mathematical analysis, we shall consider in the following special cases of eq. (22), corresponding to the two circuits described in Section 1.

2.1.3.1 $H[v, \dot{v}, \Psi(\tau)] = -(P + 4q_1 \cos 2\tau)v - [2q_1 \sin 2\tau + r_1 + r_2 v + r_3 v^2]\dot{v}$ (47)

With the expression of eq. (47), eq. (22) has the form of eq. (11), except that $\lambda_1 = 0$, σ_1 and q_1 are replaced by $1 + \epsilon p$ and $-2q_1$ respectively. Eq. (22) now represents the circuit in Fig. 1 with $k = -1$. In eq. (47), the linear damping r_1 is assumed to be positive here, for otherwise the system can be self-excited with negative linear damping only; and r_3 is positive as shown before.

At first, we shall find the zeroth order solution. We calculate $C_0(\tau)$ and then a_0 and b_0. Inserting eqs. (23) and (47) into the first of eq. (30), yields:

$$Z_0(\tau) = P_1 \sin\tau + Q_1 \cos\tau + P_2 \sin 2\tau + Q_2 \cos 2\tau + P_3 \sin 3\tau + Q_3 \cos 3\tau, \quad (48)$$

where

$$\left.\begin{aligned} P_1 &= r_1 a_0 + \tfrac{1}{4} r_3 a_0 (a_0^2 + b_0^2) + q_1 b_0 - P b_0, \\ Q_1 &= -r_1 b_0 - \tfrac{1}{4} r_3 b_0 (a_0^2 + b_0^2) - q_1 a_0 - P a_0, \\ P_2 &= \tfrac{1}{2} r_2 (a_0^2 - b_0^2), \\ Q_2 &= -r_2 a_0 b_0, \\ P_3 &= r_3 (\tfrac{1}{4} a_0^3 - \tfrac{3}{4} a_0 b_0^2) - 3 q_1 b_0, \\ \text{and} \quad Q_3 &= r_3 (\tfrac{1}{4} b_0^3 - \tfrac{3}{4} a_0^2 b_0) - 3 q_1 a_0. \end{aligned}\right\} \quad (49)$$

Substituting eq. (48) into the third of eq. (32) with $n=0$, after integration gives:

$$C_0(\tau) = \tfrac{1}{2}Q_1\tau\sin\tau - \tfrac{1}{2}P_1\tau\cos\tau + P_1'\sin\tau + Q_1'\cos\tau - \tfrac{1}{3}P_2\sin 2\tau - \tfrac{1}{3}Q_2\cos 2\tau - \tfrac{1}{8}P_3\sin 3\tau - \tfrac{1}{8}Q_3\cos 3\tau, \qquad (50)$$

where $P_1' = \frac{1}{2}P_1 + \frac{2}{3}P_2 + \frac{3}{8}P_3$,

and $Q_1' = \frac{1}{3}Q_2 + \frac{1}{8}Q_3$. } (51)

In eq. (50) letting $\tau = 2\pi$, and from eq. (39), we have

$$P_1 = Q_1 = 0. \qquad (52)$$

Putting the values of P_1 and Q_1 which are given in eq. (49), into eq. (52) and solving for a_0 and b_0, we get the sets of solutions:

$$a_0 = 0, \quad b_0 = 0; \qquad (53)$$

$$a_0^2 + b_0^2 = \frac{4}{r_3}\left[-r_1 \pm \sqrt{q_1^2 - p^2}\right], \qquad \frac{a_0}{b_0} = \mp\sqrt{\frac{q_1 - p}{q_1 + p}}. \qquad (54)$$

Inspection of eq. (54) reveals the following:

(a) Since r_1 and r_3 are positive, only the upper sign in the first of eq. (54) is possible, and consequently the second of eq. (54) takes the upper sign too.

(b) Solution (54) exists if, and only if,

$$q_1^2 > r_1^2 + p^2.$$

(c) The solution does not contain r_2, and this is why we do not take the term involving r_2 as the highest power in the non-linearity.

(d) $a_0^2 + b_0^2$, the square of the amplitude of the zeroth order solution, is inversely proportional to r_3 , the coefficient of the only non-linear term besides that containing r_2 . If r_3 approaches zero, the amplitude tends to infinity, so that, for a solution of finite amplitude, non-linearity cannot be avoided.

(e) The second of eq. (54), which represents the phase of the zeroth order solution, is independent of the non-linearity.

We then calculate the first order solution. From eq. (47), it follows that:

$$\left.\begin{aligned} H_v\left[v_0, \dot{v}_0, \Psi(\tau)\right] &= -p - 4q_1\cos 2\tau - r_2\dot{v}_0 - 2r_3 v_0\dot{v}_0 , \\ \text{and} \quad H_{\dot{v}}\left[v_0, \dot{v}_0, \Psi(\tau)\right] &= -2q_1\sin 2\tau - r_1 - r_2 v_0 - r_3 v_0^2 . \end{aligned}\right\} \quad (55)$$

Inserting eq. (55), $C_0(\tau)$, $\dot{C}_0(\tau)$ obtained from eq. (50), $A(\tau)$, $\dot{A}(\tau)$, $B(\tau)$ and $\dot{B}(\tau)$ from the first two of eq. (32), into the last three of eq. (30), gives $Z_1(\tau)$, $Z_2(\tau)$ and $Z_3(\tau)$; then from eq. (34) with $n = 1, 2,$ and 3 , after simplification, we have:

$$\left.\begin{aligned} C_1(2\pi) &= -\pi\left[r_1 + r_3\left(\tfrac{3}{4}a_0^2 + \tfrac{1}{4}b_0^2\right)\right], \\ \dot{C}_1(2\pi) &= -\pi\left[p + q_1 + \tfrac{1}{2}r_3 a_0 b_0\right], \\ C_2(2\pi) &= -\pi\left[-p + q_1 + \tfrac{1}{2}r_3 a_0 b_0\right], \\ \dot{C}_2(2\pi) &= -\pi\left[r_1 + r_3\left(\tfrac{3}{4}b_0^2 + \tfrac{1}{4}a_0^2\right)\right], \\ C_3(2\pi) &= -\pi\left\{-pP_1' + r_1Q_1' + q_1\left(P_1' + \tfrac{1}{8}P_3\right) - \tfrac{1}{6}r_2\left(Q_2a_0 + P_2b_0\right)\right. \\ &\qquad \left. + r_3\left[\tfrac{1}{2}\left(a_0^2+b_0^2\right)Q_1' + \tfrac{1}{2}\left(P_1' + \tfrac{1}{8}P_3\right)a_0b_0 + \tfrac{1}{4}\left(Q_1' + \tfrac{1}{8}Q_3\right)\left(a_0^2 - b_0^2\right)\right]\right\}, \\ \dot{C}_3(2\pi) &= \pi\left\{-pQ_1' - r_1P_1' - q_1\left(Q_1' - \tfrac{1}{8}Q_3\right) + \tfrac{r_2}{6}\left(P_2a_0 - Q_2b_0\right)\right. \\ &\qquad \left. + r_3\left[-\tfrac{1}{2}\left(a_0^2+b_0^2\right)P_1' - \tfrac{1}{2}\left(Q_1' - \tfrac{1}{8}Q_3\right)a_0b_0 + \tfrac{1}{4}\left(P_1' - \tfrac{1}{8}P_3\right)\left(a_0^2 - b_0^2\right)\right]\right\}. \end{aligned}\right\} \quad (56)$$

Inserting the values of P's and Q's into eq. (56), then substituting it into eq. (40) and solving for α_1, and β_1, we obtain

$$\left.\begin{aligned}\alpha_1 &= \frac{1}{S_0}\left[r_2^2(a_0^2+b_0^2)S_1 + \tfrac{1}{3}r_2 a_0 b_0 S_0 - P_3(S_3+b_0^2 S_4) + Q_3 S_5\right],\\ \beta_1 &= \frac{1}{S_0}\left[r_2^2(a_0^2+b_0^2)S_2 - \tfrac{1}{3}r_2(a_0^2-b_0^2)S_0 + Q_3(S_3+a_0^2 S_4) + P_3 S_6\right],\end{aligned}\right\} \quad (57)$$

where $S_0 = r_1^2+p^2-q_1^2-q_1 r_3 a_0 b_0 + r_1 r_3(a_0^2+b_0^2) + \frac{3}{16}r_3^2(a_0^2+b_0^2)^2$,

$$S_1 = \frac{1}{6}(2pa_0 + q_1 a_0 + r_1 b_0),$$

$$S_2 = \frac{1}{6}(2pb_0 - q_1 b_0 - r_1 a_0),$$

$$S_3 = \frac{1}{8}\left[q_1 r_1 + \tfrac{1}{2}r_1 r_3 a_0 b_0 + \tfrac{1}{4}r_3 p(a_0^2-b_0^2)\right],$$

$$S_4 = \frac{1}{8}r_3\left(q_1 + \tfrac{1}{2}r_3 a_0 b_0\right),$$

$$P_3 = r_3\left(\tfrac{1}{4}a_0^2 - \tfrac{3}{4}a_0 b_0^2\right) - 3q_1 b_0,$$

$$Q_3 = r_3\left(\tfrac{1}{4}b_0^3 - \tfrac{3}{4}a_0^2 b_0\right) - 3q_1 a_0,$$

$$S_5 = -\frac{1}{8}\left[p^2+r_1^2 - pq_1 - \tfrac{1}{2}r_3 p a_0 b_0 + \tfrac{1}{4}r_1 r_3(3b_0^2+5a_0^2) + \tfrac{1}{4}r_3^2(3a_0^2b_0^2+a_0^4)\right],$$

and $$S_6 = -\frac{1}{8}\left[3(p^2+r_1^2) - 4q_1^2 - pq_1 - \tfrac{1}{2}r_3 p a_0 b_0 - 4r_3 q_1 a_0 b_0 + \tfrac{1}{4}r_1 r_3(13a_0^2+7b_0^2) + \tfrac{1}{4}r_3^2(3a_0^4+3a_0^2b_0^2+2b_0^4)\right].$$

We have calculated the values of a_0, b_0, $C_0(t)$ α_1 and β_1. Inserting these values into eq. (25), periodic solutions to the first order of ϵ are obtained. We now inwestigate the stability of the solutions.

Solution (a): $a_0 = b_0 = 0$.

From eq. (56), it follows that

$$C_1(2\pi) + \dot{C}_2(2\pi) = -2\pi r_1 < 0,$$

and $$C_1(2\pi)\dot{C}_2(2\pi) - \dot{C}_1(2\pi)C_2(2\pi) = \pi^2\left[r_1^2 - (q_1^2-p^2)\right].$$

Hence this solution is stable if $q_1^2 < r_1^2 + p^2$, otherwise it is directly unstable. Thus the condition of self-excitation is: $q_1^2 > r_1^2 + p^2$. Note that this inequality is free from non-linearity.

Solution (b): $$a_0^2 + b_0^2 = \frac{4}{r_3}\left[-r_1 + \sqrt{q_1^2 - p^2}\right], \qquad \frac{a_0}{b_0} = -\sqrt{\frac{q_1+p}{q_1-p}}.$$

It is calculated that:

$$C_1(2\pi) + \dot{C}_2(2\pi) = 2\pi\left[r_1 - 2\sqrt{q_1^2 - p^2}\right],$$

and $$C_1(2\pi)\dot{C}_2(2\pi) - \dot{C}_1(2\pi)C_2(2\pi) = 4\pi^2\sqrt{q_1^2-p^2}\left[-r_1 + \sqrt{q_1^2-p^2}\right].$$

This solution is stable if $\sqrt{q_1^2-p^2} > r_1$ or $q_1^2 > r_1^2 + p^2$. Since the condition of existence of this solution is the same as that of its stability, this solution is always stable.

We now summarize: The equation

$$\ddot{v} + v = -\epsilon\left\{(p + 4q_1\cos 2\tau)v + [2q_1\sin 2\tau + r_1 + r_2 v + r_3 v^2]\dot{v}\right\}$$

always has a solution with zero amplitude, which is stable unless $q_1^2 > r_1^2 + p^2$, then it is unstable. As soon as the values of the parameters reach the unstable region of the zero-amplitude solution, a stable solution with finite amplitude appears, and is of the form:

$$v = V\sin(\tau + \psi) + \epsilon\left[C_0(\tau) + \alpha_1\cos\tau + \beta_1\sin\tau\right] + O(\epsilon^2),$$

where $$V^2 = \frac{4}{r_3}\left[-r_1 + \sqrt{q_1^2 - p^2}\right],$$

$$\psi = \tan^{-1}\left(-\sqrt{\frac{q_1+p}{q_1-p}}\right),$$

$C_0(\tau)$, α_1, and β_1 are from eqs. (50) and (57) respectively, and $O(\epsilon^2)$ contains terms of $\epsilon^2, \epsilon^3, \cdots$.

The manner in which V , the amplitude of the

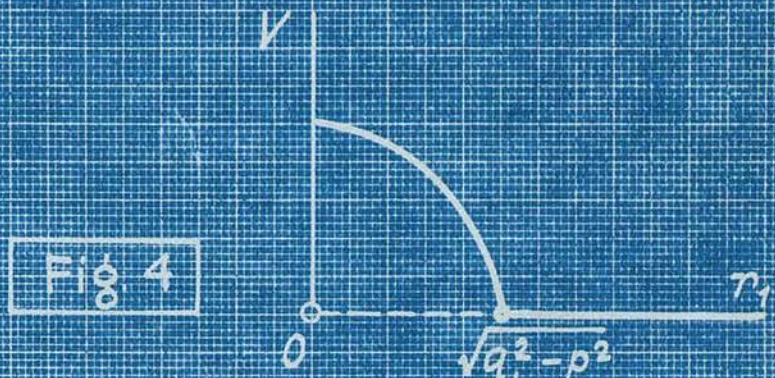

Fig. 4

Fig. 5

Fig. 6

zeroth order solution, varies as the linear damping r_1, the amplitude of the parameter-variation q_1, or the difference between the natural frequency of the circuit and one-half that of the parameter-variation p is varied, is sketched in Figs. 4, 5, and 6 respectively. The full lines (other than OV) stand for stable and the dotted lines for unstable solutions. These curves will be compared in Section 3 with those obtained by experiment.

2.1.3.2. $H\left[v, \dot{v}, \Psi(\tau)\right] = -r\dot{v} + 2q_2 v\cos 2\tau - \sum_{n=1}^{5} p_n v^n$. (58)

In eq. (58), r, q_2, and p_n ($n = 2, 3, 4, 5$) are the same constants as those in eq. (14), p_3 is negative, r and p_5 are positive, and $p_1 = \frac{1}{\epsilon}(\sigma_2 - 1)$. Eq. (22) is then identical with eq. (14), which represents the circuit in Fig. 3, except that $\lambda_2 = 0$.

Substituting eqs. (23) and (58) into the first of eq. (30) gives $Z_0(\tau)$. Inserting the expression of $Z_0(\tau)$ into eq. (34) with $n = 0$, and from eq. (39), we have:

$$r a_0 - q_2 b_0 - p_1 b_0 - \tfrac{3}{4} p_3 b_0 (a_0^2 + b_0^2) - \tfrac{5}{8} p_5 b_0 (a_0^2 + b_0^2)^2 = 0,$$

$$r b_0 - q_2 a_0 + p_1 a_0 + \tfrac{3}{4} p_3 a_0 (a_0^2 + b_0^2) + \tfrac{5}{8} p_5 a_0 (a_0^2 + b_0^2)^2 = 0.$$

The solutions of these equations are

$$V_0^2 = a_0^2 + b_0^2 = 0, \quad \text{i.e. } a_0 = b_0 = 0;$$

and
$$\left.\begin{aligned} V^2 = a_0^2 + b_0^2 &= \frac{1}{5p_5}\left[-3p_3 \pm \sqrt{9p_3^2 - 40p_5(p_1 \mp \sqrt{q_2^2 - r^2})}\right], \\ \tan\psi = \frac{a_0}{b_0} &= \frac{q_2 \pm \sqrt{q_2^2 - r^2}}{r}. \end{aligned}\right\} \quad (59)$$

The upper and lower signs in the second of eq. (59) correspond respectively to the upper and lower signs

before the radical $\sqrt{q_2^2-r^2}$ in the first of eq. (59). In view of eq. (59), it follows that:

the phases of the periodic solutions are independent of the non-linearity; and

the solutions to the zeroth order of ϵ do not contain r_2 and r_4 which are the coefficients of v^2 and v^4 respectively.

Solution (59) may not exist, or may have from one to four values, according to the relations between the constants.

Let

$$V_1^2 = \frac{1}{5p_5}\left[-3p_3+\sqrt{9p_3^2-40p_5\left(p_1-\sqrt{q_2^2-r^2}\right)}\right],$$

$$V_2^2 = \frac{1}{5p_5}\left[-3p_3-\sqrt{9p_3^2-40p_5\left(p_1-\sqrt{q_2^2-r^2}\right)}\right],$$

$$V_3^2 = \frac{1}{5p_5}\left[-3p_3+\sqrt{9p_3^2-40p_5\left(p_1+\sqrt{q_2^2-r^2}\right)}\right],$$

and

$$V_4^2 = \frac{1}{5p_5}\left[-3p_3-\sqrt{9p_3^2-40p_5\left(p_1+\sqrt{q_2^2-r^2}\right)}\right].$$

As V^2 must be positive, we have first, common to the four sets, a necessary condition of existence of solutions:

$$|q_2| > r$$

For individual cases, further conditions are:

(a) V_1 is possible if $9p_3^2 > 40p_5\left(p_1-\sqrt{q_2^2-r^2}\right)$,

(b) V_2 is possible if $9p_3^2 > 40p_5\left(p_1-\sqrt{q_2^2-r^2}\right) > 0$,

(c) V_3 is possible if $9p_3^2 > 40p_5\left(p_1+\sqrt{q_2^2-r^2}\right)$,

(d) V_4 is possible if $9p_3^2 > 40p_5\left(p_1+\sqrt{q_2^2-r^2}\right) > 0$.

(59a)

We now examine the stability of these solutions.

Inserting the partial derivatives of $H[v, \dot{v}, \Psi(\tau)]$ with respect to v and $\dot{v}$ which are obtained from eq. (58), into the second and third of eq. (30), and with the help of eq. (23), gives $Z_1(\tau)$ and $Z_2(\tau)$. Inserting the two expressions of $Z_1(\tau)$ and $Z_2(\tau)$ into eq. (34) with $n=1$ and 2, results, after simplification, in

$$C_1(2\pi) = -\pi\left[r - \tfrac{3}{2}p_3 a_0 b_0 - \tfrac{5}{2}p_5 a_0 b_0 (a_0^2+b_0^2)\right],$$

$$\dot{C}_1(2\pi) = \pi\left[-q_2 - p_1 - \tfrac{3}{4}p_3(a_0^2+b_0^2) - \tfrac{3}{2}p_3 a_0^2 - \tfrac{15}{8}p_5(a_0^2+b_0^2)^2 - \tfrac{5}{4}p_5(a_0^2+b_0^2)(a_0^2-b_0^2)\right],$$

$$C_2(2\pi) = \pi\left[-q_2 + p_1 + \tfrac{3}{4}p_3(a_0^2+b_0^2) + \tfrac{3}{2}p_3 b_0^2 + \tfrac{15}{8}p_5(a_0^2+b_0^2)^2 + \tfrac{5}{4}p_5(a_0^2+b_0^2)(b_0^2-a_0^2)\right],$$

and

$$\dot{C}_2(2\pi) = -\pi\left[r + \tfrac{3}{2}p_3 a_0 b_0 + \tfrac{5}{2}p_5 a_0 b_0 (a_0^2+b_0^2)\right].$$

It follows then that

$$C_1(2\pi) + \dot{C}_2(2\pi) = -2\pi r < 0,$$

and

$$C_1(2\pi)\dot{C}_2(2\pi) - \dot{C}_1(2\pi)C_2(2\pi) = \pi^2 \Omega_n, \quad (n=0, 1, 2, \cdots 5),$$

where $\Omega_0 = r^2 + p_1^2 - q_2^2$ corresponds to $V = V_0 = 0$,

$$\Omega_n = 3p_1p_3V_n^2 + \left(\tfrac{9}{4}p_3^2 + 5p_1p_5\right)V_n^4 + \tfrac{45}{8}p_3p_5V_n^6 + \tfrac{25}{8}p_5^2V_n^8$$

corresponds to $V = V_n \neq 0$, $(n=1, 2, 3, 4)$. The explicit expressions for Ω_n $(n=1, 2, 3, 4)$ are:

$$\Omega_1 = \sqrt{q_2^2 - r^2}\sqrt{9p_3^2 - 40p_5(p_1 - \sqrt{q_2^2-r^2})}\ V_1^2 > 0,$$

$$\Omega_2 = -\sqrt{q_2^2 - r^2}\sqrt{9p_3^2 - 40p_5(p_1 - \sqrt{q_2^2-r^2})}\ V_2^2 < 0,$$

$$\Omega_3 = -\sqrt{q_2^2 - r^2}\sqrt{9p_3^2 - 40p_5(p_1 + \sqrt{q_2^2-r^2})}\ V_3^2 < 0,$$

and

$$\Omega_4 = \sqrt{q_2^2 - r^2}\sqrt{9p_3^2 - 40p_5(p_1 + \sqrt{q_2^2-r^2})}\ V_4^2 > 0.$$

Therefore, we have the stability criteria:

(a) $V_0 = 0$ is stable if $q_2^2 < p_1^2 + r^2$ and is directly unstable if $q_2^2 > p_1^2 + r^2$;

(b) V_1 and V_4 are always stable;

(c) and V_2 and V_3 are always directly unstable.

Note that the condition of self-excitation depends only on the linear terms of the equation and has the same form as the previous example.

We shall in the following examine how the solutions vary as q_2 , r , or p is varied. Firstly, the case of varying q_2 and constant r, p_1, p_3 and p_5 is considered. Solving for q_2 from inequalities (59a), we have:

(a) The Condition of existence of V_1 is

i) $|q_2| > r$, if $40 p_1 p_5 < 9 p_3^2$;

ii) $|q_2| > \sqrt{r^2 + (p_1 - \frac{9 p_3^2}{40 p_5})^2}$, if $40 p_1 p_5 > 9 p_3^2$.

(b) The Conditions of existence of V_2 are

i) $r < |q_2| < \sqrt{p_1^2 + r^2}$, if $40 p_1 p_5 < 9 p_3^2$ and $p_1 > 0$;

ii) $\sqrt{r^2 + (p_1 - \frac{9 p_3^2}{40 p_5})^2} < |q_2| < \sqrt{p_1^2 + r^2}$, if $40 p_1 p_5 > 90 p_3^2$;

(c) The Conditions of existence of V_3 are

$r < |q_2| < \sqrt{r^2 + (\frac{9 p_3^2}{40 p_5} - p_1)^2}$ and $9 p_3^2 > 40 p_1 p_5$.

(d) The Conditions of existence of V_4 are

i) $r < |q_2| < \sqrt{r^2 + (\frac{9 p_3^2}{40 p_5} - p_1)^2}$, if $9 p_3^2 > 40 p_1 p_5 > 0$;

ii) $\sqrt{r^2 + p_1^2} < |q_2| < \sqrt{r^2 + (\frac{9 p_3^2}{40 p_5} - p_1)^2}$, if $p_1 < 0$.

It should be noticed that the term "existence" used in these cases has mathematical sense only, for V_2 and V_3 , which have been shown to be unstable, can never appear in practice.

Inspection of the above conditions indicates four cases to be considered:

(a) $40p_1p_5 > 9p_3^2$. In this case only V_1 (stable) and V_2 (unstable) are possible and they exist under limitations. Besides V_1 and V_2, V_0 always exists in all cases: it is stable unless $|q_2| > \sqrt{r^2+p_1^2}$ when it becomes unstable. Curves of V plotted against $|q_2|$ are sketched in Fig. 7(a), in which the full lines denote stable solutions and the dotted lines unstable solutions. Fig. 7(a) shows that V_1 and V_2 exist when $|q_2| > \sqrt{r^2+\left(p_1 - \frac{9p_3^2}{40p_5}\right)^2}$ and V_2 disappears at $|q_2| = \sqrt{p_1^2+r^2}$, while V_0 changes from stable to unstable. Fig. 7(a) also shows the effect of hysteresis if $|q_2|$ is actually increased and then decreased again. As $|q_2|$ is increased from zero, the stable V_0 is followed until $|q_2|$ reaches $\sqrt{r^2+p_1^2}$: the solution then jumps to V_1. As $|q_2|$ is decreased, V_1 remains until $|q_2|$ reaches $\sqrt{r^2+\left(p_1-\frac{9p_3^2}{40p_5}\right)^2}$, the solution then jumps back to V_0. The process is indicated by the arrows.

(b) $p_1 < 0$. All the solutions in this case are possible except V_2. V_1 (stable) exists when $|q_2| > r$, V_3 (unstable) exists when $|q_2|$ is between r and $\sqrt{r^2+\left(\frac{9p_3^2}{40p_5}-p_1\right)^2}$, and V_4 (stable) exists when $|q_2|$ is between $\sqrt{r^2+p_1^2}$ and $\sqrt{r^2+\left(\frac{9p_3^2}{40p_5}-p_1\right)^2}$. The solutions are shown in Fig. 7(b). Before $|q_2|$ is actually increased to $\sqrt{r^2+p_1^2}$, $V = V_0$; when $\sqrt{r^2+p_1^2}$ is reached, $V = V_4$; when $|q_2|$ reaches

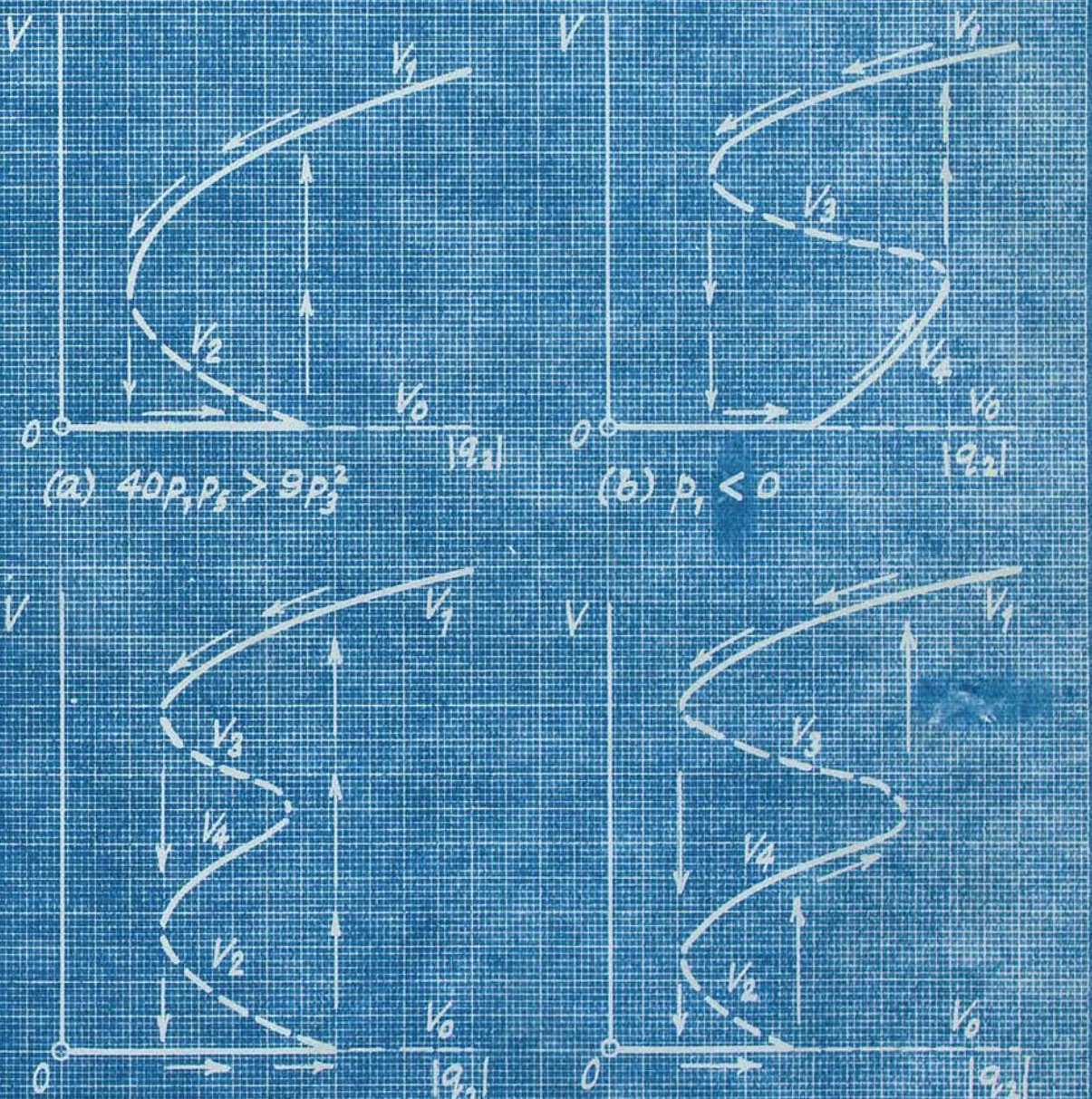
V
V1
V2
V0
0
|Q2|
(a) $40P_1P_3 > 9P_3^2$
V
V1
V3
V4
V0
0
|Q2|
(b) $P_1 < 0$
V
V1
V3
V4
V2
V0
0
|Q2|
(c) $80P_1P_3 > 9P_3^2 > 40P_1P_3 > 0$
V
V1
V3
V4
V2
V0
0
|Q2|
(d) $9P_3^2 > 80P_1P_3 > 0$

Fig. 7

TABLE I

		V_1	V_2	V_3	V_4
a	$40p_1p_5 > 9p_3^2$	$r < \sqrt{q_2^2-(p_1-\frac{9p_3^2}{40p_5})^2}$	$r < \sqrt{q_2^2-(p_1-\frac{9p_3^2}{40p_5})^2}$ $r > \sqrt{q_2^2-p_1^2}$		
b	$\lvert q_2\rvert > \frac{9p_3^2}{40p_5} - p_1$ $p_1 < 0$	$r < \lvert q_2\rvert$		$r > \sqrt{q_2^2-(\frac{9p_3^2}{40p_5}-p_1)^2}$ $r < \lvert q_2\rvert$	$r > \sqrt{q_2^2-(\frac{9p_3^2}{40p_5}-p_1)^2}$ $r < \sqrt{q_2^2-p_1^2}$
c	$\lvert q_2\rvert < \frac{9p_3^2}{40p_5} - p_1$ $p_1 < 0$	$r < \lvert q_2\rvert$		$r < \lvert q_2\rvert$	$r < \sqrt{q_2^2-p_1^2}$
d	$\lvert q_2\rvert > \frac{9p_3^2}{40p_5} - p_1$ $40p_1p_5 < 9p_3^2 < 80p_1p_5$	$r < \lvert q_2\rvert$	$r < \lvert q_2\rvert$ $r > \sqrt{q_2^2-p_1^2}$	$r < \lvert q_2\rvert$ $r > \sqrt{q_2^2-(\frac{9p_3^2}{40p_5}-p_1)^2}$	$r < \lvert q_2\rvert$ $r > \sqrt{q_2^2-(\frac{9p_3^2}{40p_5}-p_1)^2}$
e	$\lvert q_2\rvert > \frac{9p_3^2}{40p_5} - p_1$ $9p_3^2 > 80p_1p_5 > 0$	$r < \lvert q_2\rvert$	$r < \lvert q_2\rvert$ $r > \sqrt{q_2^2-p_1^2}$	$r < \lvert q_2\rvert$ $r > \sqrt{q_2^2-(\frac{9p_3^2}{40p_5}-p_1)^2}$	$r < \lvert q_2\rvert$ $r > \sqrt{q_2^2-(\frac{9p_3^2}{40p_5}-p_1)^2}$
f	$\lvert q_2\rvert < \frac{9p_3^2}{40p_5} - p_1$ $p_1 > 0$	$r < \lvert q_2\rvert$	$r < \lvert q_2\rvert$ $r > \sqrt{q_2^2-p_1^2}$	$r < \lvert q_2\rvert$	$r < \lvert q_2\rvert$

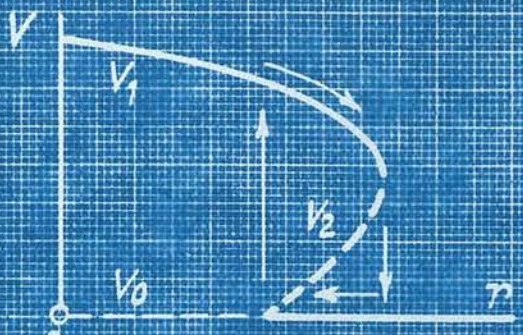

(a) $40P_1P_5 > 9P_3^2$

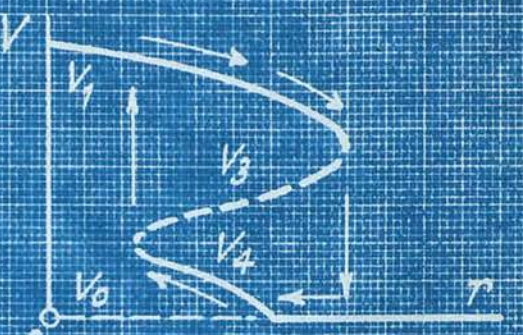

(b) $|q_2| > \frac{9P_3^2}{40P_5} - P_1$, $P_1 < 0$

(c) $|q_2| < \frac{9P_3^2}{40P_5} - P_1$, $P_1 < 0$

(d) $|q_2| > \frac{9P_3^2}{40P_5} - P_1$,
$40P_1P_5 < 9P_3^2 < 80P_1P_5$

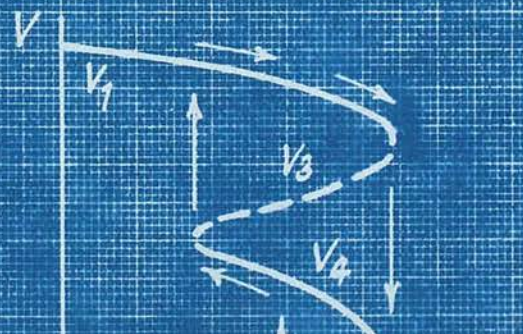

(e) $|q_2| > \frac{9P_3^2}{40P_5} - P_1$
$9P_3^2 > 80P_1P_5$,
$P_1 > 0$

(f) $|q_2| < \frac{9P_3^2}{40P_5} - P_1$
$P_1 > 0$

Fig. 8

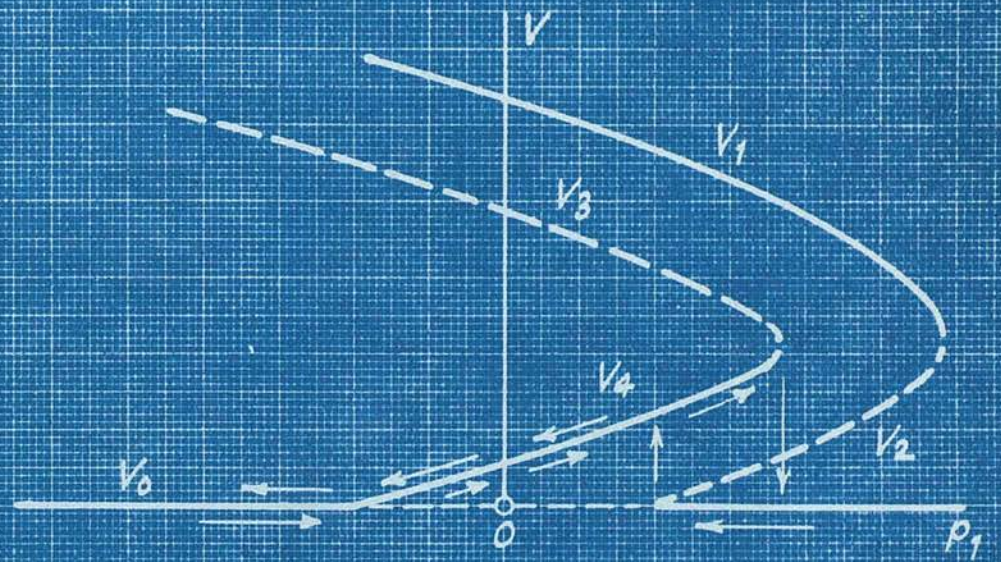

(a) $9p_3^2 > 80p_5\sqrt{q_2^2 - r^2}$

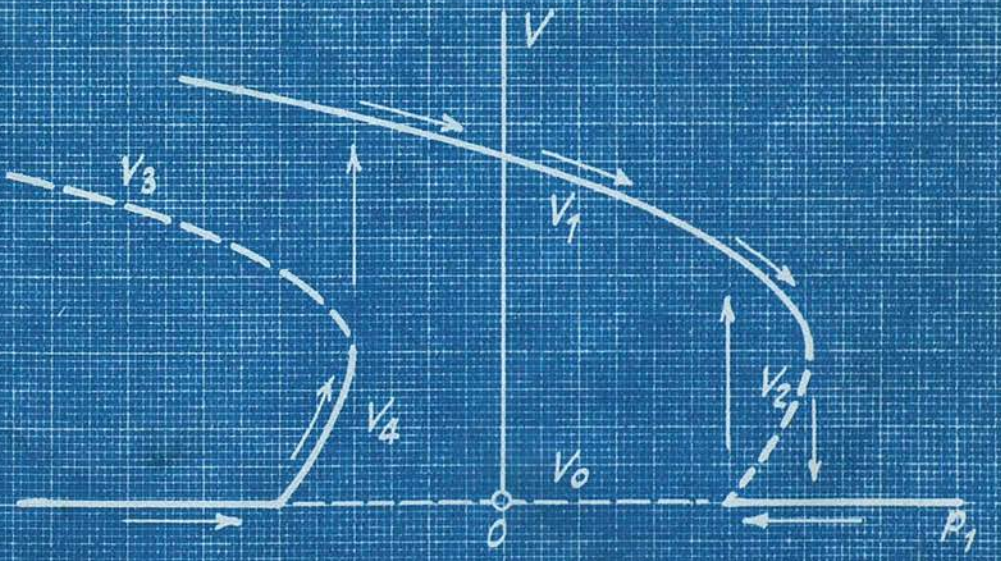

(b) $9p_3^2 < 80p_5\sqrt{q_2^2 - r^2}$

Fig. 9

remaining constant, it is found that the conditions of existence of solutions are:

for V_1 , $p_1 < \frac{9p_3^2}{40p_5} + \sqrt{q_2^2 - r^2}$,

for V_2 , $\sqrt{q_2^2 - r^2} < p_1 < \frac{9p_3^2}{40p_5} + \sqrt{q_2^2 - r^2}$,

for V_3 , $p_1 < \frac{9p_3^2}{40p_5} - \sqrt{q_2^2 - r^2}$,

for V_4 , $-\sqrt{q_2^2 - r^2} < p_1 < \frac{9p_3^2}{40p_5} - \sqrt{q_2^2 - r^2}$,

and, of course, $|q_2| > r$ is further condition for all four cases. The graphs of V against p_1 shown in Figs. 9(a) and 9(b) correspond to two different cases, $9p_3^2 >$ and $< 80p_5\sqrt{q_2^2 - r^2}$ respectively. Fig. 9(a) shows that V_1 cannot be reached if the initial condition of the system is quiescent. And there is no indication of resonance at $p_1 = 0$ for either Fig. 9(a) or 9(b).

Summarizing the results that have been obtained: The equation $\ddot{v} + v = -\epsilon\left\{r\dot{v} - 2q_2 v\cos 2\tau + \sum_{n=1}^{5} p_n v^n\right\}$ always has a solution with zero amplitude V_0, which is stable unless $q_2^2 > r^2 + p_1^2$, then it is unstable. At the condition when V_0 becomes unstable, the system represented by the above equation is self-excited and the equation has a solution of the form

$$v = V\sin(\tau + \Psi) + O(\epsilon),$$

where
$$\left.\begin{aligned} V^2 &= \frac{-3p_3 + \sqrt{9p_3^2 - 40p_5(p_1 - \sqrt{q_2^2 - r^2})}}{5p_5}, \\ \Psi &= \tan^{-1}\frac{q_2 + \sqrt{q_2^2 - r^2}}{r}; \end{aligned}\right\}$$

or
$$\left.\begin{aligned} V^2 &= \frac{-3p_3 - \sqrt{9p_3^2 - 40p_5(p_1 + \sqrt{q_2^2 - r^2})}}{5p_5}, \\ \Psi &= \tan^{-1}\frac{q_2 - \sqrt{q_2^2 - r^2}}{r}. \end{aligned}\right\}$$

The choice of the sets of V and Ψ depends upon the relations among the parameters (r , q_2, p_1 , p_3 , and p_5) of the equation. When a parameter is at first increased and then decreased, hysteresis may be expected, and is always accompanied by jumps.

Some further facts are obtained from Figs. 7, 8, and 9, as well as from Figs. 4, 5, and 6 in the previous example:

(a) When V_0 is unstable, for any set of fixed parameters the number of stable solutions is equal to that of unstable solutions.

(b) When V_0 is stable, the number of stable solutions is one more than that of unstable solutions.

(c) When V_0 is not changing, the solutions appear or disappear by pairs, one-half of them stable, the other half unstable.

(d) When V_0 is changing from stable to unstable, a stable solutions appears or an unstable disappears at the same moment; and vice versa.

2.2 Forced Oscillations.

As shown before, eq. (17) - which represents a general equation for forced oscillations - may have either an unstable or a stable solution when $\epsilon = o$, according as μ in eq. (21) is real or imaginary. When μ is real and the condition (21a) is satisfied, one can apply the same method of analysis as that for self-excitation (Section 2.1) except that the generating solution, instead of the expression in eq. (23), is

$$a_o \cos\tau + b_o \sin\tau + \int^{\tau} F(u) \sin(\tau - u)\, du .$$

In this way, the solution obtained is of constant amplitude and frequency, with period 2π.

When μ is imaginary, or $\mu = j\gamma$ with γ real, eq. (20) (the solution of Hill's equation) can be taken as the generating solution. In this case, while condition (21a) is unnecessary, we require instead: $\gamma << 1$. In this section we shall confine our attention to the case of $\mu = j\gamma$ with $\gamma << 1$, and to the particular problem corresponding to the circuit in Fig. 1, though the method is applicable to other similar systems. The main steps taken in this analysis are (1) assuming a form of solution sufficiently general to represent the final oscillations observed, thus (2) reducing the second order differential equation into two first order differential equations which are made soluble by taking advantage of the smallness of γ . The analysis

predicts oscillations with modulated amplitude and frequency.

For the circuit in Fig. 1, σ, $\Psi_1(\tau)$, $\Psi_2(\tau)$, $E(\tau)$, and $D(v,\dot{v})$ in eq. (15) take the forms: σ_1, $-\frac{1}{2}\epsilon q_1 \sin 2\tau$, $2\epsilon q_1 \cos 2\tau$, $\lambda_1 \cos 2\tau$, and $-(r_1 + r_2 v + r_3 v^2)\dot{v}$ respectively. Inserting these in eq. (15), then

$$\ddot{v} - \epsilon q_1 \sin 2\tau \dot{v} + \left[\sigma_1 - 2\epsilon q_1 \cos 2\tau\right] v = \lambda_1 \cos 2\tau - \epsilon\left[r_1 + r_2 v + r_3 v^2\right]\dot{v}.$$

With $v = x e^{\frac{1}{2}\epsilon q_1 \int^\tau \sin 2\tau\, d\tau} = x e^{\frac{1}{4} q_1 \epsilon \cos 2\tau}$, this becomes

$$\ddot{x} + \left[\sigma - 2q\,\Psi(\tau)\right] x = F(\tau) + \epsilon G(x,\dot{x}), \tag{60}$$

where $\sigma = \sigma_1 - \frac{1}{8}\epsilon^2 q_1^2$,

$$2q\,\Psi(\tau) = \epsilon q_1 \cos 2\tau - \tfrac{1}{8}\epsilon^2 q_1^2 \cos 4\tau,$$

$$F(\tau) = \lambda_1 \cos 2\tau\, e^{-\frac{1}{4} q_1 \epsilon \cos 2\tau},$$

and

$$G(x,\dot{x}) = -(r_1 + r_2 v + r_3 v^2)\,\dot{v}\, e^{-\frac{1}{4} q_1 \epsilon \cos 2\tau}.$$

The generating solution of eq. (60), given by eq. (20), can be expressed in a more convenient form for subsequent manipulation. Write (6):

$$\left.\begin{aligned} x_1(\tau) &= \sum_{l=-\infty}^{\infty} c_{2l+1} \cos(2l+1+\gamma)\tau, \\ x_2(\tau) &= \sum_{l=-\infty}^{\infty} c_{2l+1} \sin(2l+1+\gamma)\tau, \end{aligned}\right\} \tag{61}$$

and let their initial conditions be:

$$\left.\begin{aligned} x_1(0) &= \dot{x}_2(0) = 1, \\ \dot{x}_1(0) &= x_2(0) = 0. \end{aligned}\right\} \tag{61a}$$

The coefficients c_{2l+1} and γ are definite functions of σ and q in eq. (60). Substituting eq. (61) into eq. (20), gives

$$x = A \sum_{l=-\infty}^{\infty} c_{2l+1} \sin\left[(2l+1+\gamma)\tau + \theta\right] + \sum_{m=-\infty}^{\infty} c_{2m+1} c_{2n+1} \int^\tau F(u) \sin\left[2(m\tau - nu) + (l+\gamma)(\tau - u)\right] du, \tag{62}$$

where and

$$A = \sqrt{A_1^2 + A_2^2}, \tag{63}$$

$$\theta = \tan^{-1}\frac{A_1}{A_2}.$$

Differentiating eq. (62) with respect to τ gives:

$$\dot{x} = A \sum_{l} (2l+1+\gamma)\, c_{2l+1} \cos\left[(2l+1+\gamma)\tau+\theta\right] + \sum_{m,n} c_{2m+1}\, c_{2n+1}\, F(\tau) \sin 2(m-n)\tau + \sum_{m,n} (2m+1+\gamma)\, c_{2m+1}\, c_{2n+1} \int^{\tau} F(u) \cos\left[2(m\tau - nu) + (1+\gamma)(\tau-u)\right] du. \quad (64)$$

Eqs. (62) and (64) are thus the solution and its derivative of eq. (60) with $\epsilon = 0$.

Assume the solution and derivative of eq. (60) with $\epsilon \neq 0$ have the same forms as eq. (62) and (64) respectively, but with A and θ as functions of τ instead of arbitrary constants: now differentiating eq. (62) and comparing the result with eq. (64), we have

$$\dot{A} \sum_{l} c_{2l+1} \sin\left[(2l+1+\gamma)\tau+\theta\right] + A\dot{\theta} \sum_{l} c_{2l+1} \cos\left[(2l+1+\gamma)\tau+\theta\right] = 0. \quad (65)$$

Differentiating eq. (64) and substituting the result together with eq. (62) into eq. (60)yields

$$\dot{A} \sum_{l} (2l+1+\gamma)\, c_{2l+1} \cos\left[(2l+1+\gamma)\tau+\theta\right] - A\dot{\theta} \sum_{l} c_{2l+1} \sin\left[(2l+1+\gamma)\tau+\theta\right] = \epsilon\, G(x, \dot{x}), \quad (66)$$

where x and $\dot{x}$ in the right hand side of eq. (66) are to be replaced by eqs. (62) and (64) with A and θ as functions of τ . To simplify the problem, we introduce K_n $(n=1, 2, 3, 4)$ defined by

$$\left.\begin{aligned} K_1 &= \sum_{l} c_{2l+1} \sin\left[(2l+1+\gamma)\tau+\theta\right], \\ K_2 &= \sum_{l} c_{2l+1} \cos\left[(2l+1+\gamma)\tau+\theta\right], \\ K_3 &= \sum_{l} (2l+1+\gamma)\, c_{2l+1} \sin\left[(2l+1+\gamma)\tau+\theta\right], \\ \text{and} \quad K_4 &= \sum_{l} (2l+1+\gamma)\, c_{2l+1} \cos\left[(2l+1+\gamma)\tau+\theta\right]. \end{aligned}\right\} \quad (67)$$

Eqs. (65) and (66) then become

$$K_1 \dot{A} + K_2 A \dot{\theta} = 0,$$

and $$K_4 \dot{A} - K_3 A \dot{\theta} = \epsilon G.$$

Solving for $\dot{A}$ and $\dot{\theta}$, we obtain

$$\dot{A} = \frac{-1}{\Delta} \epsilon K_2 G,$$

$$\dot{\theta} = \frac{1}{\Delta A} \epsilon K_1 G,$$

where $$\Delta = \begin{vmatrix} K_1 & K_2 \\ K_4 & -K_3 \end{vmatrix} = -(K_1 K_3 + K_2 K_4).$$

From the initial conditions - eq. (61a) - it can easily be shown that for all τ[6]

$$\Delta = -[x_1 \dot{x}_2 - \dot{x}_1 x_2] = -1.$$

Thus the two simultaneous first-order differential, equations to be solved are:

$$\left.\begin{aligned} \dot{A} &= \epsilon K_2 G, \\ \text{and} \quad \dot{\theta} &= -\frac{1}{A} \epsilon K_1 G. \end{aligned}\right\} \quad (68)$$

It can be seen that both A and θ change with time slowly since ϵ is small. Thus their frequencies of variation (on the assumption that they possess periodic solutions, which we later show that they really have) is small compared to the smallest frequency in x as given by eq. (62).

Without actually carrying out substitutions of x and $\dot{x}$ in eq. (68), it can be seen that $K_1 G$ and $K_2 G$ contain only sinusoidal terms of the following four types of angular velocity:

(a) 0 (constant terms),

(b) $2n\gamma$ (with $n=1,2,3,\cdots$),

(c) $2m$ (with $m=1,2,3,\cdots$),

(d) $m\left[(2l-1)\pm(2n-1)\gamma\right]$ (with $l,m,n=1,2,3,\cdots$).

Since $\gamma<<1$, we now average eq. (68) over a time interval $T=2\pi$, which is about the largest period of terms of type (d) but is still very short compared with periods of terms of type (b). Thus we have

$$\left.\begin{aligned}\frac{1}{T}\int_{\tau}^{T+\tau}\dot{A}(\tau)\,d\tau &= -\frac{\epsilon}{T}\int_{\tau}^{T+\tau}K_2(\tau)\,G(\tau)\,d\tau,\\ \frac{1}{T}\int_{\tau}^{T+\tau}\dot{\theta}(\tau)\,d\tau &= \frac{-\epsilon}{T}\int_{\tau}^{T+\tau}\frac{1}{A(\tau)}K_1(\tau)\,G(\tau)\,d\tau.\end{aligned}\right\}\quad(69)$$

The left of eq. (69) reduce to $\dot{A}(\tau)$ and $\dot{\theta}(\tau)$ respectively, provided that small higher derivatives of A and θ are neglected. On the right side θ and A are considered as constants, and after the process of average, terms of type (a) remain unaffected, those of types (c) and (d) practically vanish, and those of type (b) survive almost unchanged during the time T short compared with their periods. It should be noted that our conclusions regarding terms of types (b) and (d) rest on the tacit assumption that

$$2n\gamma<<1 \qquad \text{and} \qquad m(2n-1)\gamma<<1 .$$

These are really the criteria of the present method. However, they are not so restrictive as they appear, because terms of large values of m and n only occur together with coefficients c_{2l+1} of large l in eq. (61), and these coefficients are usually very small compared with c_1 if q is not too large (6), say $q<1$. Thus only terms involving the first few

coefficients c_{2l+1} need be retained in the right-hand side of eq. (69), and the values of m and n are limited to small integers.

This done, eq. (69) may be reduced to:

$$\left.\begin{aligned}\dot{A}(\tau) &= \epsilon\left[s_0 + \sum_{n=1}^{N} s_{1n}\cos 2n(\gamma\tau+\theta) + \sum_{n=1}^{N} s_{2n}\sin 2n(\gamma\tau+\theta)\right],\\ \dot{\theta}(\tau) &= \frac{-\epsilon}{A}\left[\nu_0 + \sum_{n=1}^{N} \nu_{1n}\cos 2n(\gamma\tau+\theta) + \sum_{n=1}^{N} \nu_{2n}\sin 2n(\gamma\tau+\theta)\right],\end{aligned}\right\} \quad (70)$$

where the upper limit N of the summations is determined by the criterion $2n\gamma << 1$ which in turn is determined by the values of q and σ in eq. (60). The s and ν values are defined by:

$$\left.\begin{aligned}s_0 &= \frac{1}{T_0}\int_0^{T_0} K_2(\tau)\,G(\tau)\,d\tau,\\ s_{1n} &= \frac{1}{2T_0}\int_0^{T_0} K_2(\tau)\,G(\tau)\cos 2n(\gamma\tau+\theta)\,d\tau,\\ s_{2n} &= \frac{1}{2T_0}\int_0^{T_0} K_2(\tau)\,G(\tau)\sin 2n(\gamma\tau+\theta)\,d\tau,\\ \nu_0 &= \frac{1}{T_0}\int_0^{T_0} K_1(\tau)\,G(\tau)\,d\tau,\\ \nu_{1n} &= \frac{1}{2T_0}\int_0^{T_0} K_1(\tau)\,G(\tau)\cos 2n(\gamma\tau+\theta)\,d\tau,\\ \nu_{2n} &= \frac{1}{2T_0}\int_0^{T_0} K_1(\tau)\,G(\tau)\sin 2n(\gamma\tau+\theta)\,d\tau.\end{aligned}\right\} \quad (71)$$

It is understood that A and θ inside these integrals are temporarily regarded as constants, as the object of the integrations is to single out terms with particular frequencies. T_0 is the common period of all the frequencies concerned. (As γ can always, for practical purposes, be represented by a rational fraction $\frac{k_1}{k_2}$ in its lowest terms with $k_1 << k_2$, T_0 is therefore $2k_2\pi$).

Further discussion of the solutions of eq. (70) depends on the value of N and the forms of s and ν

as functions of A . We shall choose the simple case for which experimental observation has been made (section 3). In our experiment, q or ϵq_1 is small, of the order of ϵ . We thus have (6)

$$c_1 >> c_3 >> c_5 >> \cdots,$$

$$c_1 >> c_{-1} >> c_{-3} >> \cdots,$$

and $e^{-\frac{1}{4}\epsilon q_1 \cos 2\tau} \doteq 1$.

Hence it would be sufficient to take the terms in eqs. (62) and (64) involving c_1 only; and by the initial conditions (61a), $c_1 = 1$. Eqs. (62), (64) and (70), therefore become respectively

$$\left.\begin{aligned} x &= A\sin\left[(1+\gamma)\tau + \theta\right] - \tfrac{1+\gamma}{3}\lambda_1 \cos 2\tau, \\ \dot{x} &= A(1+\gamma)\cos\left[(1+\gamma)\tau + \theta\right] + \tfrac{2}{3}\lambda_1(1+\gamma)\sin 2\tau, \end{aligned}\right\} \quad (72)$$

$$\left.\begin{aligned} \dot{A}(\tau) &= \epsilon\left[s_0 + s_{11}\cos 2(\gamma\tau+\theta) + s_{21}\sin 2(\gamma\tau+\theta)\right], \\ \dot{\theta}(\tau) &= \frac{-\epsilon}{A}\left[\nu_0 + \nu_{11}\cos 2(\gamma\tau+\theta) + \nu_{21}\sin 2(\gamma\tau+\theta)\right], \end{aligned}\right\} \quad (73)$$

where

$$\left.\begin{aligned} s_0 &= -\tfrac{1}{2}A\left[r_1 + \tfrac{1}{2}r_3 w_1^2 + \tfrac{1}{4}r_3 A^2\right], \\ s_{11} &= \tfrac{1}{4}r_2 w_1, \\ s_{21} &= \nu_0 = \nu_{11} = 0, \\ \nu_{21} &= \tfrac{1}{4}r_2 w_1 A, \\ w_1 &= -\tfrac{1}{3}\lambda_1, \end{aligned}\right\} \quad (74)$$

and terms of the order of γ have been omitted from eqs. (74).

Our task now is to show that A and $\dot{\theta}$ in eq. (72), which can be solved from eq. (73), are periodic. Putting $\Phi = \gamma\tau + \theta$ = the total phase, and $w = -\frac{1}{4}\epsilon r_2 w_1$, the second of eqs. (73) becomes

$$\dot{\Phi} = \gamma + w\sin 2\Phi. \quad (75)$$

There are two different solutions of eq. (75) corresponding to $\gamma^2 > \text{or} < w^2$. Only one will give periodic results. This solution, with $\gamma^2 > w^2$, is:

$$\Phi = \tan^{-1}\frac{1}{\gamma}\left[\sqrt{\gamma^2-w^2}\,\tan\sqrt{\gamma^2-w^2}\,\tau - w\right]. \tag{76}$$

Therefore the angular velocity $\dot{\Phi}$ is

$$\dot{\Phi} = \gamma + \frac{2w\tan\Phi}{1+\tan^2\Phi}$$

$$= \gamma\left[1 + \frac{w\gamma_1\sin 2\gamma_1\tau - 2w^2\cos^2\gamma_1\tau}{\gamma^2\cos^2\gamma_1\tau + (\gamma_1\sin\gamma_1\tau - w\cos\gamma_1\tau)^2}\right], \tag{77}$$

where $\gamma_1 = \sqrt{\gamma^2-w^2}$. Eq. (77) shows that $\dot{\Phi}$ consists of two terms: a constant term and an oscillating term of frequency $\frac{\gamma_1}{\pi}$. The denominator of the second term is always positive, hence finite amplitide of the frequency-oscillation is assured. To show the periodic nature of $\dot{\Phi}(\tau)$, a reasonable set of constants has been assumed ($\gamma = 10^{-4}$, $w = 10^{-5}$), and a plot of $\frac{1}{\gamma}\dot{\Phi}(\tau)$ versus $\gamma_1\tau$ is given in Fig. 10.

Returning to the first of eq. (73), we have now

$$\dot{A} = (w_0 - w\cos 2\Phi)A - w_3 A^3, \tag{78}$$

$$\left.\begin{aligned}\text{where}\quad & w_0 = -\tfrac{1}{2}\epsilon\left(r_1 + \tfrac{1}{2}r_3 w_1^2\right),\\ \text{and}\quad & w_3 = \frac{1}{8}\epsilon r_3 .\end{aligned}\right\} \tag{79}$$

Eq. (78) is of Bernoulli's type, with Φ as known function of τ given by eq. (76). Its solution is

$$\frac{1}{A^2(\tau)} = \frac{\dot{\Phi}(\tau)}{\gamma A^2(0)}\,e^{-2w_0\tau} + 2w_3 e^{-2iw_0\tau}\dot{\Phi}(\tau)\int^{\tau}\frac{1}{\dot{\Phi}(t)}\,e^{2w_0 t}\,dt . \tag{80}$$

The first term on the right side of eq. (80) dies out

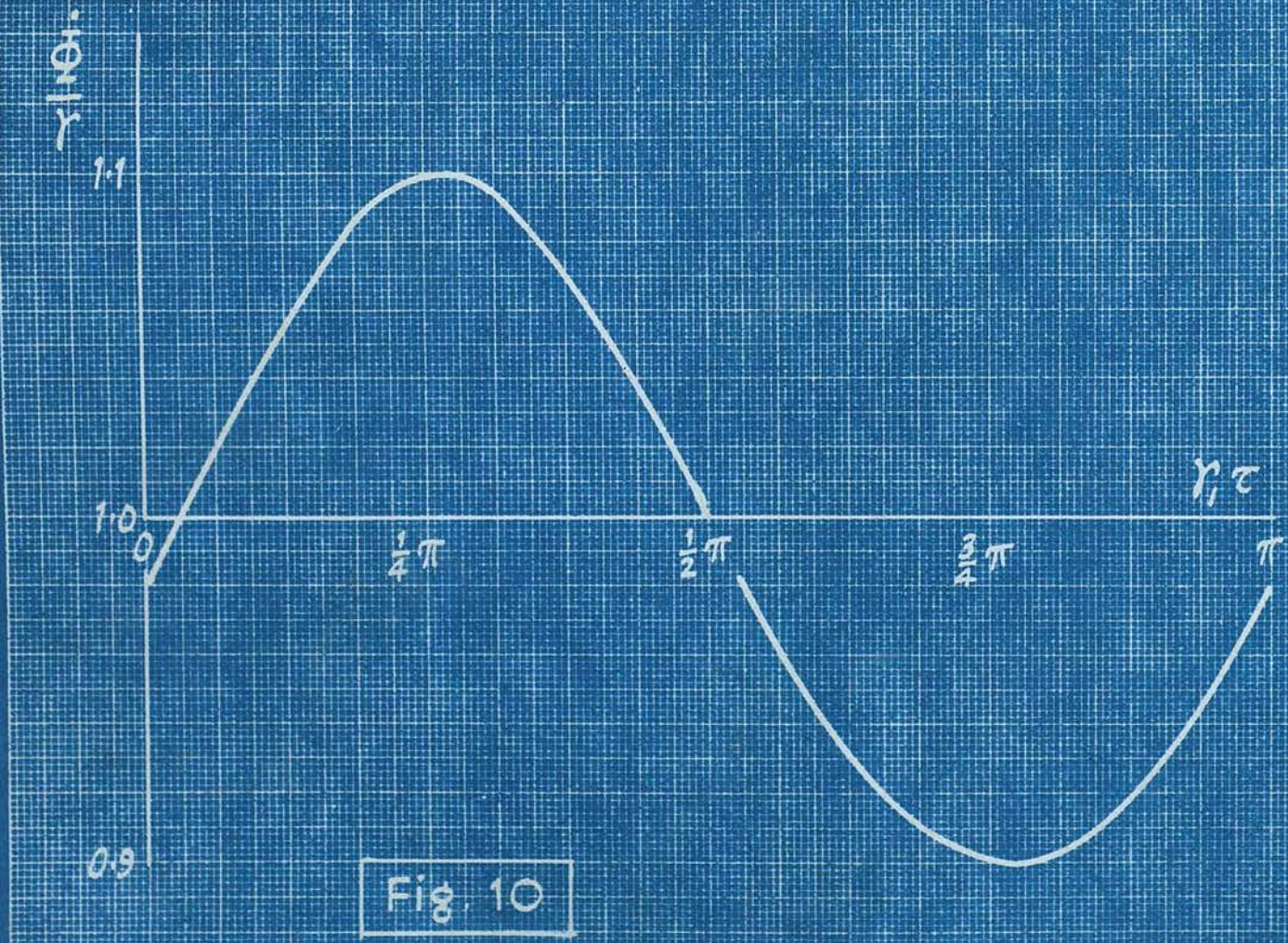
$\frac{\dot{\Phi}}{\gamma}$
1·1
1·0
0·9
0
$\frac{1}{4}\pi$
$\frac{1}{2}\pi$
$\frac{3}{4}\pi$
π
$\gamma_1 \tau$

Fig. 10

for τ large if $w_0 > 0$ (which needs $r_1 < \frac{1}{2} r_3 w_1^2$), and the second term is periodic. Without carrying out the exact evaluation of the integral in the second term which is rather complicated, its essential qualitative feature can be discussed. Since $\gamma^2 > w^2$ in eq. (75), $\dot{\Phi}$ cannot change its sign for all values of t, hence the integrand in eq. (80) has no singularity. Then the factor $\frac{1}{\dot{\Phi}}$, being a periodic function with period $\frac{\pi}{\gamma_1}$, can be expanded into a Fourier series. For each of the typical terms containing $\sin pt$ or $\cos pt$ ($p = 2n\gamma_1$) in the Fourier series, we have

$$e^{-2w_0\tau}\int^{\tau} e^{2w_0 t}\sin pt\,dt = \frac{1}{4w_0^2+p^2}\left(2w_0\sin p\tau - p\cos p\tau\right),$$

and $$e^{-2w_0\tau}\int^{\tau} e^{2w_0 t}\cos pt\,dt = \frac{1}{4w_0^2+p^2}\left(2w_0\cos p\tau + p\sin p\tau\right), \quad p = 2n\gamma_1, \quad n = 1, 2, \cdots.$$

Thus the right side of eq. (80) is periodic of period $\frac{\pi}{\gamma_1}$, with a dominant positive constant term since $\gamma^2 > w^2$. It follows then that A is also periodic with the same period $\frac{\pi}{\gamma_1}$. For a specific set of values of w_0, w, w_3, and γ, the solution of $A(\tau)$ will be given later in Part II, where a graphical method is used. An interesting aspect of the graphical solution is that the maximum of amplitude occurs almost concurrently with the minimum of frequency and vice versa, in accordance with experimental observations. It also turns out that in the final solution as given by the first of eq. (72), the first term by far predominates, the ratio of the amplitude of the

second term to that of the first term is of the order of ϵ . Hence the solution obtained here agrees with experimental observations in all qualitative feature.

3. EXPERIMENTAL ARRANGEMENTS AND RESULTS.

Here, the experimental data from the circuits in Figs. 1 and 3, and the results of numerical calculation followed from Section 2, are given. The details of the circuits in Figs. 1 and 3 are shown in Figs. 11 and 12 respectively. V1 and V2 in Fig. 11 are EF50 valves with the practically identical characteristics shown in Figs. 12 and 13 corresponding to the curves of the anode current I_a against the grid bias E_g and the suppressor grid bias E_s respectively. The alternating voltages applied to the two suppressor grids, are applied in phase-opposition by an audio-frequency oscillator through a transformer with a centre-tap connected with potentiometers R_{s1} and R_{s2}. The magnitude and frequency of the voltages are variable. The control grid of V1 is connected to an inductance L' coupled to a second inductance L in series with a variable resistor. R is the sum of the variable resistance and the resistance of L. L and C form a tank circuit. L_f, a choke coil with high inductance, and C_f, a variable condenser, form a resonant filter to exclude a.c. components from the d.c. supply. For each setting the filter is tuned until the amplitude of the oscillations, seen on the screen of an oscilloscope connected across the control grids, is a maximum. C_{b1} and C_{b2} are blocking condensers. The screen grid is operated with the same voltage E_a as

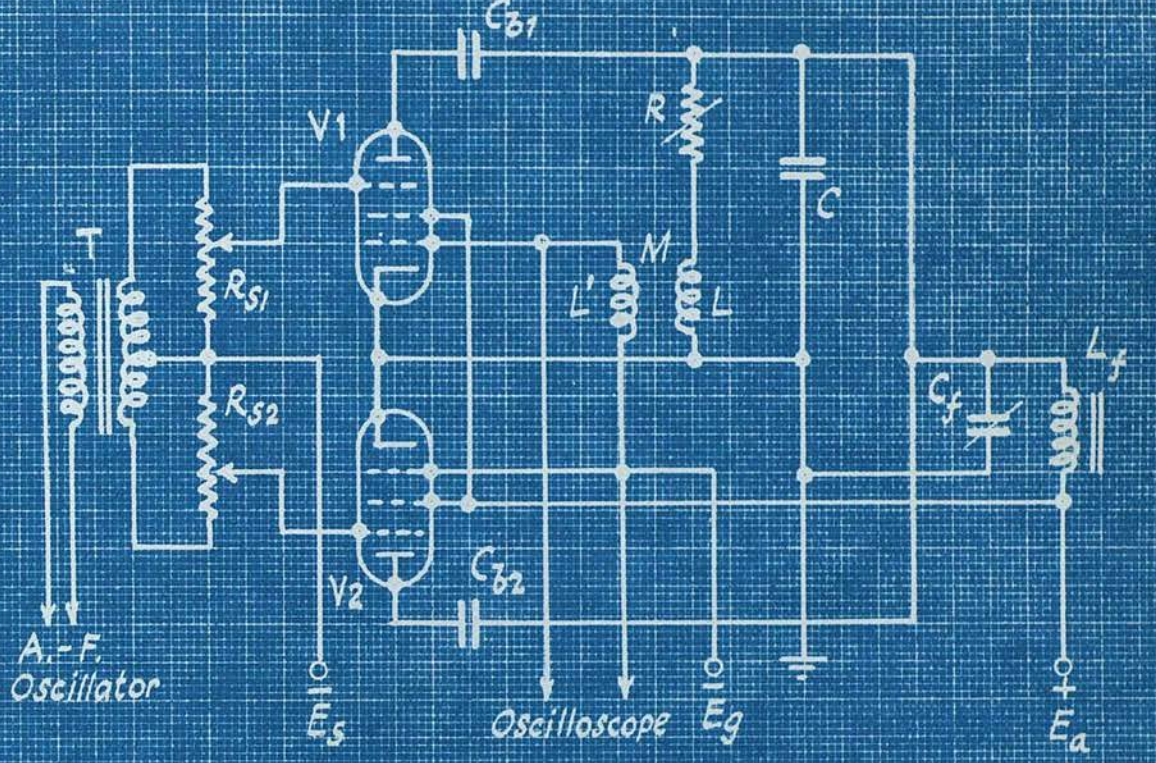
C_{b1}
V1
R
C
T
R_{S1}
M
L'
L
L_f
C_f
R_{S2}
V2
C_{b2}
A.-F. Oscillator
E_s
Oscilloscope
E_g
E_a

Fig. 11

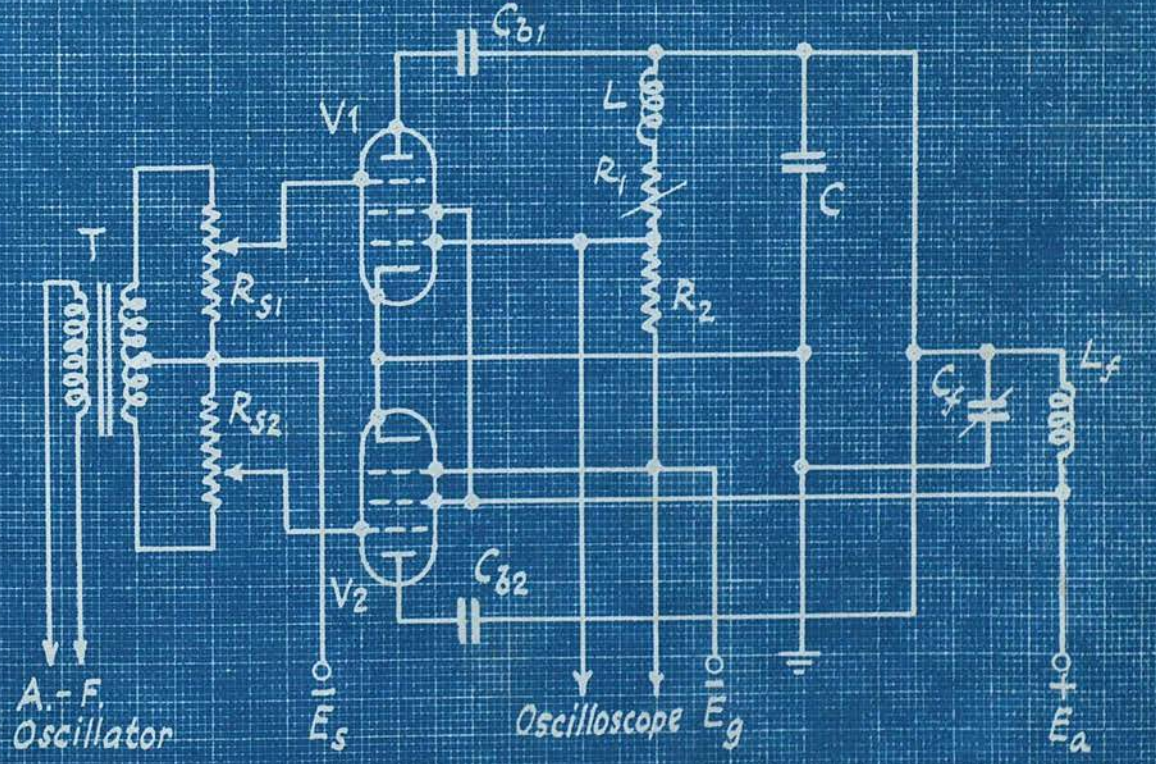
C_{b1}
V1
L
R_1
C
T
R_{S1}
R_2
L_f
C_f
R_{S2}
V2
C_{b2}
A.-F. Oscillator
E_s
Oscilloscope
E_g
E_a

Fig. 12

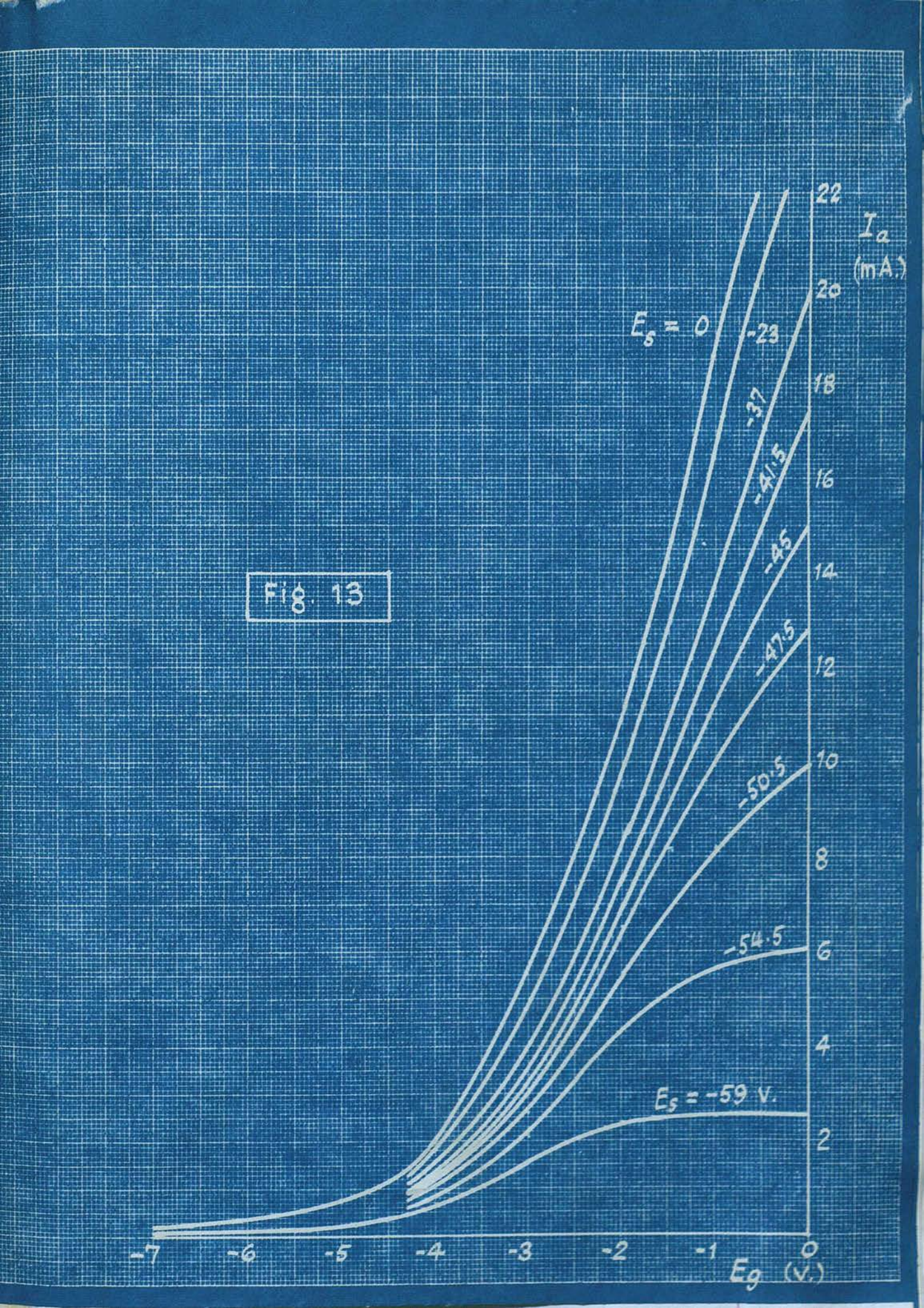
Fig. 13
I_a (mA.)
22
20
18
16
14
12
10
8
6
4
2
$E_s = 0$
-23
-37
-41.5
-45
-47.5
-50.5
-54.5
$E_s = -59$ V.
-7
-6
-5
-4
-3
-2
-1
0
E_g (V.)

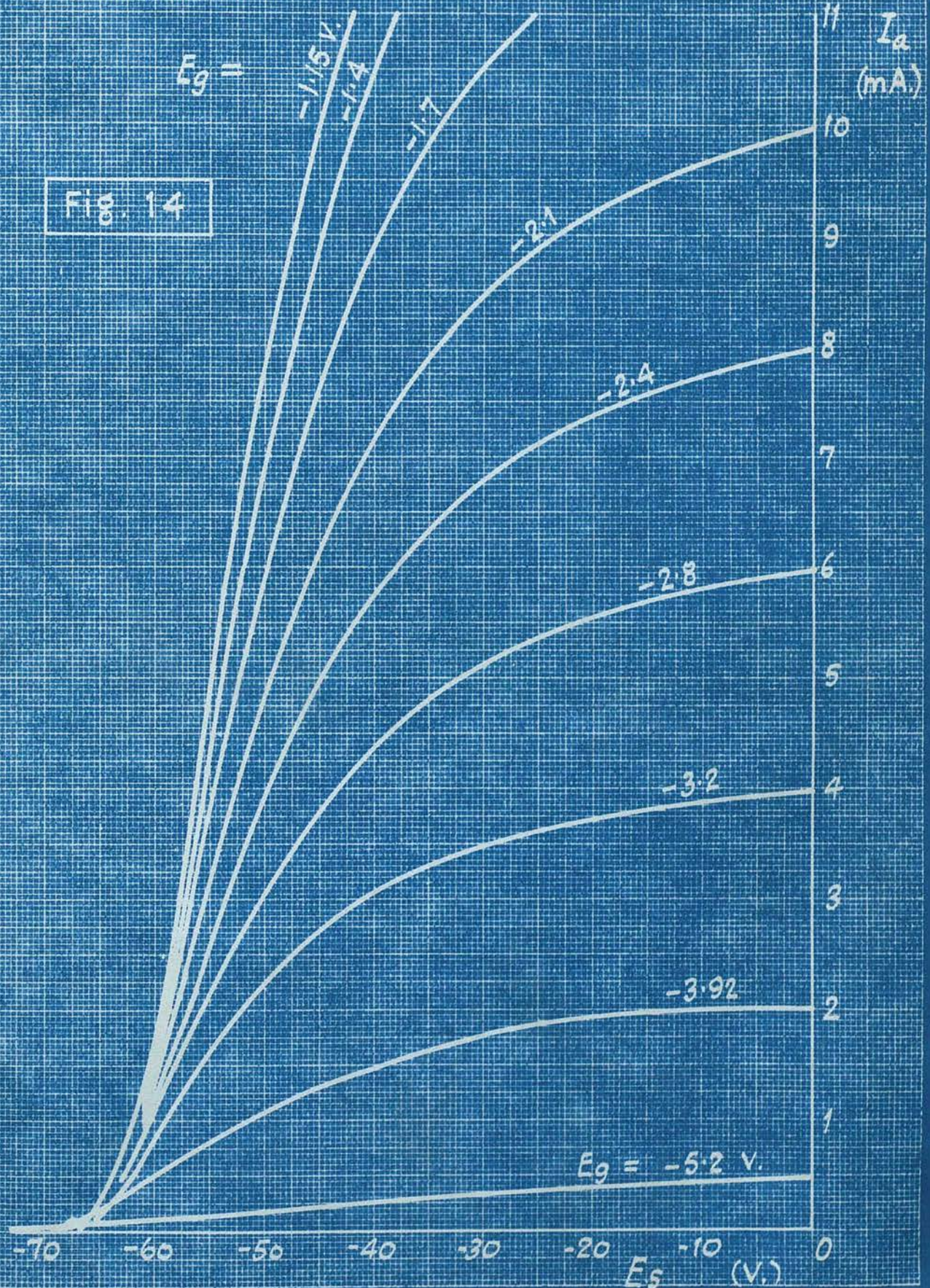
Eg =
-1.6 V.
-1.8
-2.1
-2.4
-2.8
-3.2
-3.92
Eg = -5.2 V.
Ia (mA.)
11
10
9
8
7
6
5
4
3
2
1
0
-70
-60
-50
-40
-30
-20
-10
Es (V.)

Fig. 14

the anode. The negative terminal of E_a and the positive terminals of E_s and E_g are all earthed.

The circuit in Fig. 12 is the same as that in Fig. 11 except that L' is replaced by a resistance R_2, and the branch $L-R$, instead of being connected to earth, is connected to the control grid of $V1$. R_1 in Fig. 12 represents the same quantity as R in Fig. 11.

Let λ_{01} and λ_{02} denote the amplitudes of the voltages across the suppressor grids, f_2 the frequency of the oscillator, and f_1 the natural frequency of the circuit. With the parameters adjusted to suitable values, and f_2 varied, the following effects are observed for both circuits in Figs. 11 and 12:

(a) <u>With $\lambda_{01} = \lambda_{02} = \lambda_0$, λ_0 being a sufficient large value</u>.

When f_2 is not very near $2f_1$, there is practically no oscillation on the screen of the oscilloscope. When f_2 approaches $2f_1$, sinusoidal oscillations at the frequency exactly $\frac{1}{2}f_2$ appear. The amplitude of oscillations in the circuit of Fig. 11 is a maximum when $f_2 = 2f_1$, and decreases gradually to zero as f_2 is shifted away from $2f_1$. In the circuit of Fig. 12, the amplitude does not reach a maximum when $f_2 = 2f_1$, and may be different for the same value of f_2 according as this particular value is approached from a higher or a lower frequency; and oscillations with considerable amplitude may appear or disappear suddenly.

(b) With $\lambda_{01} = \lambda_0$, $\lambda_{02} = 0$. When $f_2 \doteq 2f_1$, the oscillations are similar to those in case (a). When f_2 is not near $2f_1$, there are oscillations with frequency f_2 and with very small amplitude. When f_2 is adjusted at a value between those of the above two cases, i.e., neither too near nor too far from $2f_1$, oscillations are observed with amplitude and frequency both modulated. The modulation of the amplitude and the frequency are simultaneous, and are very small. When the amplitude is a maximum, the frequency is minimum, and vice versa. The minimum frequency is about $\frac{1}{2} f_2$. The maximum frequency varies with different operating conditions, and the greatest of maximum frequency observed is f_2. A typical wave form of this kind is shown in Fig. 15.

In the following some quantitative results of self-excitation (i.e. $\lambda_{01} = \lambda_{02} = \lambda_0$) are given. For the circuit of Fig. 11, the operating conditions are:

$E_a = 300$ V, $E_s = -47.5$ V, $E_g = -2.4$ V,

$L = 215$ mH $C = 0.0007$ μF, $M = -0.7$ mH;

then $f_1 = \frac{1}{2\pi\sqrt{LC}} = 4100$ c/s. Values of the amplitude V of v, the voltage across L', against various quantities are measured:

(a) $\lambda_0 = 6$ V, $f_2 = 8200$ c/s, R varied;

(b) $R = 363\Omega$, $f_2 = 8200$ c/s, λ_0 varied;

(c) $R = 363\Omega$, $\lambda_0 = 8$ V, f_2 varied.

For the circuit of Fig. 12, the working conditions are:

$E_a = 300$ V, $E_s = -47.5$ V, $E_g = -2.4$ V,

$L = 89$ mH, $C = 0.01$ μF, $R_2 = 300\Omega$.

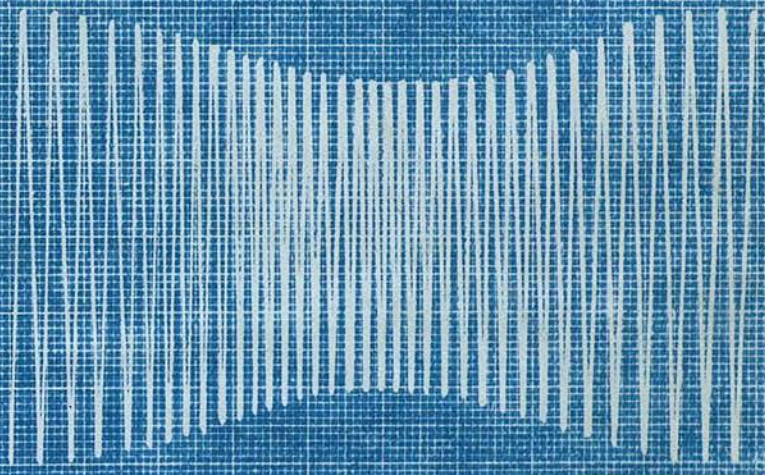

Fig. 15

The following measurements of the amplitude V of v, the voltage across R_2, against other parameters are made:

(d) $f_2 = 15300$ c/s, $\lambda_0 = 20.6$ V, R_1 varied;

(e) $f_2 = 13900$ c/s, $\lambda_0 = 16.8$ V, R_1 varied;

(f) $f_2 = 15300$ c/s, $R_1 = 33.3\,\Omega$, λ_0 varied;

(g) $f_2 = 13900$ c/s, $R_1 = 33.3\,\Omega$, λ_0 varied;

(h) $\lambda_0 = 14.7$ V, $R_1 = 33.3\,\Omega$, f_2 varied.

The measured results of cases (a) - (h) are shown by the full lines in Figs. 16-23, respectively.

The dotted lines in Figs. 16-23 are calculated from the results of the mathematical analysis in Section 2.1. The process of numerical calculation will be given in the following. The zeroth-order solution of eq. (11) for the circuit of Fig. 11, as shown before, is eq. (54). Write $p = \frac{1}{\epsilon}(\sigma_1 - 1) = \frac{1}{\epsilon}\left(\frac{1}{LCw^2} - 1\right)$, $q_1 = \frac{n_1 \lambda_0 M}{2\epsilon LCw}$, $w = \pi f_2$, and from the definitions of r_1 and r_3 given by eq. (10), eq. (54) becomes

$$V^2 = \frac{4}{3l_3 M}\left[-(RC + Ml_1) + \sqrt{\left(\frac{n_1\lambda_0 M}{2}\right)^2 - \left(\frac{1}{\pi f_2} - \pi LC f_2\right)^2}\right]. \quad (81)$$

Similarly, for the circuit of Fig. 12, putting $p_1 = \frac{1}{\epsilon}(\sigma_2 - 1)$, $w = \pi f_2$, and inserting eq. (13) into eq. (59), gives the equation for calculating the amplitude of the voltage across R_2:

$$V^2 = \frac{1}{5l_5}\left\{-3l_3 \pm \sqrt{9l_3^2 - 40l_5\left(l_1 + \frac{1}{R_2} - \frac{LC\pi^2 f_2^2}{R_2} \mp \sqrt{\left(\frac{n_1\lambda_0}{2}\right)^2 - \left[\pi f_2 C\left(1 + \frac{R_1}{R_2}\right)\right]^2}\right)}\right\}. \quad (82)$$

In eqs. (81) and (82), l_1, l_3, l_5, and n_1, are to be determined. First, l_1, l_3, and l_5 are found

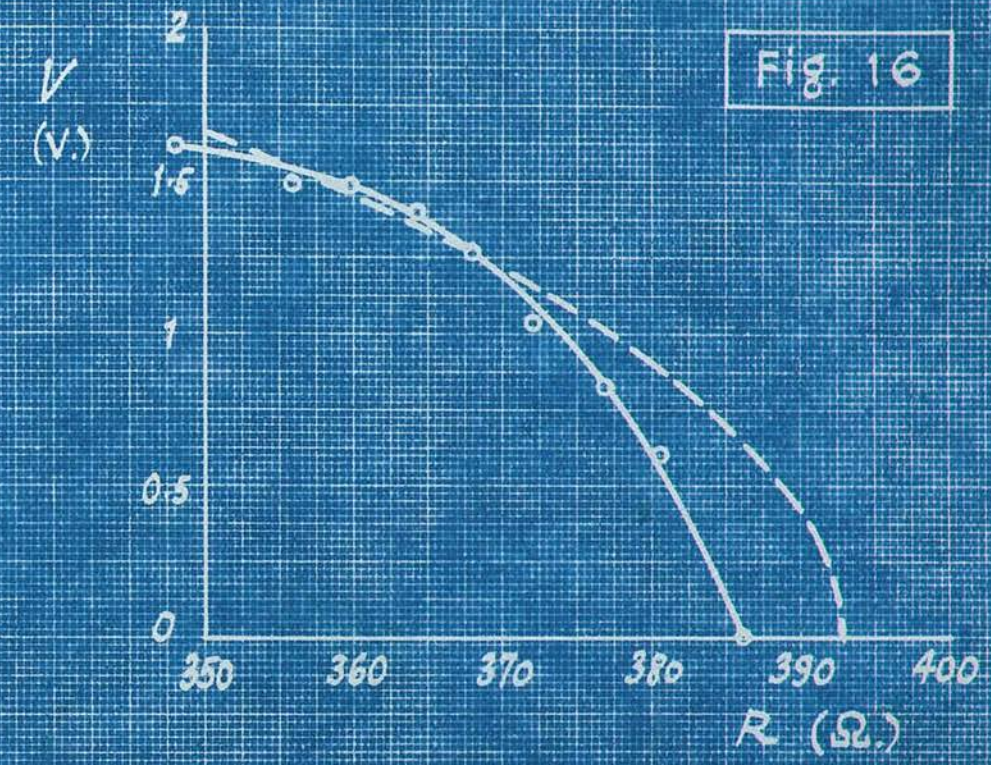

Fig. 16

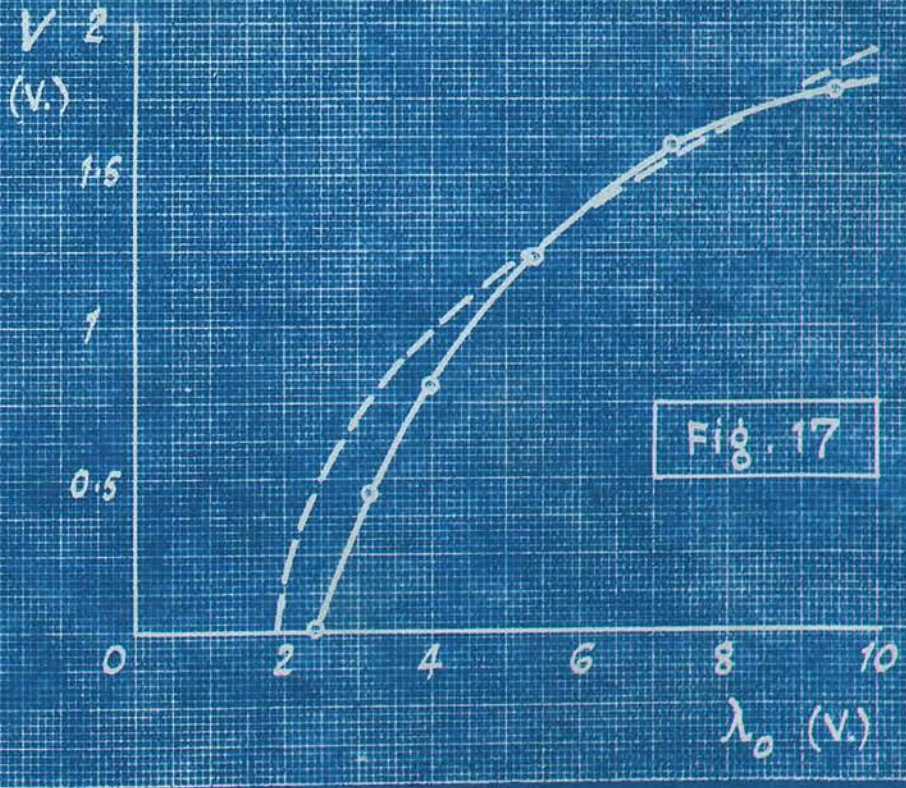

Fig. 17

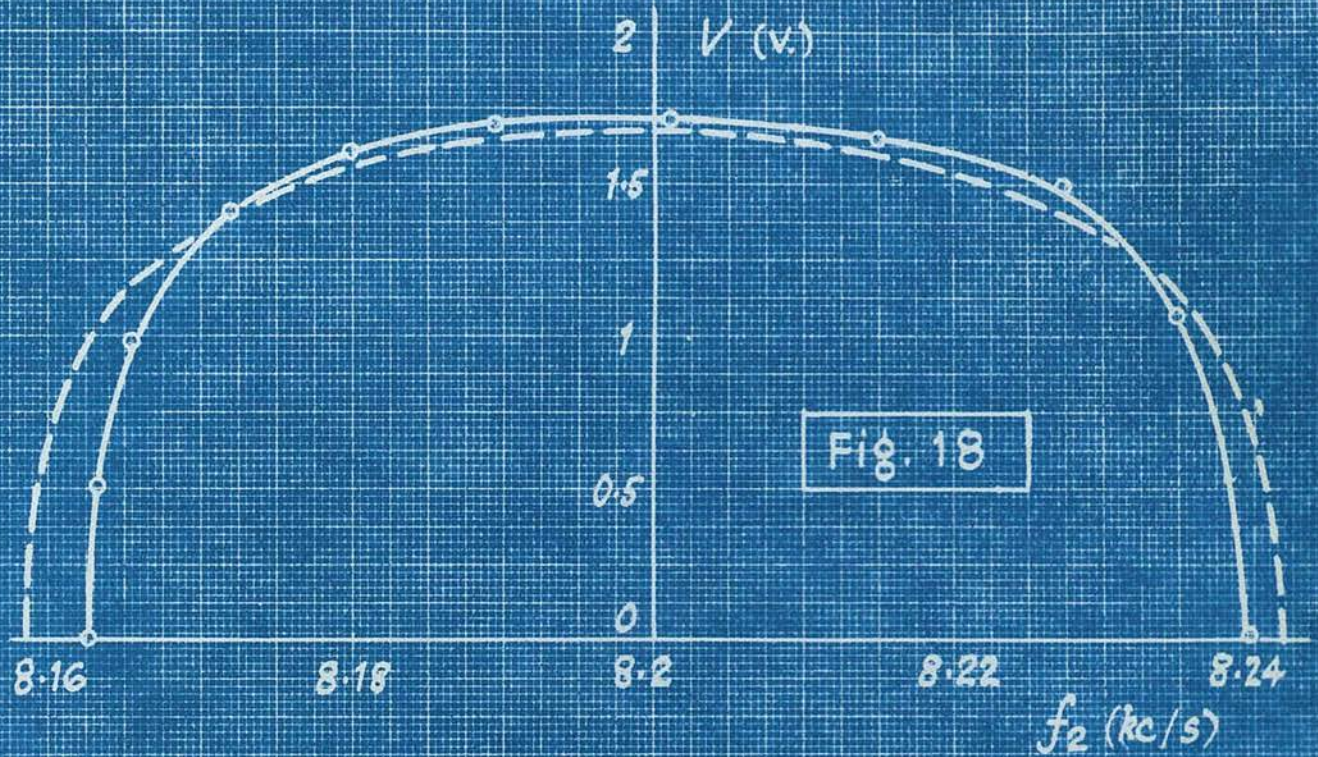

Fig. 18

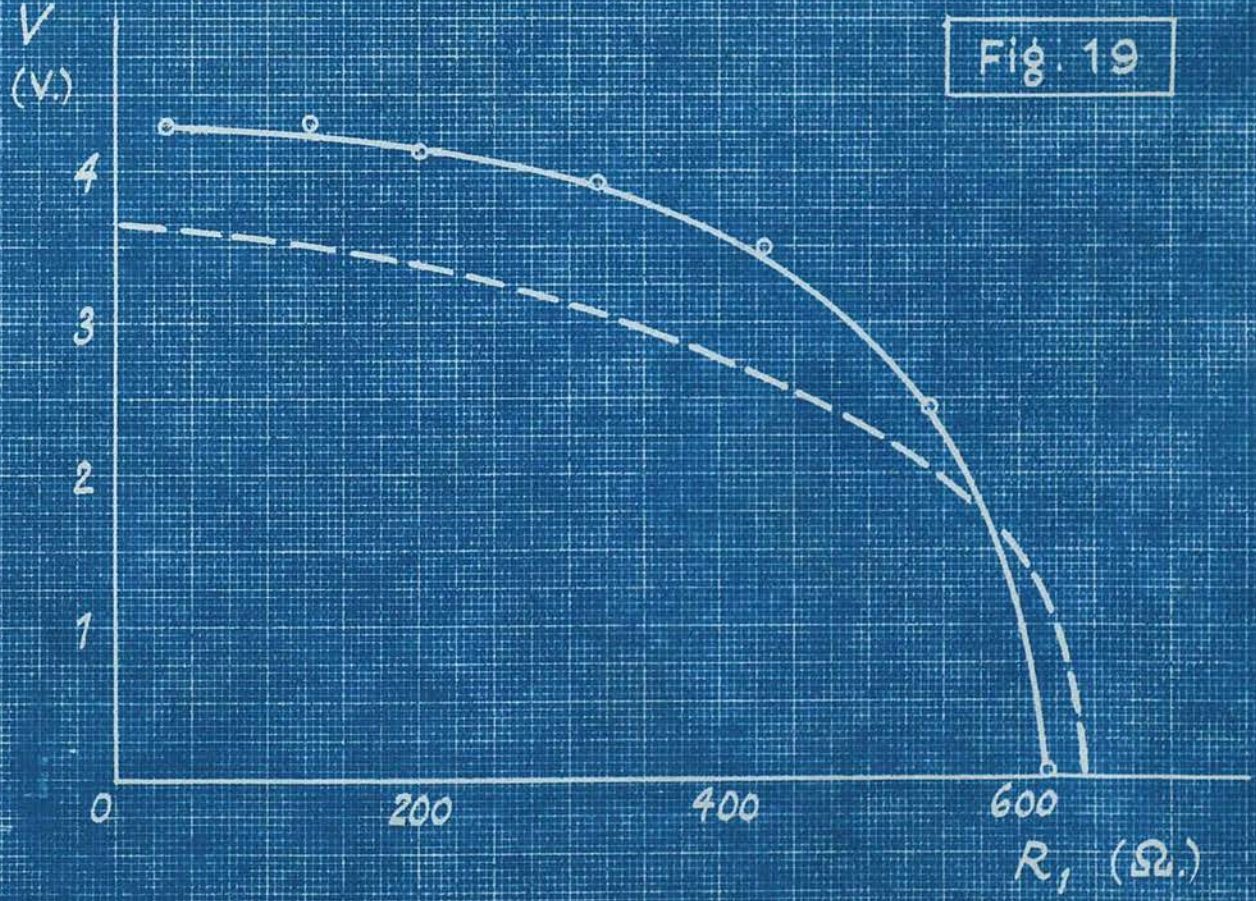

Fig. 19

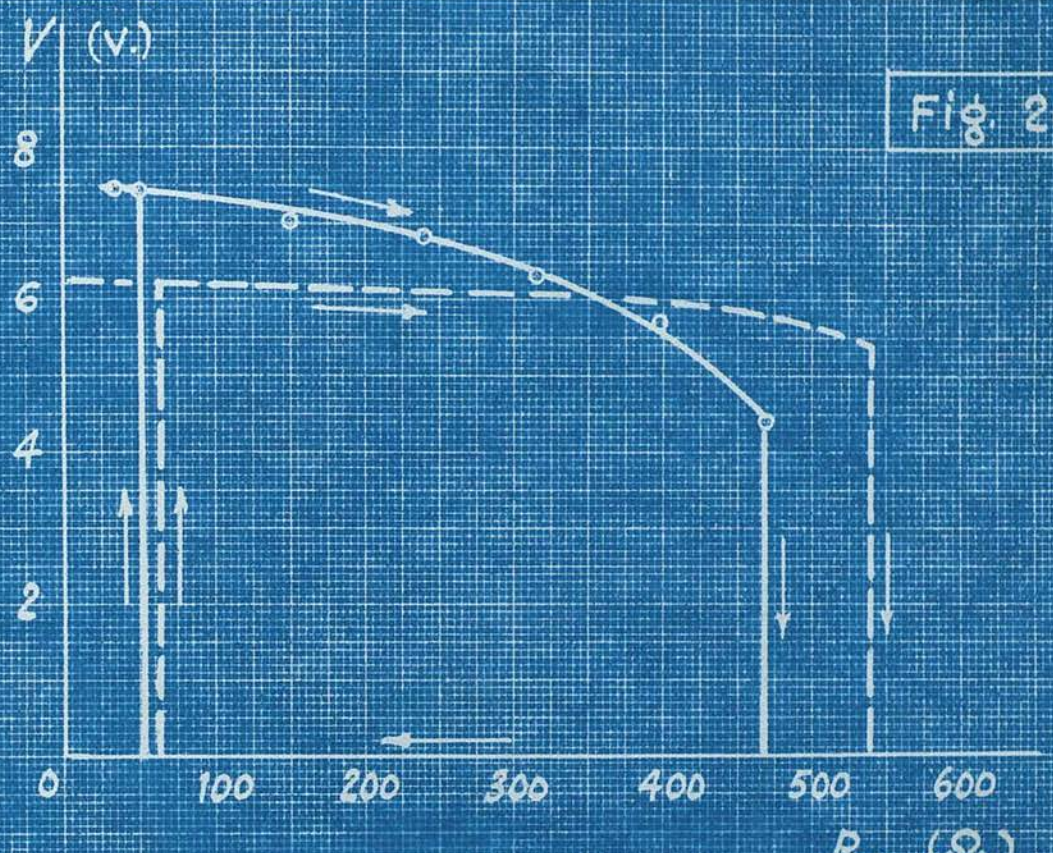

Fig. 20

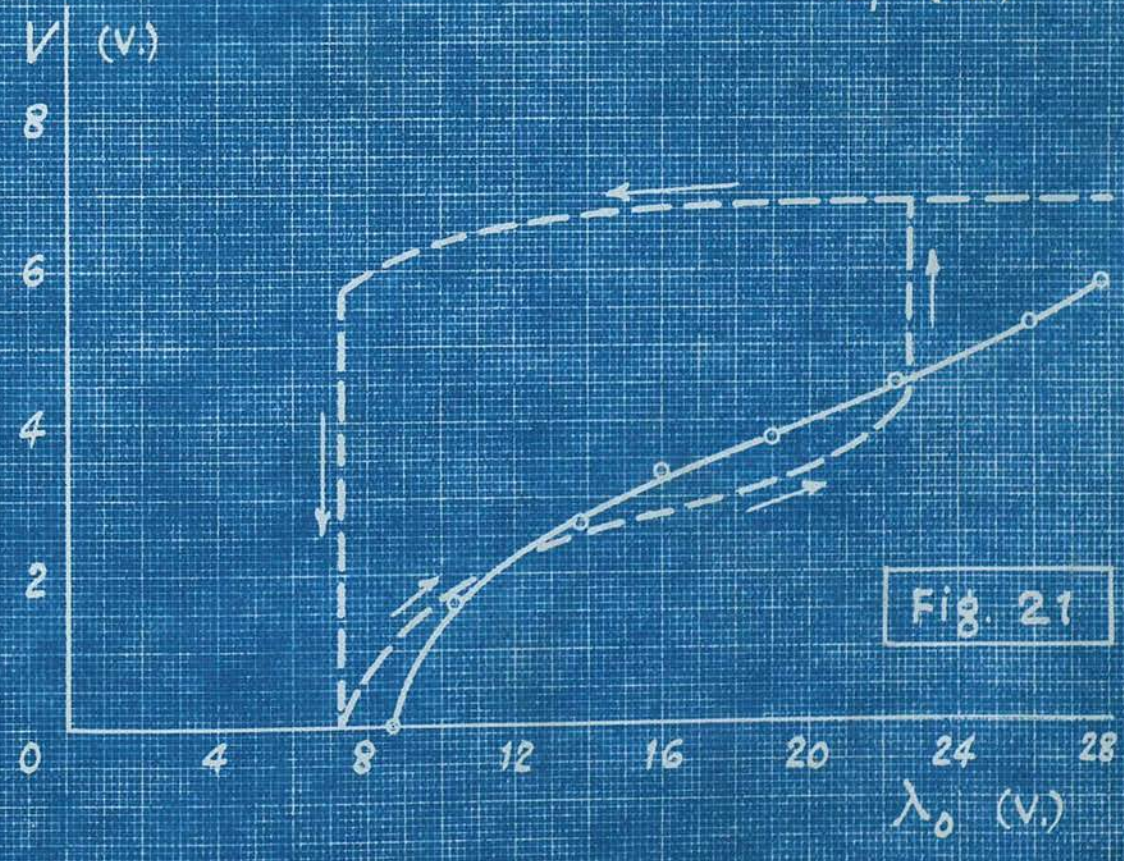

Fig. 21

Fig. 22

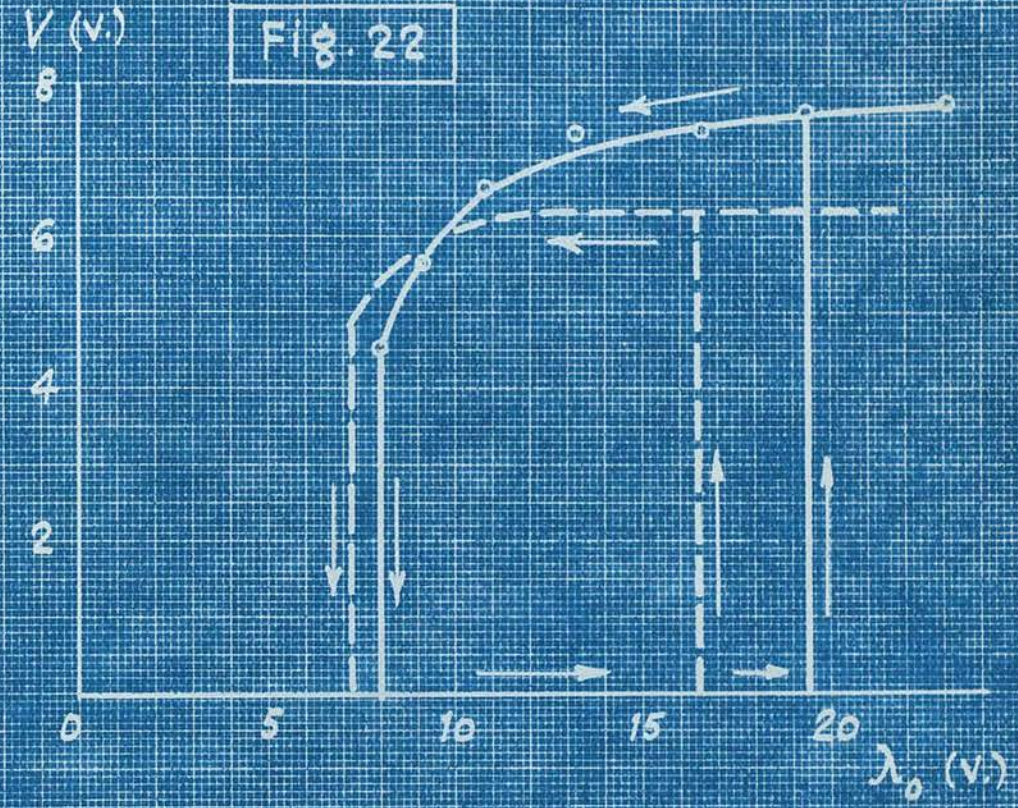

Fig. 23

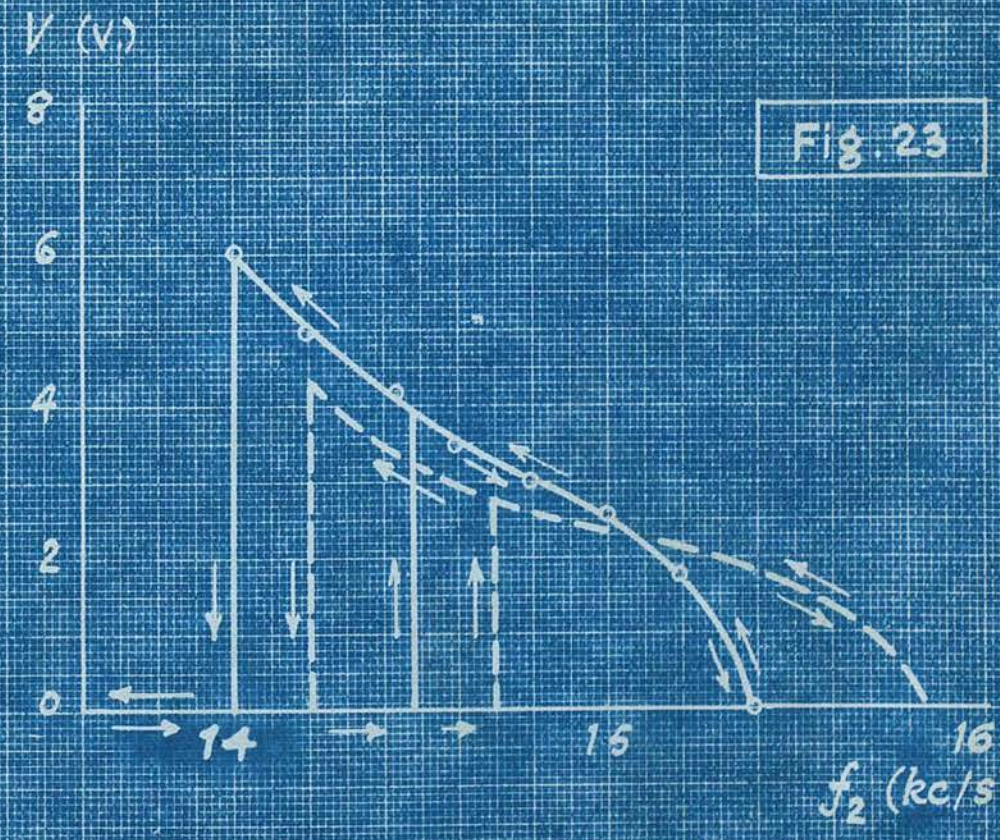

from the curve $E_s = -47.5\,V$ in Fig. 13. The point ($E_g = -2.4\,V$, $E_s = -47.5\,V$) is taken as the origin, and the curve is approximated by a polynomial of the form $I_a = \sum_{n=1}^{5} l_n E_g^n$.

The values of the l_s' found are:

$$l_1 = 3.49 \times 10^{-3},$$

$$l_2 = 0.386 \times 10^{-3},$$

$$l_3 = -0.212 \times 10^{-3},$$

$$l_4 = -0.0154 \times 10^{-3},$$

and $$l_5 = 0.0067 \times 10^{-3}.$$

The I_a/E_g curve represented by the polynomial with these values of l_s' together with points obtained from actual measurement are plotted in Fig.24. Next n_1 is determined from families of characteristic curves of I_a/E_g and I_a/E_s . The slopes of I_a/E_s curves at $E_s = -47.5\,V$ against E_g are plotted in Fig. 25(a), and the slope of the curve in Fig. 25(a) at $E_g = -2.4\,V$ is $0.148\ mA/V^2$. The slopes of I_a/E_g curves at $E_g = -2.4\,V$ against E_s are plotted in Fig. 25(b): the slope of the curve in Fig. 25(b) at $E_s = -47.5\,V$ is $0.144\ mA/V^2$. Then

$$n_1 = \tfrac{1}{2}(0.148 + 0.144) \times 10^{-3} = 0.146 \times 10^{-3}\ A/V^2.$$

All the quantities on the right of eqs. (81) and (82) are given and fixed, and values of V against varying R, λ_0 or f_2 can be calculated.

As an example of numerical calculation, we shall calculate one point in the case of Fig. 16. Here

Fig. 24

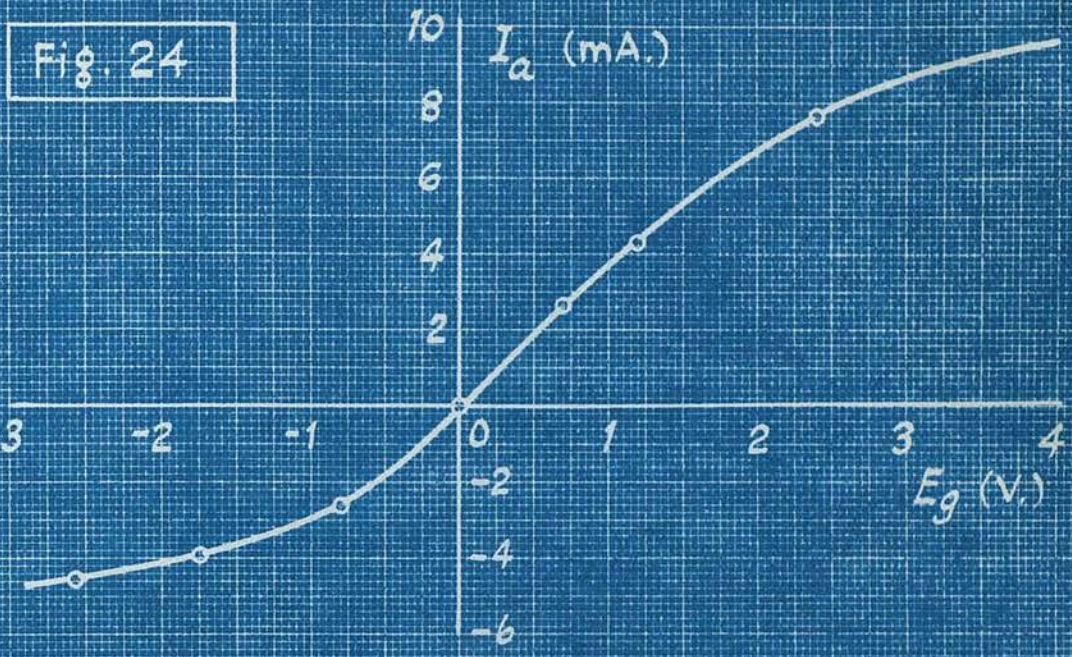

Fig. 25 a

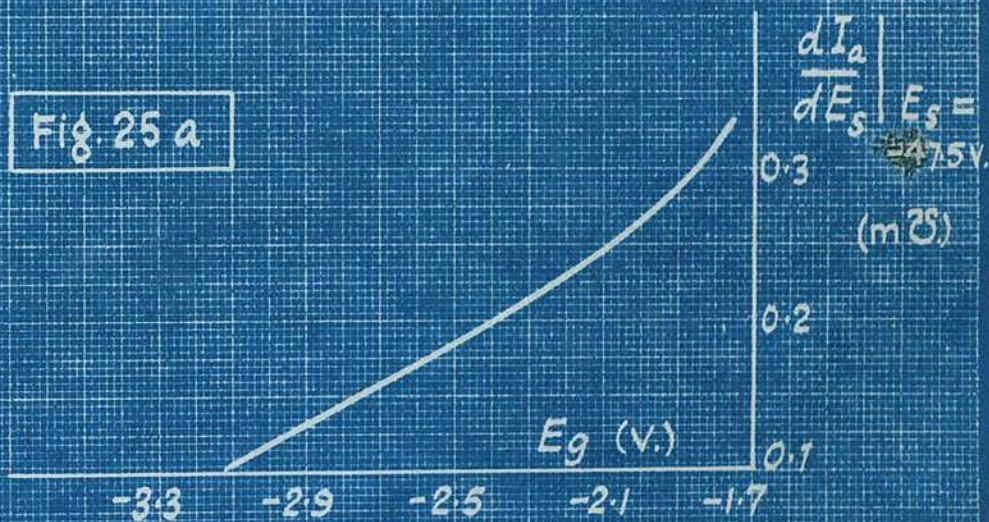

Fig. 25 b

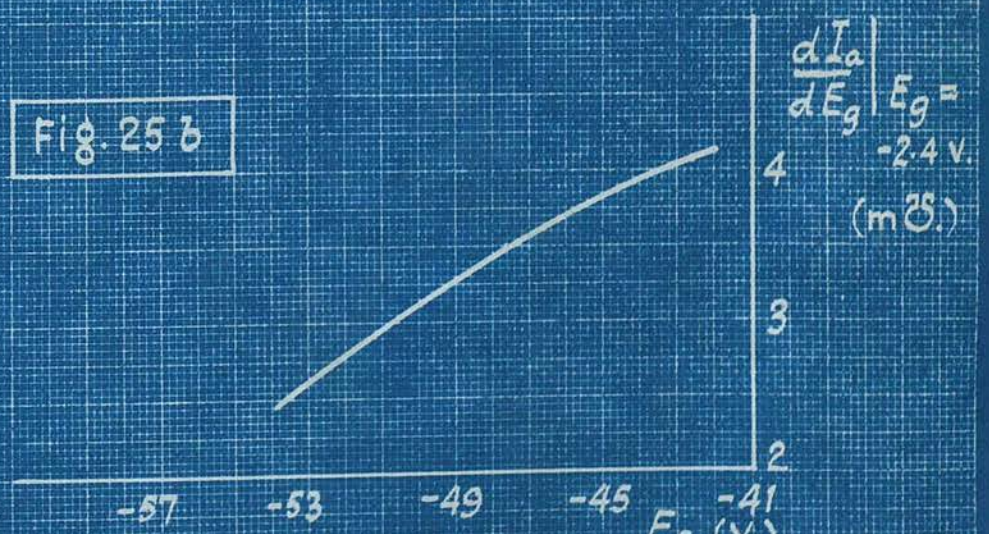

$$n_1 = 0.146 \times 10^{-3}\ A/V^2,$$

$$l_1 = 3.49 \times 10^{-3}\ A/V,$$

$$l_3 = -0.212 \times 10^{-3}\ A/V^3,$$

$$M = -0.7 \times 10^{-3}\ H,$$

$$C = 0.007 \times 10^{-6}\ F,$$

$$\lambda_0 = 6.0\ V,$$

$$L = 215 \times 10^{-3}\ H,$$

$$f_2 = 8200\ c/s,$$

and let $R = 380\Omega$.

Putting these values into eq. (81), we have

$$V = \left\{ \frac{4}{3\times(-.212\times10^{-3})\times(-0.7\times10^{-3})} \left(-(380\times0.007\times10^{-6} - 0.7\times10^{-3}\times3.49\times10^{-3}) + \left[\left(\frac{0.146\times10^{-3}\times6\times0.7\times10^{-3}}{2} \right)^2 - \left(\frac{1}{\pi\times8200} - \pi\times215\times10^{-3}\times0.007\times10^{-6}\times8200 \right)^2 \right]^{\frac{1}{2}} \right) \right\}^{\frac{1}{2}}$$

$$= 0.9\ V.$$

It should be noted that before attempting the calculation, the values of terms containing ϵ in Eqs.(11) and (14) must be small enough, otherwise the mathematical analysis is invalid. In the cases of the circuits of Figs. 11 and 12, these values are of the order of 0.01 and 0.1 respectively.

In Figs. 16-18, the curvatures of calculated curves are slightly smaller than those obtained by experiment for large values of V, and are slightly larger for small values. Also for small values of V, the calculated curves are just outside the experimental ones. The errors of theoretical and experimental results are within 10%. The first order solution is also calculated, but the correction found

is less than 1%, i.e., well within the experimental error.

The cases in Figs. 19, 20, 21, 22, &23 correspond to those in Figs. 8(c), 8(d), 7(b), 7(c), and 9(a) respectively. In these figures, the calculated curves are flatter than those from experiment. For small values of V, the calculated curves are outside the experimental, and for large values of V the experimental values of V are considerably larger than those calculated. The errors are, in places, ~~of the order of~~ about 20%. The large errors may be attributed as follows:

(a) In the derivation of differential equations, it has been assumed that the control grid draws no current and that the I_a/E_s characteristic is a straight line. These conditions are fulfilled when V and λ_0 are small,-e.g, the case in Fig. 11 ($V < 2$ v, $\lambda_0 < 10$ v) - but are not realized in the present case in which λ_0 may be larger than 20 v and the amplitude V of the alternating voltage across the control grid, biased at -2.4 v, may be as much as 8 v.

(b) The results are calculated from the zeroth order solution only. As the terms involving ϵ are of the order of 0.1 as mentioned before, it can be expected that higher-order solutions will improve the results. However, the results agree well qualitatively, jumps and hysteresis occurring as predicted, except in the

case in Fig. 21 in which the jumps do not appear. It is believed that a jump will take place in this case if λ_0 is larger than 28 V, which was the largest value obtainable experimentally.

Another experimental result, a wave with modulated amplitude, is shown in Fig. 25(a), which represents the voltage across R_2 in Fig. 12 with the following operating conditions: $E_a = 300$ V, $E_b = -45$ V, $E_g = -3$ V, $\lambda_{01} = \lambda_0 = 18.7$ V, $\lambda_{02} = 0$, $L = 115$ mH, $C = 0.007$ μF, $R_1 = 200\ \Omega$, $R_2 = 9000\ \Omega$, and $f_2 = 11500$ c/s. The curve in Fig. 26(b) is a 30-c/s. timing wave. Comparison of the waves in Figs. 26(a) and (b) shows that the frequency of the amplitude-variation of the curve in Fig. 26(a) is about 15 c/s. The frequency of the wave in Fig. 26(a) also varies periodically, synchronously with the amplitude modulation. The forms of the wave in Fig. 26(a) at its maximum and minimum amplitude (or minimum and maximum frequency) are sketched in Figs. 26(c) and (d) respectively. The frequency of the wave in Fig. 26(d) is f_2, i.e., 11500 c/s. for the present case, and that of the wave in Fig. 26(c) is $\frac{1}{2} f_2$.

The wave forms of Fig. 26(c) and of the envelope of the wave in Fig. 26(a) are much distorted from a sinusoid; this is because R_2, to which the non-linear terms in eq. (14) are proportional, is fairly large so that the non-linearity is of the order of 1. Problems like this are beyond the power of existing mathematical analysis.

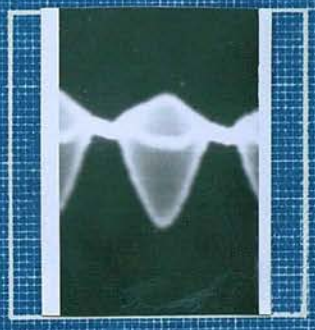

(a)

(c)

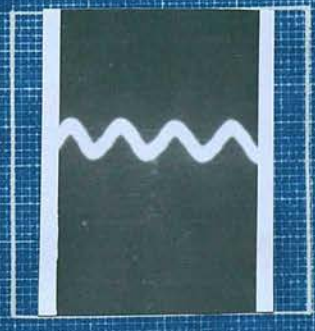

(b)

(d)

Fig. 26

PART II

A GRAPHICAL ANALYSIS FOR NON-LINEAR SYSTEMS.

1. GENERAL PRINCIPLES AND METHOD OF CONSTRUCTION.

The object of Part II is to discuss the graphical analysis of equations of the form

$$\frac{d^2x}{dt^2} + f(x,t)\frac{dx}{dt} + g(x,t) = h(t), \qquad (1)$$

where $f(x,t)$, $g(x,t)$ and $h(t)$, which are functions of the variables inside their brackets, need not be small; $f(x,t)$ and $h(t)$ can be non-analytic. Eq. (1), which occurs in systems with a non-linear and time-varying damping and restoring force, and with an arbitrary applied external force, can represent most non-linear problems met with in practice.

Integrating eq. (1), with respect to t leads to

$$\frac{dx}{dt} + F(x,t) + G(x,t) = H(t), \qquad (2)$$

where
$$\left.\begin{aligned} F(x,t) &= \int f(x,t)\,dx, \\ G(x,t) &= \int g(x,t)\,dt, \\ \text{and} \quad H(t) &= \int h(t)\,dt. \end{aligned}\right\} \qquad (3)$$

Denote x, $g(x,t)$ and $G(x,t)$ respectively by x_0, g_0, and G_0 at $t=t_0$, and by $x_0+\Delta x$, $g_0+\Delta g$, and $G_0+\Delta G$ at $t = t_0+\Delta t$.

Since $\frac{dx}{dt} = \lim_{\Delta t \to 0} \frac{\Delta x}{\Delta t}$, if Δt is sufficiently small, we write

$$\frac{dx}{dt} = \frac{\Delta x}{\Delta t}. \qquad (4)$$

Similarly $\frac{dG}{dt} = \frac{\Delta G}{\Delta t}$, or $\Delta G = \frac{dG}{dt}\Delta t$; (5)

and $\frac{dg}{dx} = \frac{\Delta g}{\Delta x}$, or $\Delta g = g'\Delta x$, (6)

where $g' = \frac{dg}{dx}$, and Δx is small. At the instant $t = t_0 + \Delta t$, with the help of the second of eq. (3) and eq. (6), eq. (5) becomes

$$\Delta G = g\Delta t = (g_0 + \Delta g)\Delta t = (g_0 + g'\Delta x)\Delta t. \quad (7)$$

Thus at $t = t_0 + \Delta t$,

$$\left.\begin{aligned} G &= G_0 + \Delta G = G_0 + (g_0 + g'\Delta x)\Delta t, \\ F(x,t) &= F(x_0 + \Delta x,\ t_0 + \Delta t), \\ \text{and} \quad H(t) &= H(t_0 + \Delta t). \end{aligned}\right\} \quad (8)$$

Inserting eqs. (4) and (8) into eq. (2), gives

$$\frac{\Delta x}{\Delta t} + F(x_0+\Delta x, t_0+\Delta t) + G_0 + g_0\Delta t + g'\Delta x\Delta t = H(t_0+\Delta t).$$

Therefore, the solution $(x_0 + \Delta x)$ of the equation

$$\left(\frac{1}{\Delta t} + g'\Delta t\right)\Delta x + F(x_0+\Delta x, t_0+\Delta t) + g(x_0,t_0)\Delta t = H(t_0+\Delta t) - G(x_0,t_0) \quad (9)$$

is considered as the approximate solution of eq. (2) at $t = t_0 + \Delta t$.

Let $\alpha = \tan^{-1}\left(\frac{1}{\Delta t} + g'\Delta t\right)$,

and $\beta = \tan^{-1}\Delta t$;

eq. (9) then becomes

$$\Delta x \tan\alpha + F(x_0+\Delta x, t_0+\Delta t) + g(x_0,t_0)\tan\beta = H(t_0+\Delta t) - G(x_0,t_0). \quad (10)$$

Eq. (10) can be solved by a graphical method if the values of x_0 , G_0 , and g_0 are known. The process of construction is shown in the following. In Fig. 1, $F(x)$ is drawn against x at $t = t_0 + \Delta t$, $OA = H(t_0+\Delta t)$, $AB = G(x_0,t_0)$, $OD = x_0$, $OC = g(x_0,t_0)$, and $cc' \parallel DD' \parallel OA$. From B draw

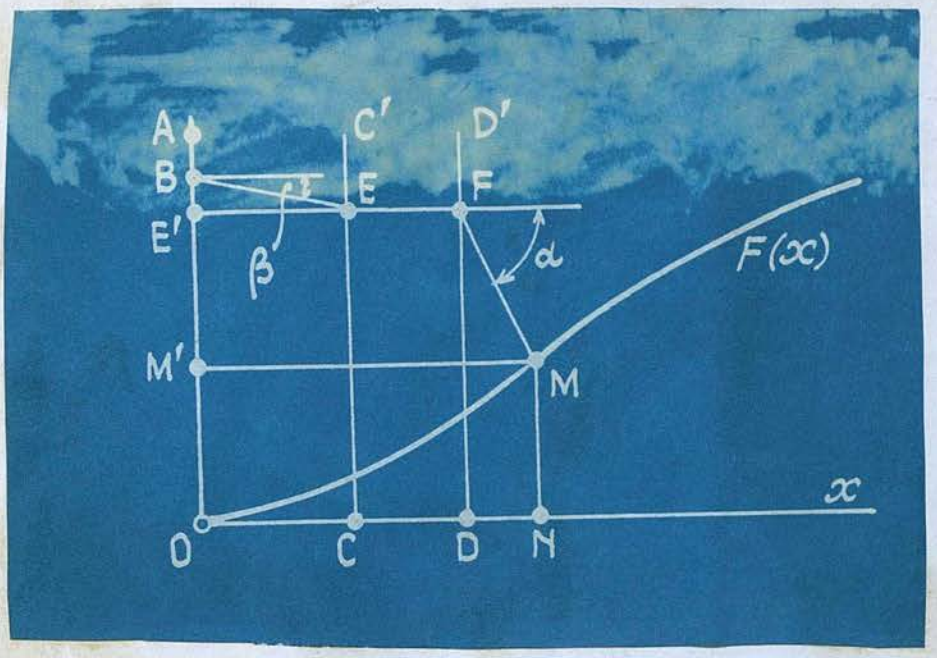

Fig. 1

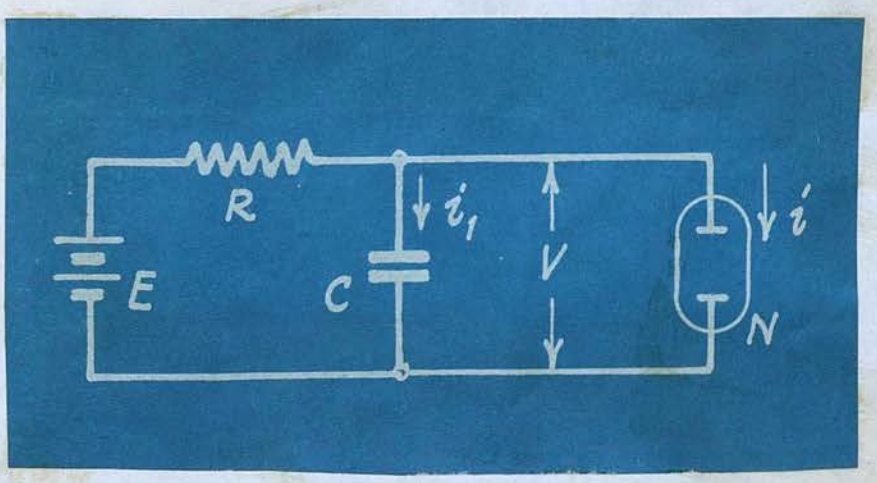

Fig. 2

BE making the angle β with $0x$, and intersecting Cc' at E. Draw $EF \parallel 0x$, and intersecting DD' at F. From F draw FM at the angle α with $0x$, and meeting $F(x)$ at M. Draw $MN \parallel 0A$ to intersect $0x$ at N. DN is then equal to Δx, and ON is equal to x at $t = t_0 + \Delta t$. Draw $FE' \parallel MM' \parallel 0X$. It is obvious that

$$H(t_0+\Delta t) - G(x_0,t_0) = 0B = BE' + E'M' + M'O$$

$$= g(x_0,t_0)\tan\beta + \Delta x \tan\alpha + F(x_0+\Delta x, t_0+\Delta t),$$

so that ON is the required value of x. Therefore, if the initial values of x and G at $t=0$ are given, their subsequent values can be found by this procedure.

The error in this construction can be attributed to two sources: the replacement of differentials by finite differences in eqs. (4), (5), and (6), and constructional errors. The former can in principle be minimized by choosing sufficiently small interval Δt. In the following applications comparisons will be made, whenever possible, between results obtained graphically and those from numerical calculations and experiments. The errors found therefrom are within 5%.

In the following some practical examples are evaluated in order to illustrate this graphical method.

2. APPLICATIONS.

2.1. Circuits containing Gaseous Conductors.

Fig. 2 shows a circuit containing a gaseous conductor N (such as a neon tube), a resistance R, a condensor C, and a source of direct voltage, E. The characteristic of the tube is represented by a non-linear empirical relation $i = f(v)$, where v and i are respectively the voltage across it and the current passing through it. The equations of the circuit are:

$$R(i_1 + i) + v = E,$$

and $$i_1 = C\frac{dv}{dt}.$$

These are reduced to the equation

$$\frac{dv}{d\tau} + F(v) = E, \qquad (11)$$

where $$\tau = \frac{t}{RC},$$

and $$F(v) = Rf(v) + v.$$

Letting $$\frac{dv}{d\tau} = \frac{\Delta v}{\Delta \tau} = \Delta v \tan\alpha,$$

eq. (11) becomes

$$\Delta v \tan\alpha + F(v) = E. \qquad (12)$$

Eq. (12) is solved graphically with the following values of the elements in the circuit in Fig. 2:

$$R = 15000\,\Omega, \quad C = 1\,\mu F, \quad E = 210\,V,$$

and the v/i relation of the neon tube is given in the table:

v(v)	162	150	140	138	140	144	149	157	165
i(mA)	0	2	4.6	7	10	14	18	23	28

Firstly, as shown in Fig. 3, $F(v)$ is plotted against v by adding v and $f(v)$ multiplied by R $(=15000\Omega)$. The upper part of the curve $F(v)$ is repeated in Fig. 4 with a larger scale of the ordinates. In the same figure, the process of graphical construction is also shown. A line AB representing $E=210V$ is drawn parallel to the ordinates. $v=132.1V$ is taken as the value of v at $\tau=0$. Mark a point O on the line AB with $v=132.1V$. Draw $o1'$ at the angle α with the ordinates. Here $\alpha=\tan^{-1}45$ therefore $\Delta\tau=\frac{1}{\tan\alpha}=\frac{1}{45}$. $o1'$ intersects $F(v)$ at $1'$. Draw $1'1$ parallel to the abscissa and to intersect AB at 1. $o1$ is then the value of Δv, the increment of v after $\Delta\tau$, since eq. (12) is satisfied at this instant. From 1 draw $12'\,//\,o1'$ meeting $F(v)$ at $2'$. Draw $2'2\,//\,1'1$ intersecting AB at 2. $o2$ is the increment of v after $2\Delta\tau$. The process is repeated so that we obtain a series of values of v for increasing τ as well as a zig-zag curve between AB and the straight part cD of $F(v)$, and at every instant, eq. (12) is satisfied. When the point 22 on AB is reached, the line drawn from it parallel to $o1'$ cannot intersect cD but another branch GH of $F(v)$. The subsequent zig-zag curve is drawn between AB and GH until the minimum point of the curve DHG is reached, then it changes to between AB and cD. One cycle is completed when the zig-zag curve returns to cD.

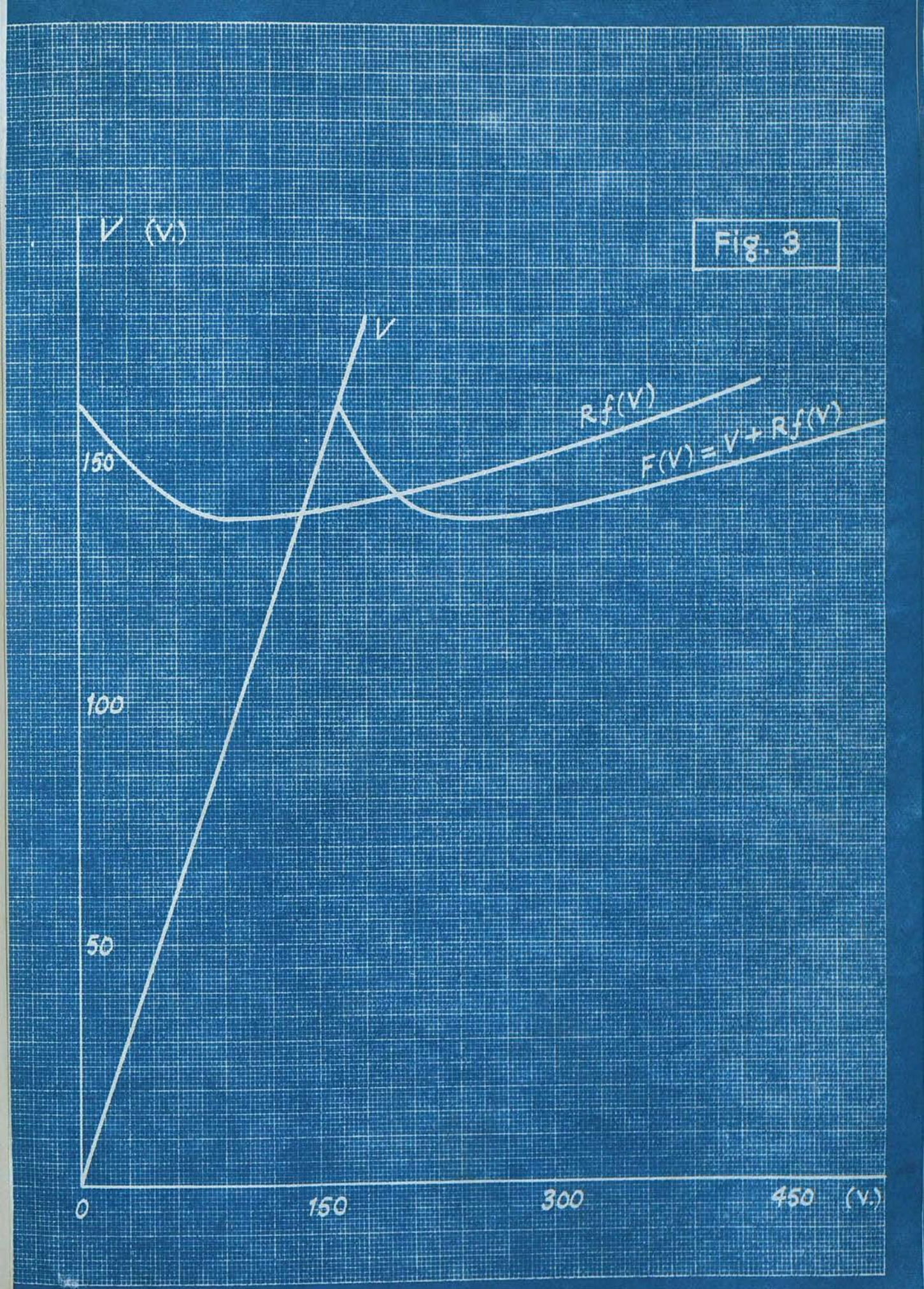
V (v)
Fig. 3
V
Rf(V)
F(V) = V + Rf(V)
150
100
50
0
150
300
450 (v.)

Fig. 4

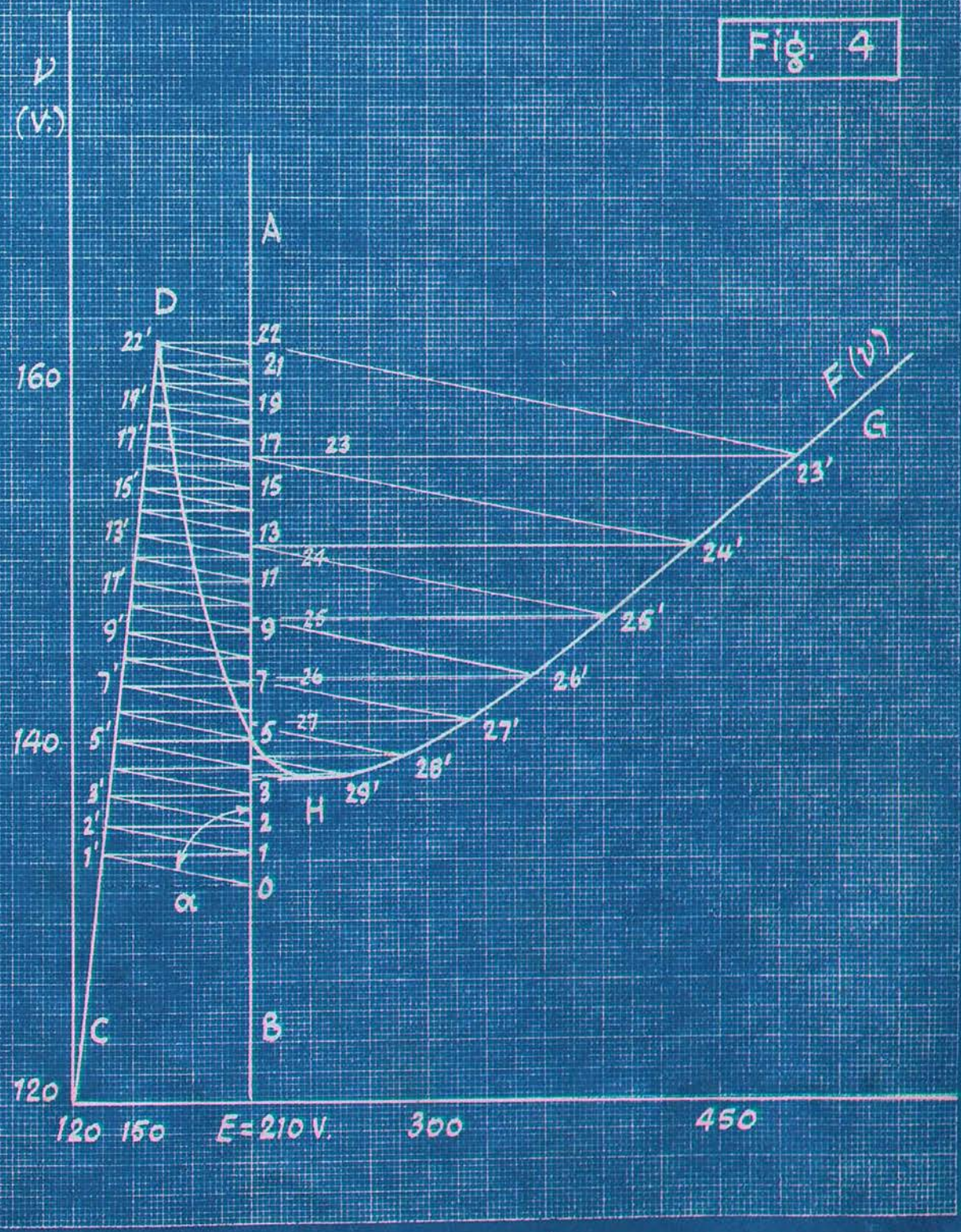
V
(V.)
160
140
120
A
B
C
D
H
α
F(V)
G
22'
19'
17'
15'
13'
11'
9'
7'
5'
3'
2'
1'
22
21
19
17
15
13
11
9
7
5
3
2
1
0
23
24
25
26
27
23'
24'
25'
26'
27'
28'
29'
120
150
E=210 V.
300
450

More cycles can be obtained in the same manner. The curve of v versus $\frac{\tau}{\Delta\tau}$ is plotted in Fig. 5. It is found that the amplitude of the oscillations is $24v$. Their period is $25.8\,\Delta\tau$. Therefore the frequency is

$$f = \frac{1}{t} = \frac{1}{RC\tau} = \frac{1}{15000 \times 10^{-6} \times 25.8 \times \frac{1}{45}} = 116\ c/s.$$

The curve in Fig. 6 is the wave form sketched from a oscillograph connected across the neon tube in Fig. 2. The amplitude and frequency measured are $24v$ and $120\ c/s$ respectively. The error between the measured frequency and that from graphical construction is:

$$\frac{120-116}{120} = 3.33\ \%.$$

From the results of construction, the following observations may be made:

(a) The ultimate oscillations do not depend upon the initial condition.

(b) For sustained oscillations, the line AB in Fig. 4 can only intersect $F(v)$ once and at the part with negative slope. And R must be large enough to ensure that these conditions can be fulfilled.

(c) The duration from the maximum to the minimum of the oscillations in Fig. 5 depends upon the slope of the part of GH of the curve $F(v)$ in Fig. 4. If GH is parallel to the abscissa, the maximum voltage drops to the minimum voltage instantaneously.

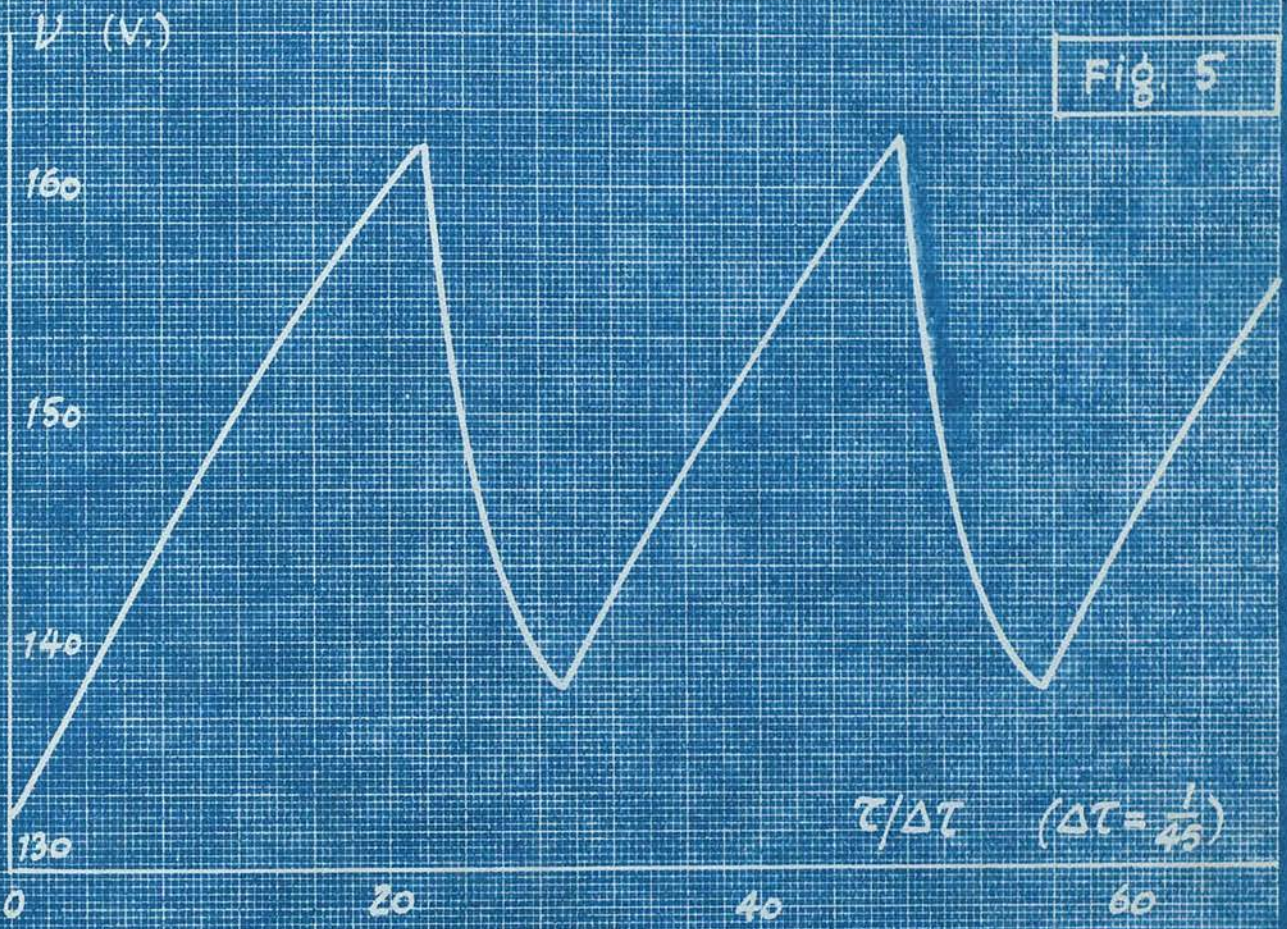

Fig. 5

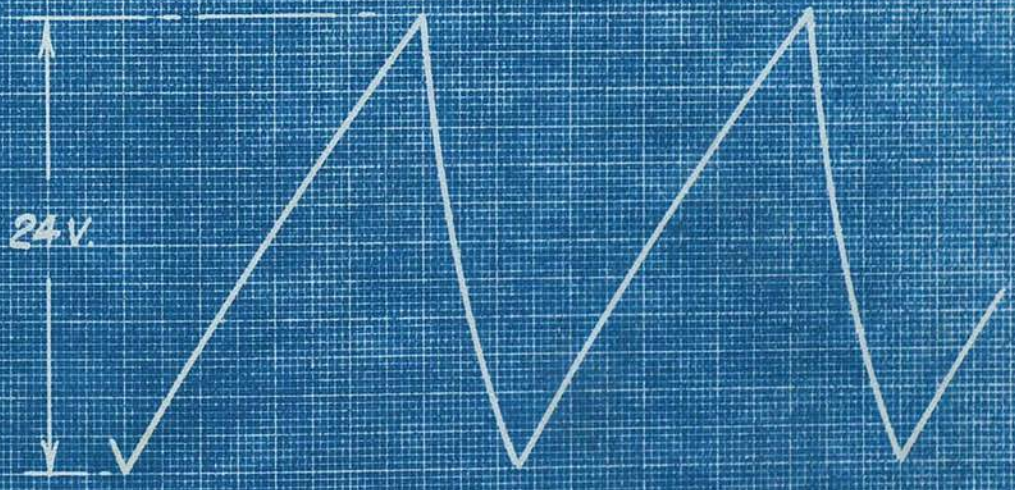

Fig. 6

2.2 Closed-cycle Control Systems with Non-Linear Friction.

The simplest kind of closed-cycle control system, namely the error-control of position, is considered. Let

θ_i = input angle,

θ_o = output angle,

θ = error angle,

then $\theta = \theta_i - \theta_o$.

The torque developed by the controller of this type of servomechanism is $T = K\theta$,

where K, being constant, can be determined from a given system. T is balanced by: (a) the torque transferred to the load, which is expressed in the form $J\frac{d^2\theta_o}{dt^2}$, where J is the moment of inertia of the motor and the load; and (b) the torque due to the friction in the system. The friction torque is in general not directly proportional to the velocity. A typical characteristic of friction as a function of velocity is shown in Fig. 7. Linear (or viscous) friction only holds for a limited range of velocity. The "stiction" and the falling part of the curve are the causes of jerky motions at low input speeds.

Therefore we have the equation for the torque

$$J\frac{d^2\theta_o}{dt^2} + f\left(\frac{d\theta_o}{dt}\right) = K\theta = K(\theta_i - \theta_o), \qquad (13)$$

where $f\left(\frac{d\theta_o}{dt}\right)$, which is the friction torque, takes

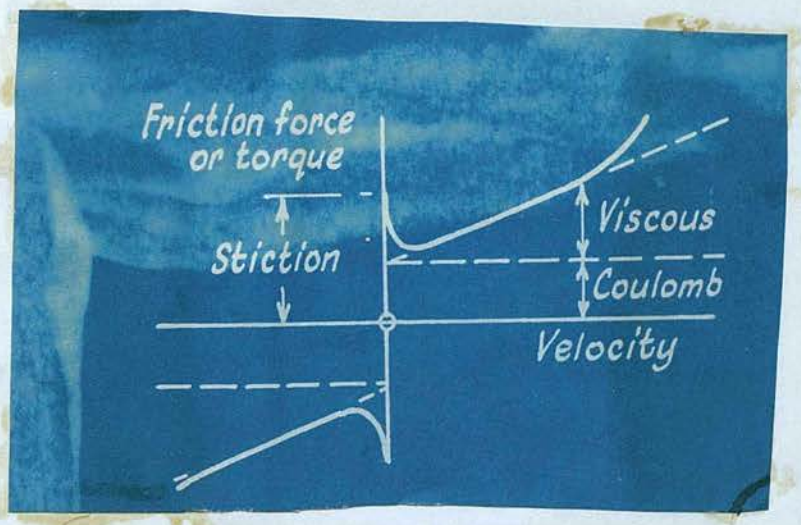
Friction force
or torque
Stiction
Viscous
Coulomb
Velocity

Fig. 7

the form of the curve in Fig. 7. Let

$$\omega = \sqrt{\frac{K}{J}},$$

$$\tau = \omega t,$$

$$\frac{d\theta_o}{d\tau} = v,$$

and $\theta_i = v_i \tau,$

where v_i is a constant, i.e., the input speed is constant.

Eq. (13) becomes:

$$\frac{dv}{d\tau} + F(v) + \int v\, d\tau = v_i \tau, \qquad (14)$$

where

$$F(v) = \frac{1}{K} f(\omega v).$$

Let $$v = z + v_i. \qquad (15)$$

Inserting eq. (15) into eq. (14), gives

$$\frac{dz}{d\tau} + F(z + v_i) + \int (z + v_i)\, d\tau = v_i \tau,$$

or $$\frac{dz}{d\tau} + F(z + v_i) + y = 0,$$

where $$y = \int z\, d\tau. \qquad (16)$$

To compare eq. (16) with eq. (2), we have

$$F(x,\tau) = F(z + v_i),$$

$$G(x,\tau) = y,$$

$$g(x,\tau) = z,$$

and $$H(\tau) = 0$$

Hence, from eq. (10), we have the equation for graphical construction:

$$\Delta Z \tan\alpha + F(Z_o + v_i + \Delta Z) + Z_o \tan\beta + y_o = 0. \qquad (17)$$

Eq. (17) shows that with a constant input speed v_i, the graphical construction can be performed as with

no input, except that the ordinate is shifted from $v=0$ to $v=v_i$, or from $z=-v_i$ to $z=0$. Eq. (17) is solved graphically for two different values of v_i, with the same initial conditions that, at $\tau=0$, $y=0$, $v=0$, or $z=-v_i$. In Fig. 8 v_i is so small that the system is operating on the falling part of the friction/ velocity characteristic curve. The process of construction is the same as that given in Section 1 and is indicated by the progressive curve $o0_1'1'_2'2'_3$ ..... At every point on the curve $o1_2'3_4$ ....., eq. (17) is satisfied. The first term on the right in eq. (17) has no effect until the point 21 is reached. When $\tau=4.44\tau$, one cycle is completed. Other cycles can be obtained in the same manner. The curve of v against $\frac{\tau}{4\tau}$ is plotted in Fig. 9. The solution of the velocity v is a periodic function of time, but over a certain time interval in each period, $v=0$, and the system is at rest. The motion is such that, as the external force is applied, the system remains at rest for a time interval, then it begins to move; after a second time interval, it comes again to rest. The process is repeated indefinitely forming a "jerky" motion. The time interval over which the speed is zero is longer as the input speed is smaller, and so is the period of the oscillations.

If v_i is large so that the system is operated on the rising part of the friction/velocity curve,

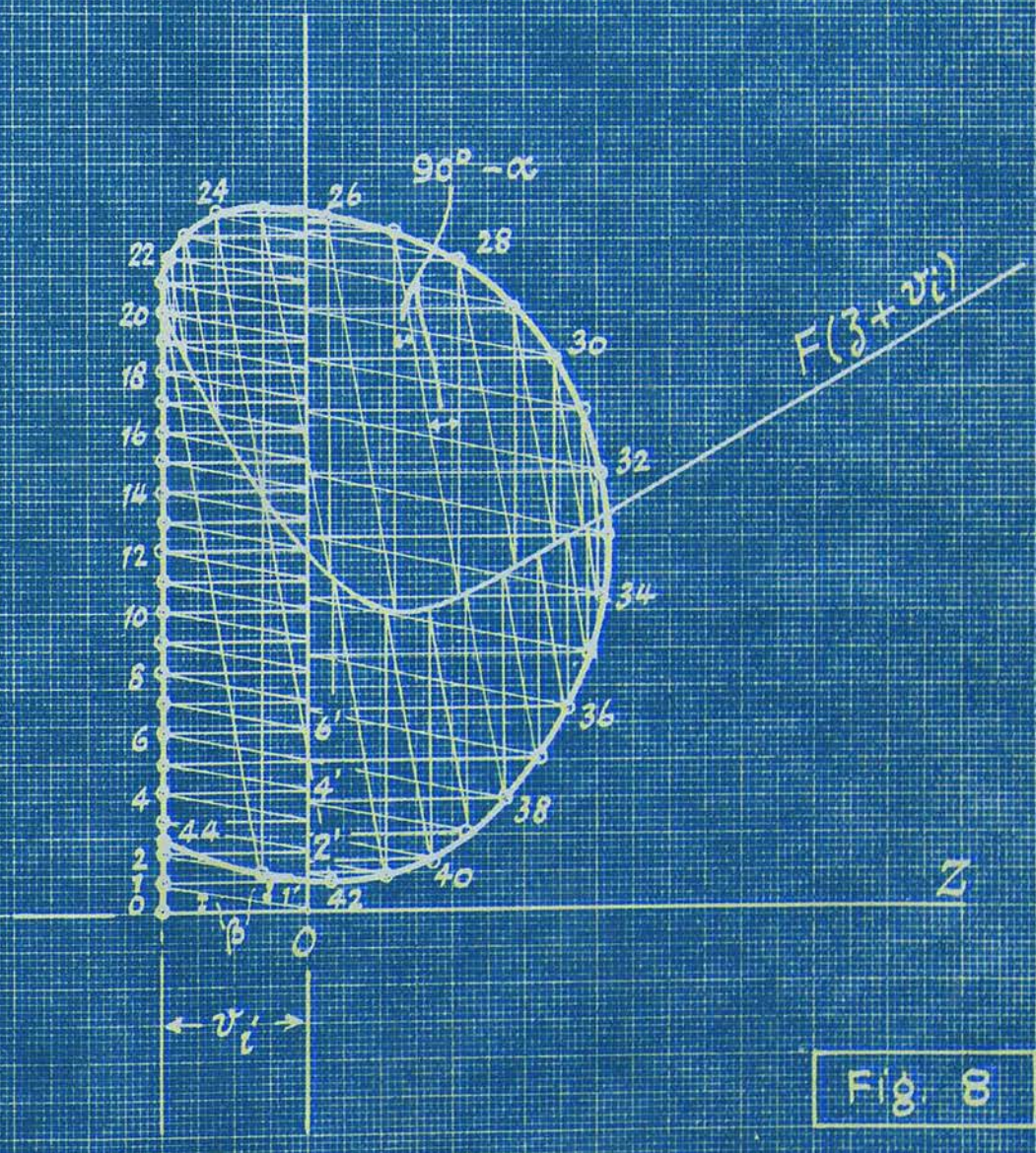
90° - α
24
26
28
22
20
30
18
16
F(3+v_i)
32
14
12
34
10
8
6
36
6'
4
4'
38
44
2
2'
40
1
1'
0
42
Z
β
O
v_i

Fig. 8

Fig. 9

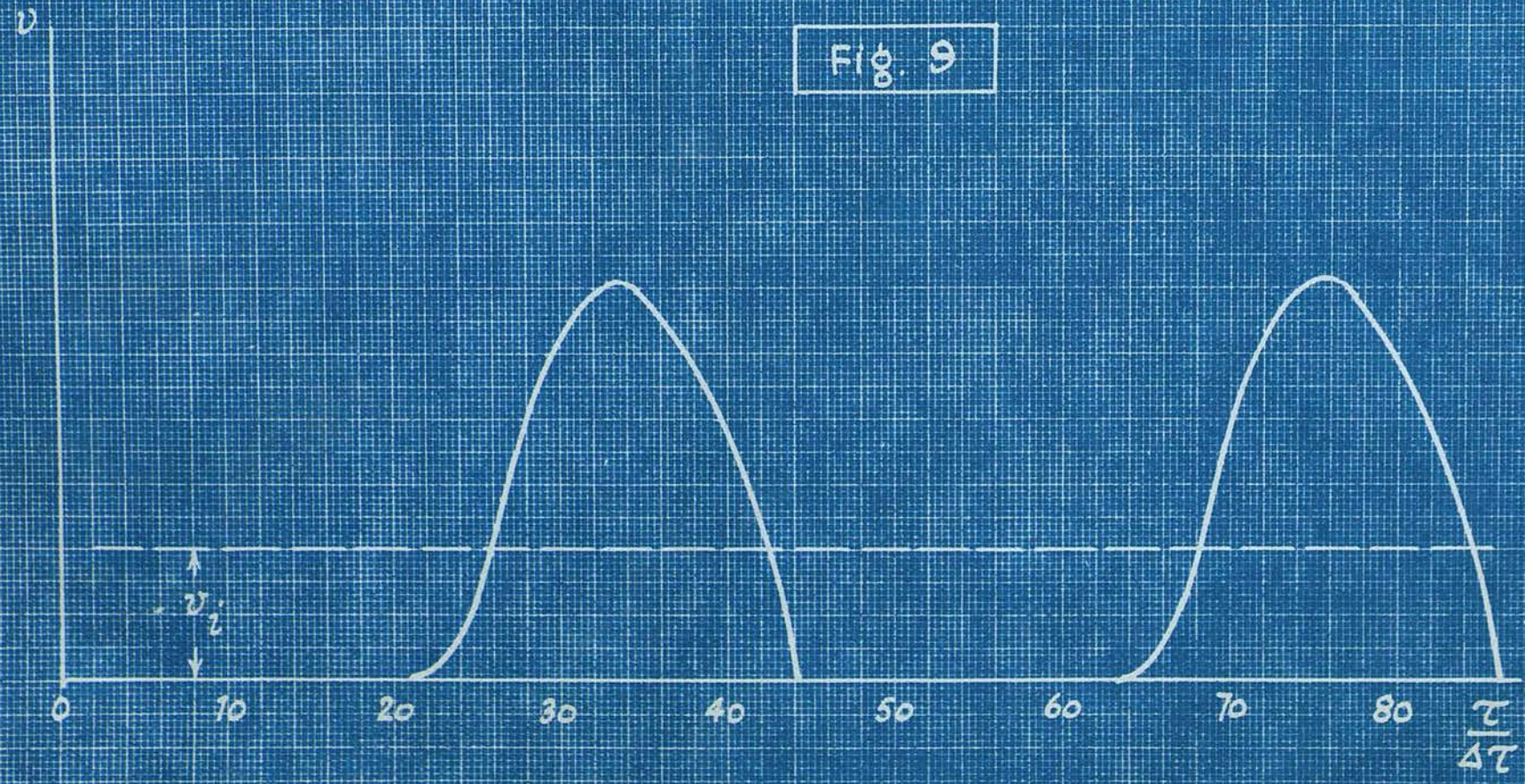

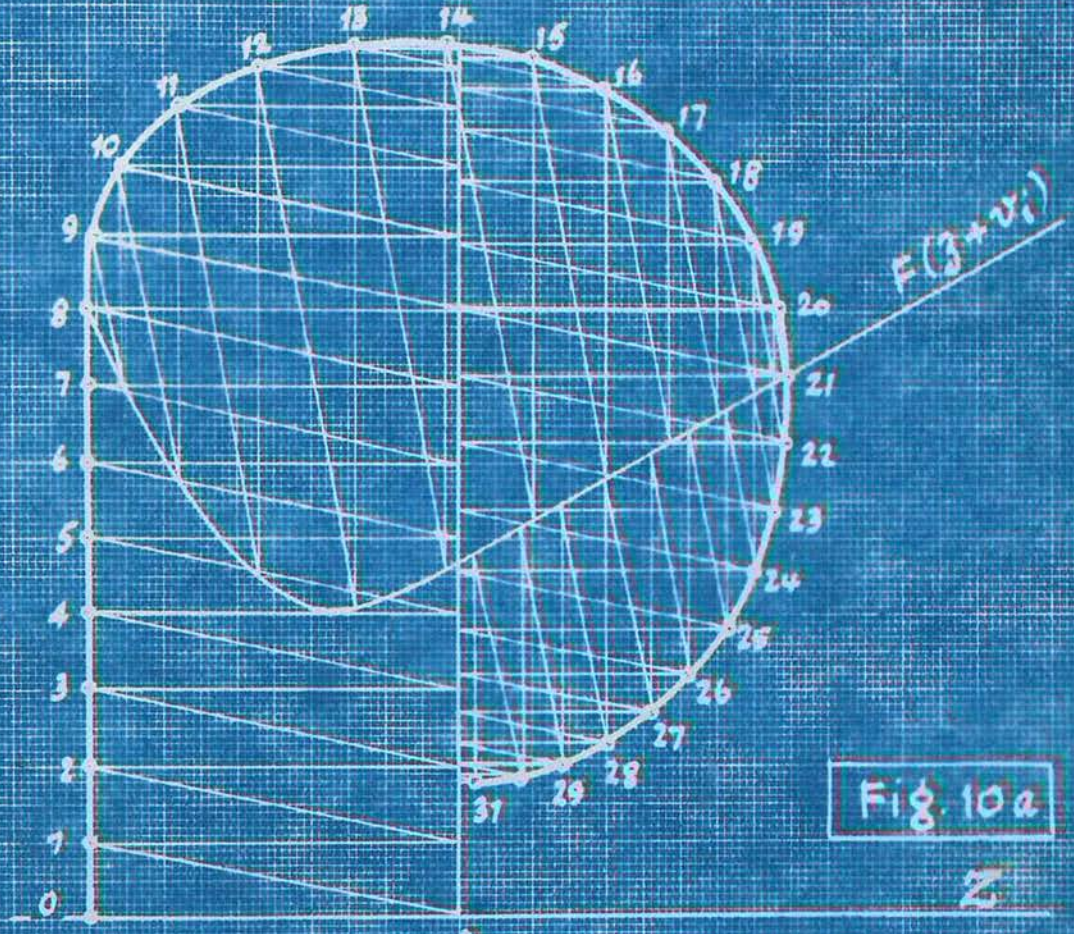

Fig: 10 a

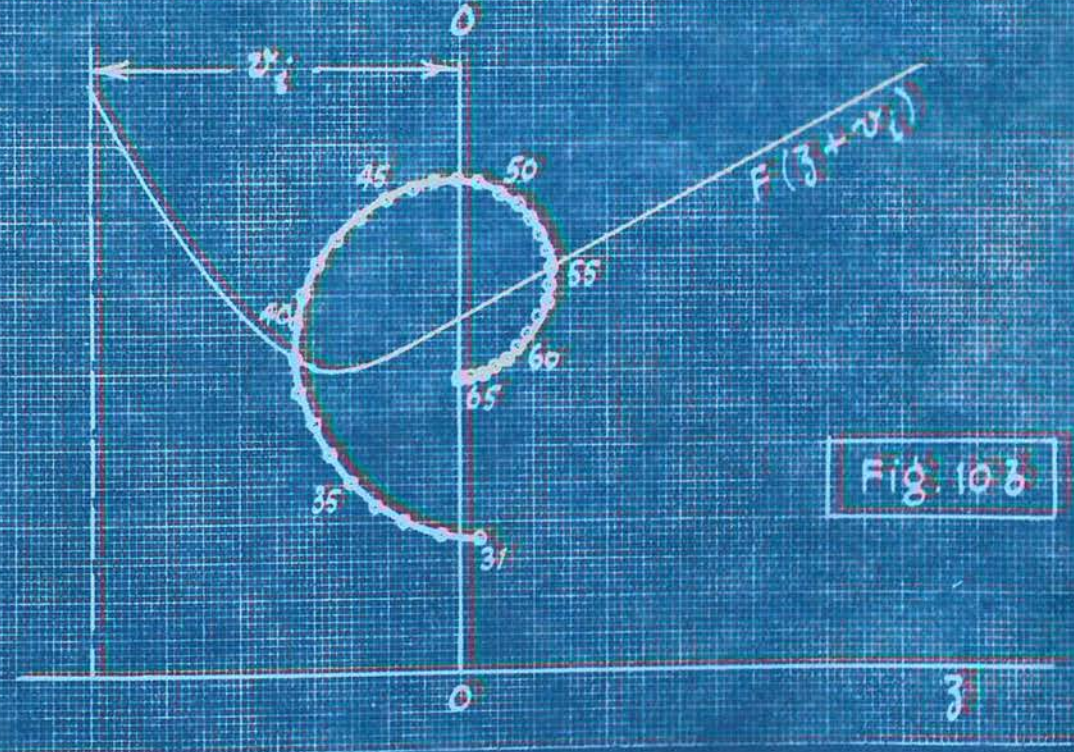

Fig: 10 b

Fig. 11

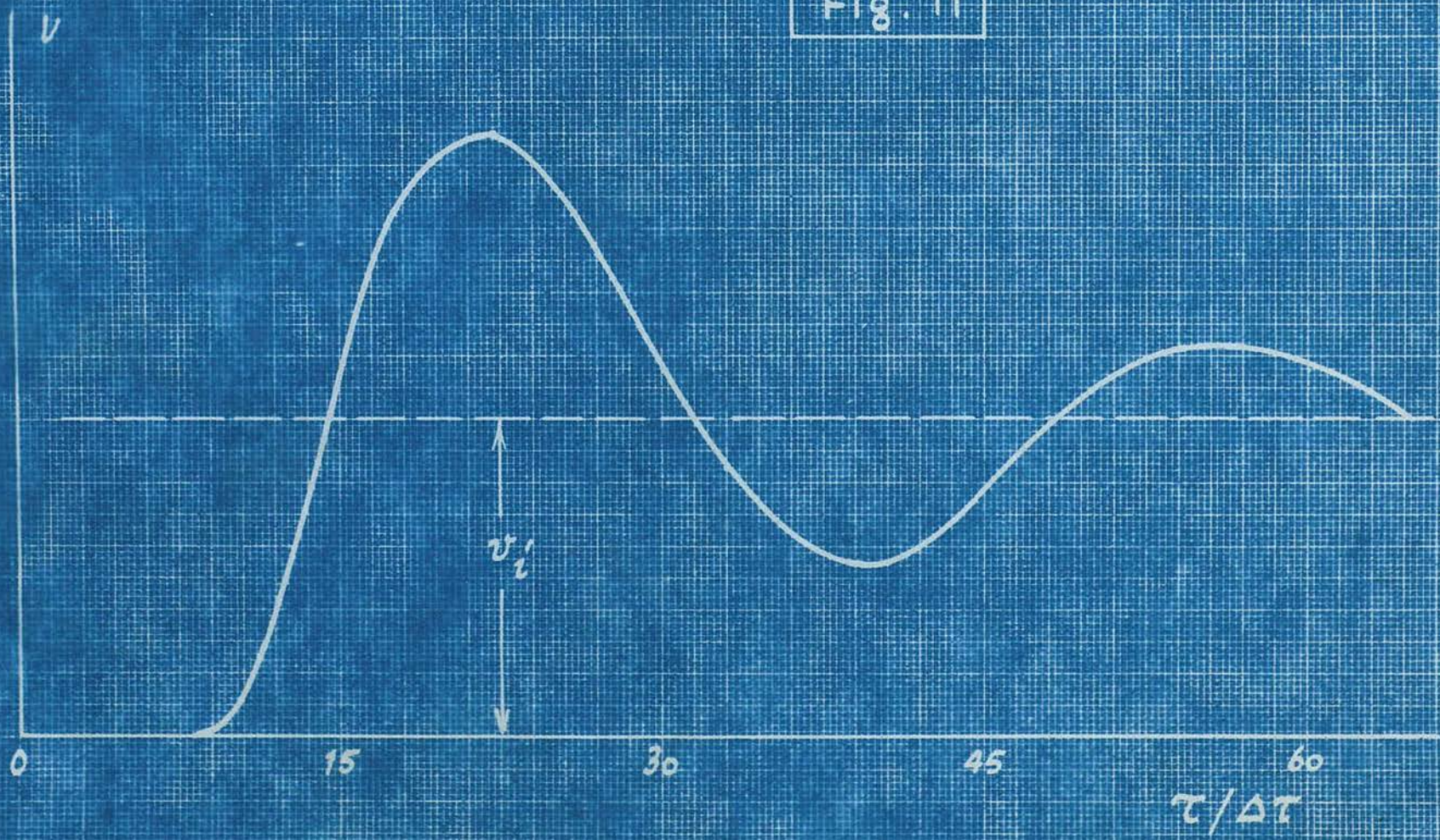

the solution for v , shown in Fig. 11 which is constructed in Fig. 10 (Fig. 10(b) is a continuation of Fig. 10 (a)), has temporary oscillations which die out as time goes on, leaving the system with a constant speed v_t . The system is thus stable under this condition.

2.3. Closed-Cycle Control Systems with Backlash.

A simple position-control servomechanism with error-rate damping is used as an example for analysis. The mechanical backlash appears between the servo motor and the load. In Fig. 12, θ_t , θ_o , and θ represent the same quantities as those used in Section 2.2.

v = velocity of centre of mass of motor and load,

v_o = velocity of load $= \frac{d\theta_o}{dt}$,

v_o is a function of v which is characterized by the backlash: when v increases in one direction, backlash has no effect,i.e., $v_o = v$; however, when v decreases (increases in the reverse direction) v_o maintains a constant maximum velocity v_{om} (friction neglected) until the backlash is taken up in the reverse direction, then $v_o = v$ almost instantaneously. Let $v_o = f(v)$, the relationship between $f(v)$ and v is plotted in Fig. 13 which shows the effect of hysteresis. It can be seen that $f(v)$ is not only a

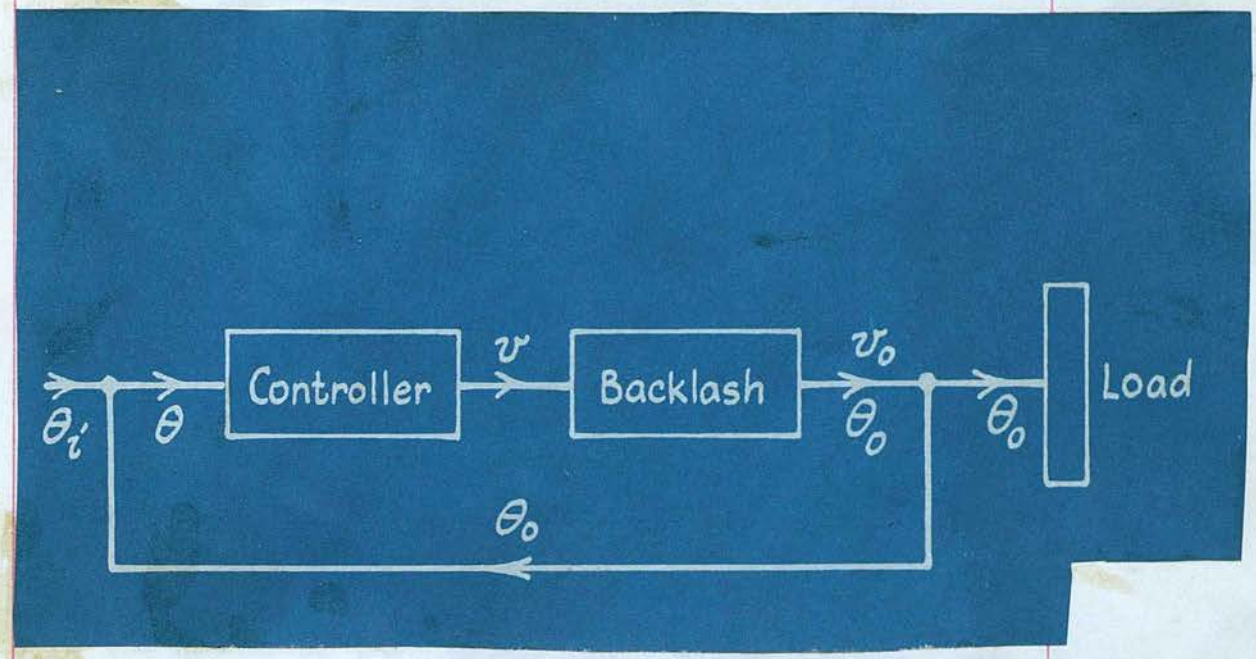
Controller
Backlash
Load
θ_i
θ
v
v_o
θ_o
θ_o
θ_o

Fig. 12

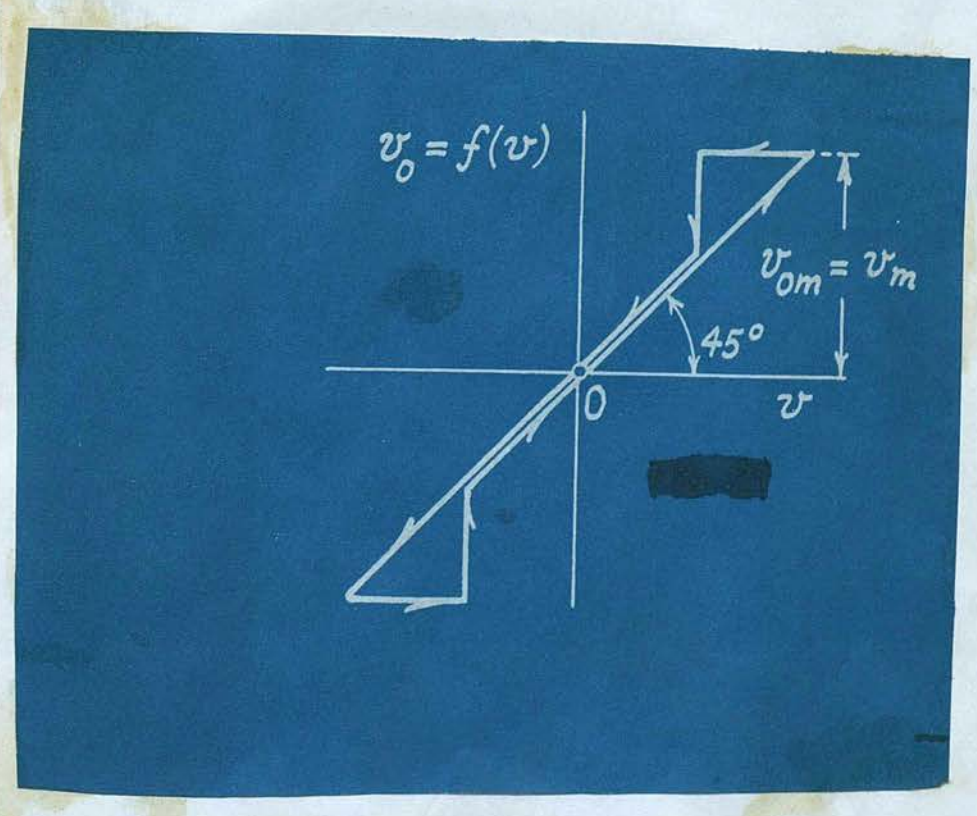
$v_o = f(v)$
$v_{om} = v_m$
45°
0
v

Fig. 13

function of V , but also of the maximum velocity V_m . Different values of V_m require different curves of $f(V)$. Further, $f(V)$ is not an analytic function at all. These introduce extreme difficulty in any attempt to solve analytically the problem of backlash.

The torque developed by the controller for an error-rate damped servomechanism is

$$T = K\theta + L\frac{d\theta}{dt},$$

where K = torque per unit error-angle,

L = torque per unit error-rate,

K and L can be calculated for a given system. Since the accelerating torque must equal the retarding torque,

$$K\theta + L\frac{d\theta}{dt} = J\frac{dV}{dt}, \tag{18}$$

where J is the moment of inertia of the motor and the load.

If $\theta_i = 0$,

then since $\theta = \theta_i - \theta_o$,

$$\theta = -\theta_o = -\int V_o\,dt = -\int f(V)\,dt. \tag{19}$$

Substituting eq. (19) into eq. (18), gives

$$\frac{dV}{dt} + cf(V) + \int f(V)\,d\tau = 0, \tag{20}$$

where $\tau = \omega t$,

$$\omega = \sqrt{\frac{K}{J}},$$

and $$c = \frac{L}{\sqrt{JK}}.$$

Since V_o equals either V or V_m , eq. (20) is

is written as the two equations:

$$\frac{dV_1}{d\tau} + cV_1 + \int_0^{\tau} V_1 d\tau = 0, \tag{21}$$

and $$\frac{dV_2}{d\tau} + cV_m + V_m\tau + \int_{\tau_1}^{\tau_1} V_1 d\tau = 0, \tag{22}$$

where the upper limit of the integral in eq. (21) is smaller than τ_1, the value of τ when V_1 reaches its maximum V_m. As $\frac{dV_m}{d\tau} = 0$, then $cV_m + \int_0^{\tau_1} V_1 d\tau = 0$, and eq. (22) is reduced to

$$\frac{dV_2}{d\tau} + V_m\tau = 0 \tag{23}$$

with the initial condition $V_2 = V_m$ at $\tau = 0$. Solving eqs. (21) and (23) alternatively gives V. When V_1 in eq. (21) reaches V_m, instead of being the solution of eq. (21), V is the solution of eq. (23). When $\int_{\tau_1}^{\tau} (V_m - V_2) d\tau = b$, where b is the backlash, impact occurs, V is then the solution of eq. (21).

This problem can be solved graphically. Comparing eq. (21) with eq. (2), we have

$$F(V, \tau) = cV_1,$$

$$G(V, \tau) = \int_0^{\tau} V_1 d\tau,$$

$$g(V, \tau) = V_1,$$

and $$H(\tau) = 0.$$

Hence, from eq. (10), the equation for graphical construction of eq. (21) is

$$\Delta V_1 \tan\alpha_1 + cV_1 + V_{10} \tan\beta = -G(V_{10}, \tau_0), \tag{24}$$

where $$\tan\alpha_1 = \left(\frac{1}{\Delta\tau} + \Delta\tau\right),$$

$$\tan\beta = \Delta\tau,$$

$\tau_0 = \tau - \Delta\tau$,

and V_{10} is the value of V_1 at τ_0.

Similarly, the equation for graphical construction of eq. (23) is

$$\Delta V_2 \tan\alpha_2 + V_m(\tau_0 + \Delta\tau) = 0, \tag{25}$$

where $\alpha_2 = \tan^{-1}\frac{1}{\Delta\tau}$. Let $\alpha_2' = \tan^{-1}\frac{2}{\Delta\tau}$, $\frac{1}{2}\Delta\tau = \Delta\tau'$, and $\frac{1}{2}\Delta V_2 = \Delta V_2'$; eq. (25) becomes

$$\Delta V_2' \tan\alpha_2' + V_m(\tau_0 + 2\Delta\tau') = 0. \tag{26}$$

Suppose $c=1$, and at $\tau=0$, $V_1 = -0.012$, $G_0 = -0.743$, Eq. (24) is firstly constructed in Fig. 14(a) with the standard method given in Section 1 with $\Delta\tau = 0.1$. V_m is obtained where the progressive curve $0\,1\,2\cdots$ intersects the straight line $f(v) = v$, since at this point $\frac{dV_1}{d\tau} = 0$. In the present case, $V_m = 0.4$, and $\tau = 13\Delta\tau$. Eq. (26) is then constructed as shown in Fig. 14(b) with $\Delta\tau' = 0.1$. At each point on the progressive curve 13, 14, 16, 18, $\cdots$, eq. (26) is satisfied. The vertical distance between each pair of points on the progressive curve (denoted by even numbers) is $2V_m\Delta\tau' = 2\times 0.4\times 0.1 = 0.08$, and the horizontal distance between each pair of points on $f(v)$ (denoted by odd numbers) is $2\Delta V_2'$. While constructing the curve 13, 14, 15, $\cdots$ another curve $14', 16', 18', \cdots$ which represents the expression $\int_{\tau_1}^{\tau} V_2\,d\tau \left(= G(\tau_0) + 2V_2\Delta\tau' \right.$, where $G(\tau_0) = \int_{\tau_1}^{\tau-\Delta\tau} V_2\,d\tau$, and $G(\tau_0) = 0$ at $\tau_0 = \tau_1$) is also constructed. The process of construction shown in

Fig. 14a

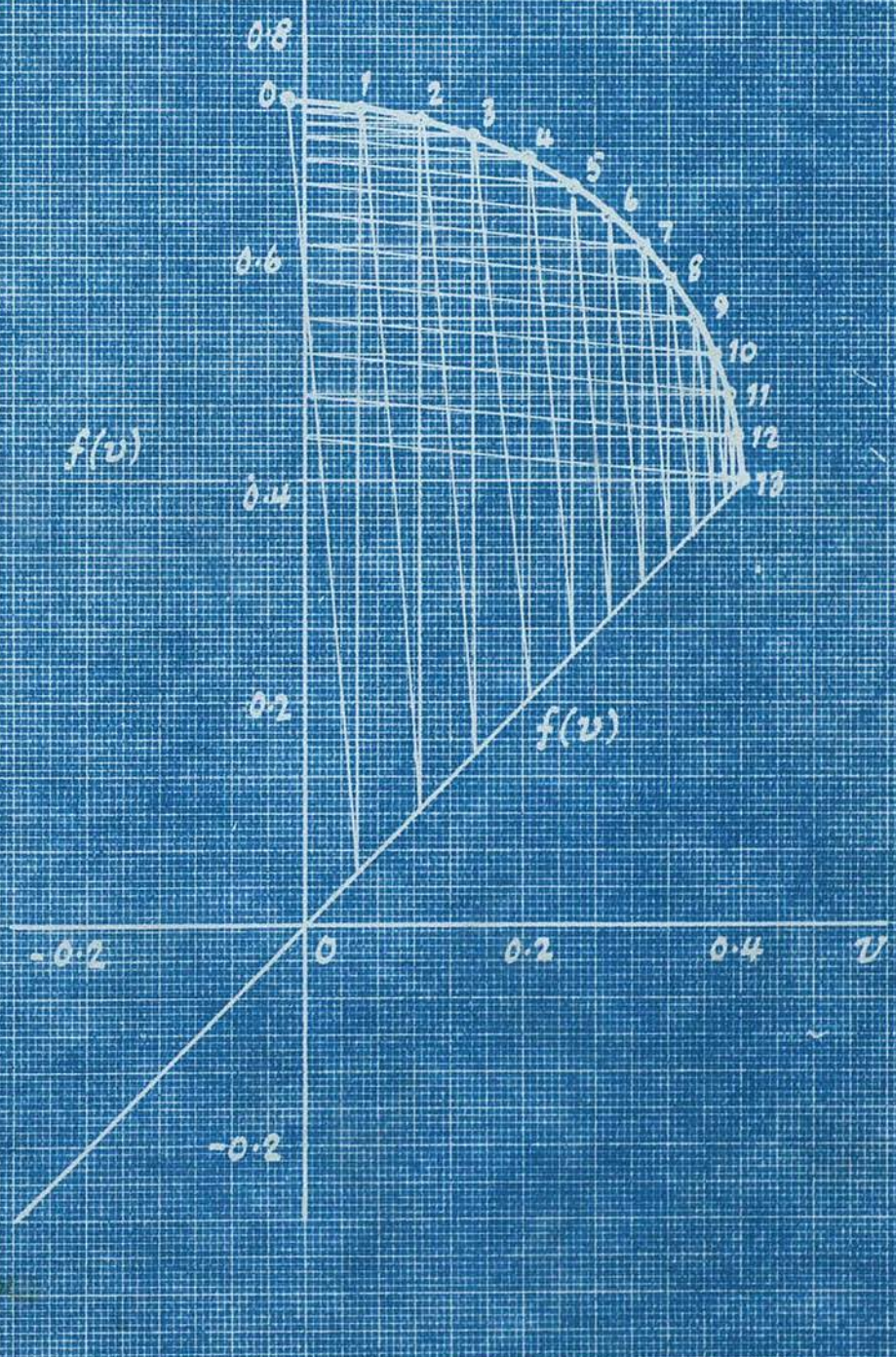

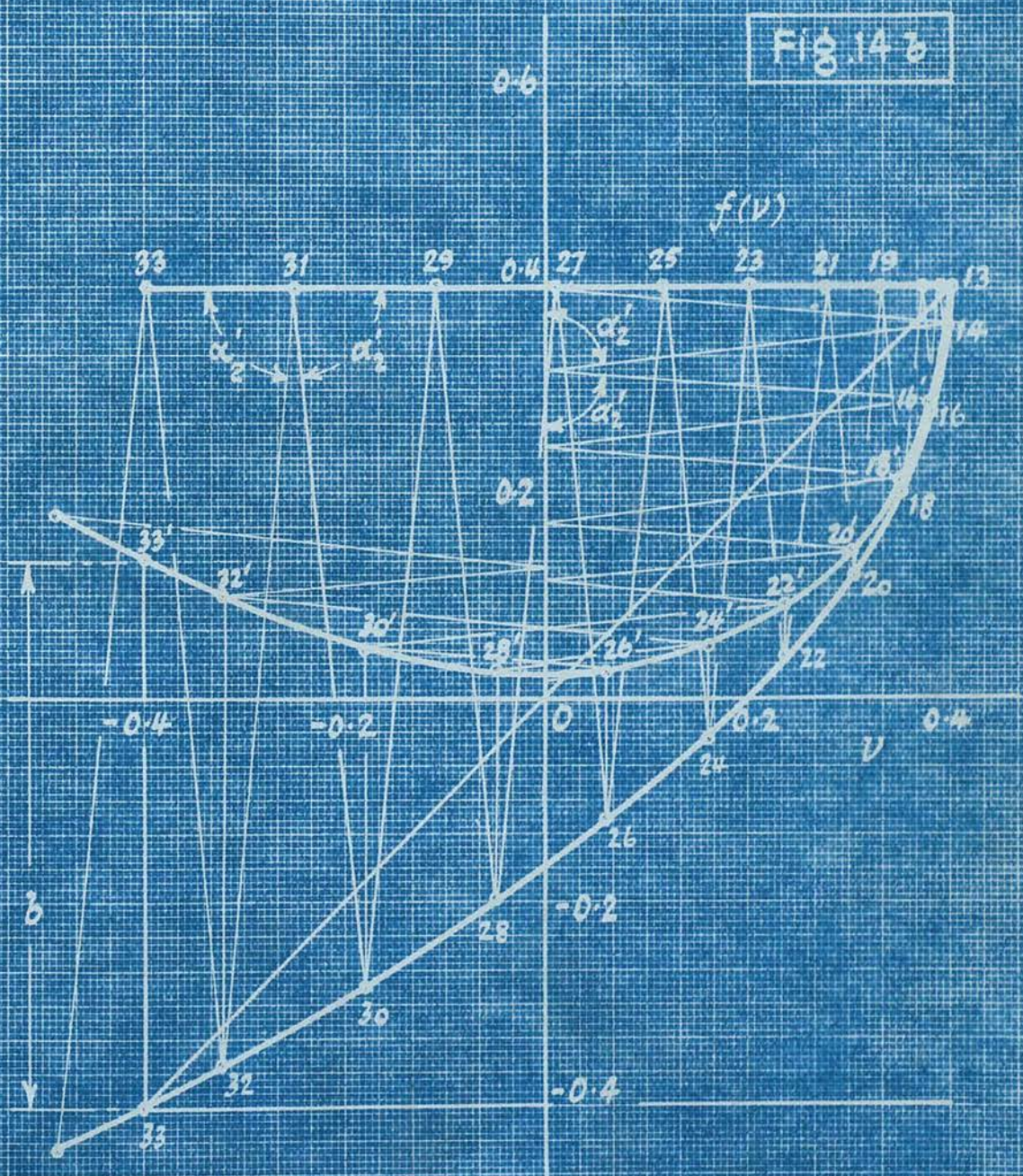
Fig. 14-a
f(V)
0·6
0·4
0·2
-0·4
-0·2
0
0·2
0·4
V
33
31
29
27
25
23
21
19
17
15
14
16
18
20
22
24
26
28
30
32
33'
32'
30'
28'
26'
24'
22'
20'
18'
16'
14'
α_2'
α_2'
α_2'
α_2'
h
b

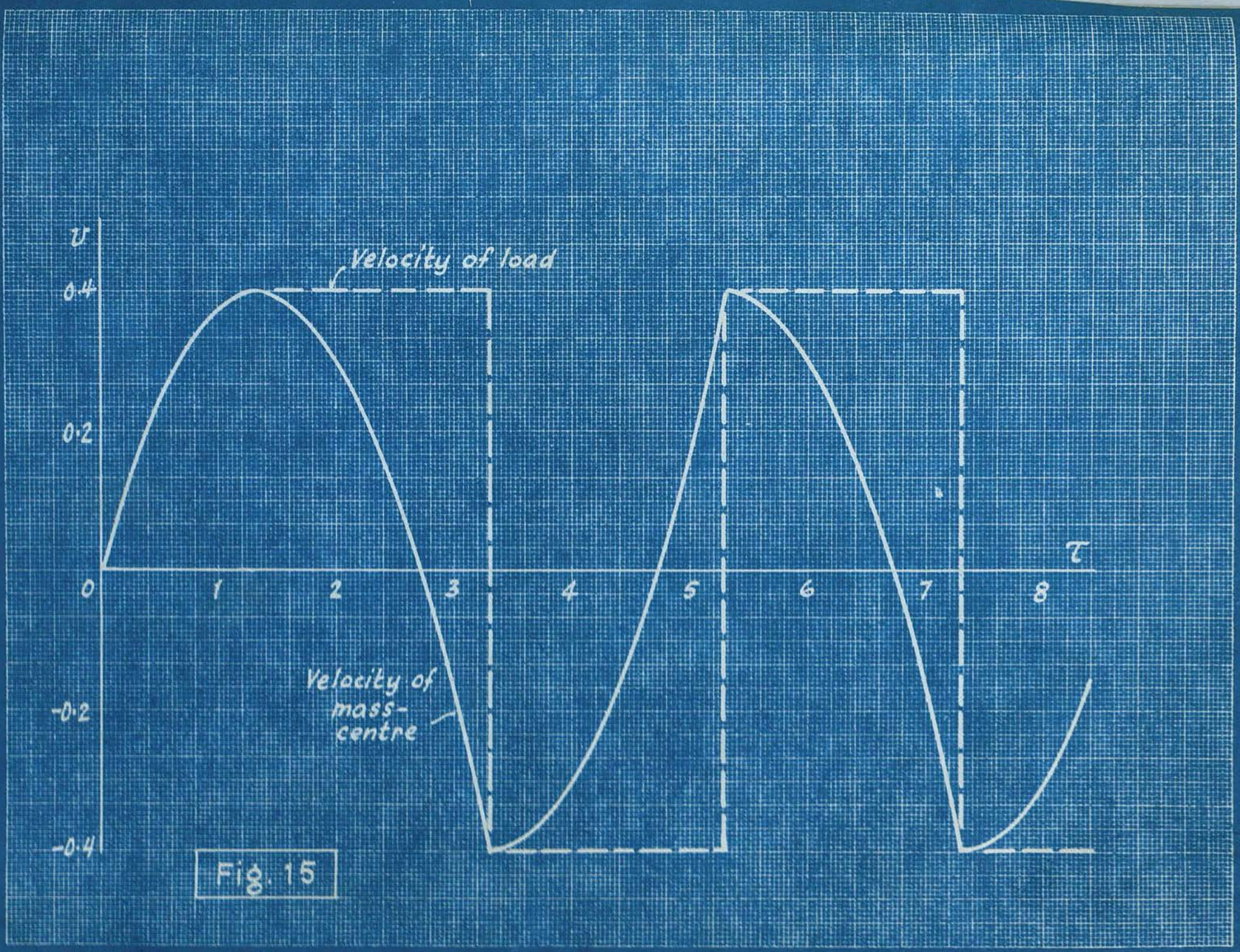
v
Velocity of load
0.4
0.2
τ
0
1
2
3
4
5
6
7
8
Velocity of mass-centre
-0.2
-0.4

Fig. 15

Fig. 14(b) is self-evident. When the vertical distance between these two curves 13, 14, 16, ··· and 13, 14', 16', ··· is b, the backlash, the first cycle of the solution is completed. The second cycle is obtained in the same manner taking, as initial values, the final values of the first. The process is repeated and sustained oscillations are ultimately obtained. If a cycle is finished after the progressive curve intersecting the straight line $f(v) = v$, i.e., after the occurrence of v_m, the following cycle is started by directly constructing eq. (26) without considering eq. (24). In our present case, the curve 13, 14, 16, ··· , intersects $f(v) = v$ at $\tau = 33\Delta\tau$, $v_2 = -v_m = -0.4$, and impact also happens at the same instant, so that the subsequent curve is only a repetition of the curve 13, 14, 16, ··· . The form of solution is shown in Fig. 15. The period of the oscillations is 4 which is in close agreement with A. Tustin's result (ref. (12), the second of Fig. 16) which is obtained from numerical calculation. The amplitude of the oscillations is 0.4, and the backlash is 0.533.

2.4. Frequency Modulation of Forced Oscillations in Section 2.2, Part 1.

Consider the equation

$$\frac{d\Phi}{d\tau} = \gamma + w\sin 2\Phi . \qquad (27)$$

In eq. (27), Φ is a function of τ to be solved, γ and w are constants. Eq. (27), which is the same as eq. (75) in Part I, is the equation of the phase of oscillations in a circuit with a periodically-varying parameter and with an external force with the frequency as the parameter-variation. This equation can easily be solved by the graphical method. Let

$$\tan\alpha = \frac{1}{\gamma\Delta\tau} ,$$

then the equation for graphical analysis is

$$\Delta\Phi \tan\alpha = 1 + \frac{w}{\gamma}\sin 2\Phi . \qquad (28)$$

The construction of eq. (28) is shown in Fig. 16 with:

$$\gamma = 10^{-4} ,$$

$$w = 10^{-5} ,$$

$$\gamma\Delta\tau = \frac{\pi}{16} ,$$

and at $\tau = 0$, $\Phi = 0$.

At each point (0, 1, 2, $\cdots$) on the curve $1 + \frac{w}{\gamma}\sin 2\Phi$ eq. (28) is satisfied. The curve of $\frac{1}{\gamma}\frac{d\Phi}{d\tau}$, the angular velocity divided by γ , versus $\gamma\tau$ is obtained by simply plotting the ordinates of the points (0, 1, 2, $\cdots$ n) on the curve in Fig. 16 against corresponding $n\gamma\Delta\tau$ as shown in Fig. 17. The resulting curve, which possesses a period $\frac{\pi}{\gamma}$

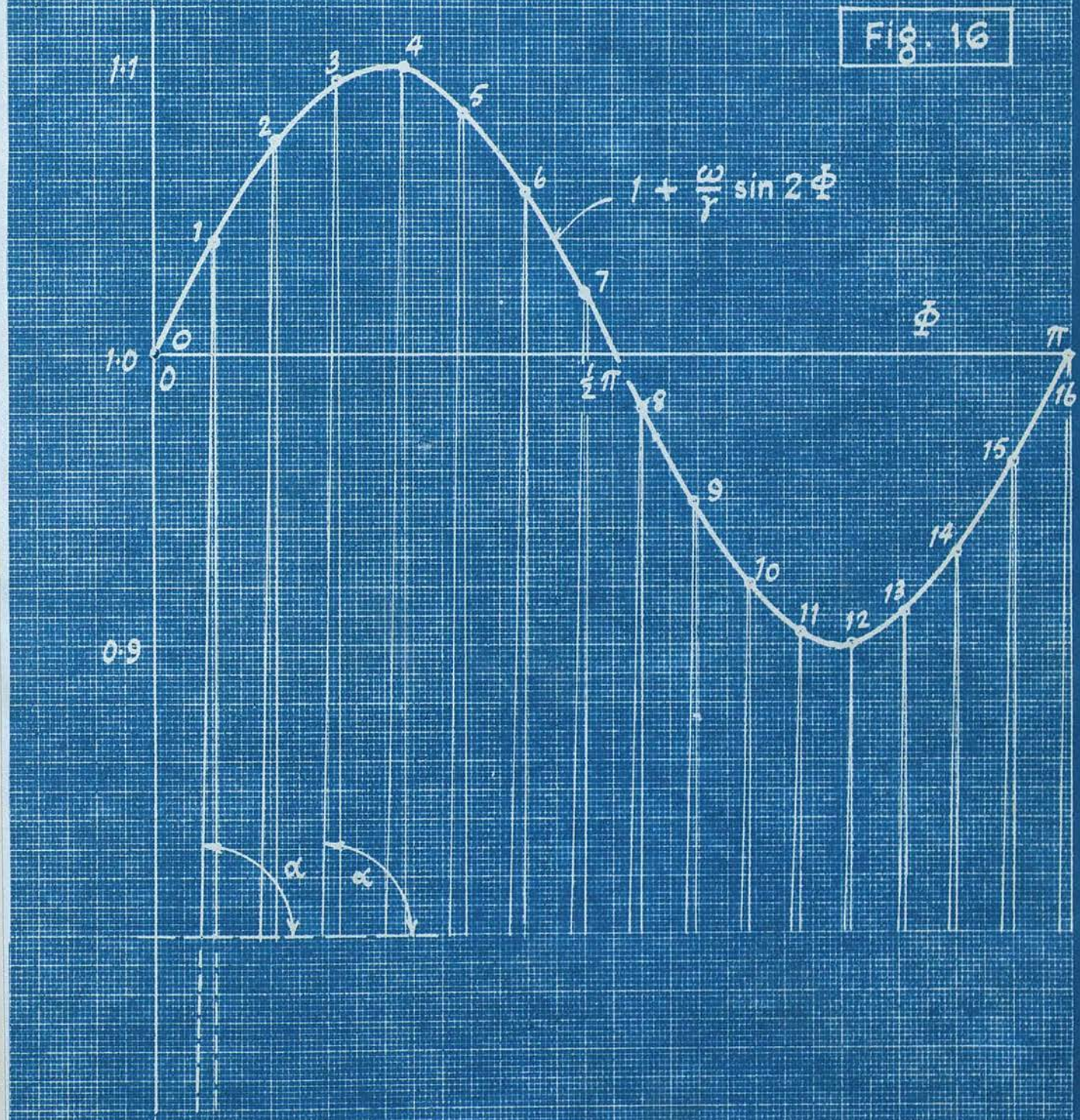
Fig. 16
1·1
1·0
0·9
0
1
2
3
4
5
6
7
8
9
10
11
12
13
14
15
16
$1 + \frac{\omega}{\gamma} \sin 2\Phi$
Φ
$\frac{1}{2}\pi$
π
α
α

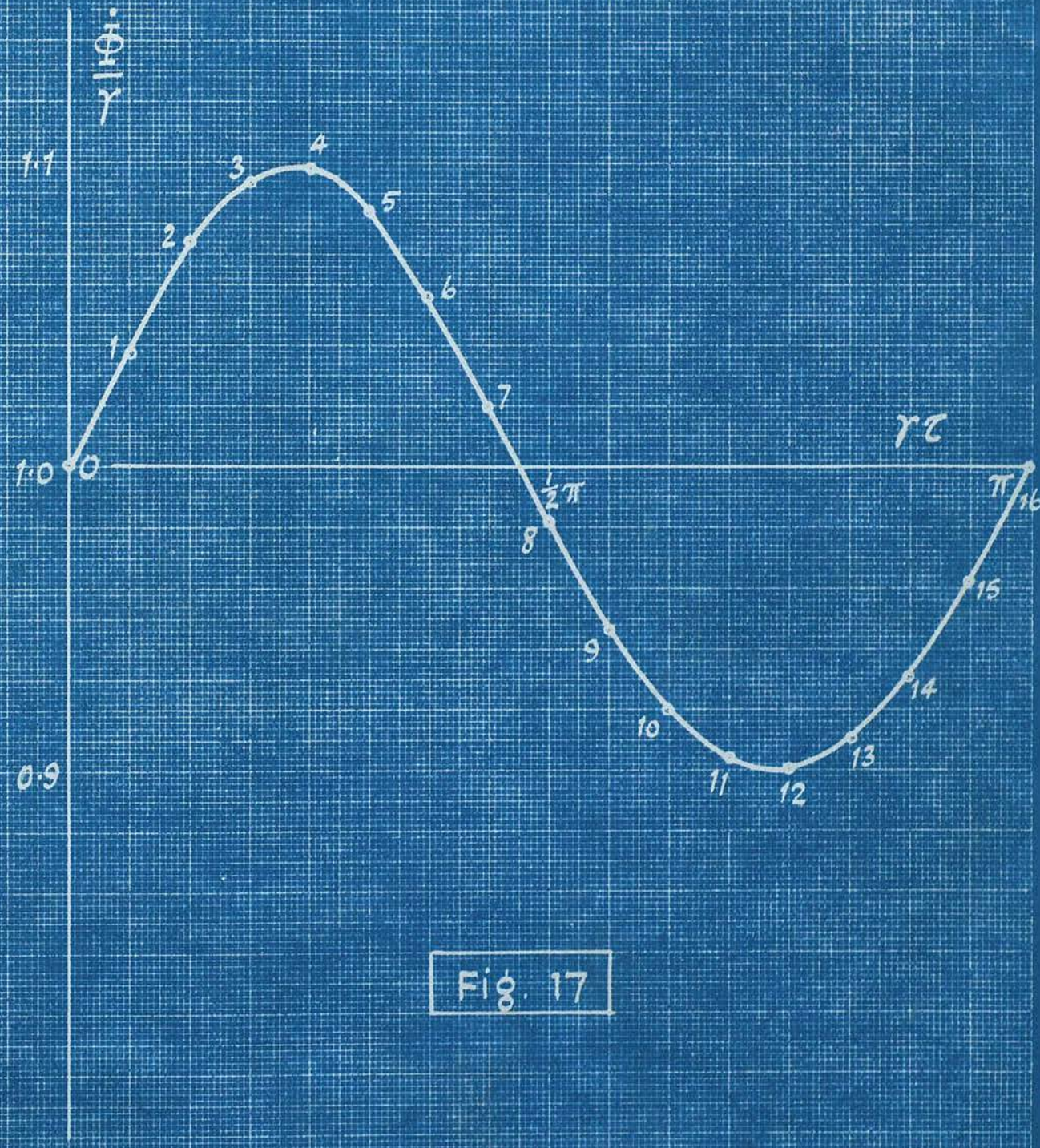
$\frac{\dot{\Phi}}{\gamma}$
1·1
1·0
0·9
0
1
2
3
4
5
6
7
8
9
10
11
12
13
14
15
16
$\gamma\tau$
$\frac{1}{2}\pi$
π

Fig. 17

and amplitude 0.1 and is slightly different from a sinusoid, agrees well with that in Fig. 10 in Part I which is obtained by directly integrating eq. (27).

2.5. Amplitude Modulation of Forced Oscillations in Section 2.2, Part I.

Consider the equation

$$\frac{dA}{d\tau} = (w_0 - w\cos 2\Phi)A - w_3 A^3. \qquad (29)$$

In this equation A is a function of τ ; w_0 , w , and w_3 are constants; and Φ is the same as that in Section 2.4. Eq. (29), which has the same form as eq. (78) in Part I, is the equation for the amplitude of oscillations in a circuit with a periodically-varying parameter and an external applied force. In Part I, we have shown that A is a periodic function of τ provided that $w_0 > 0$. Here we shall solve it graphically by taking the result of Φ obtained in Section 2.4.

Let $V = \frac{1}{A^2}$, then $\frac{dV}{d\tau} = -\frac{2}{A^3}\frac{dA}{d\tau}$.

Substituting these into eq. (29), we have

$$\frac{dV}{d\tau} + 2(w_0 - w\cos 2\Phi)V = 2w_3 . \qquad (30)$$

Eq. (30) is a linear differential equation with a periodically-varying coefficient. Letting

$$\frac{dV}{d\tau} = \frac{\Delta V}{\Delta \tau},$$

$$\tan\alpha = \frac{1}{\gamma\Delta\tau} = \frac{16}{\pi},$$

$$W_0 = W_3 = 2\times10^{-5},$$

and $$W = 10^{-5},$$

eq. (30) then becomes

$$\Delta V + \tan\alpha + 0.2\,(2-\cos 2\Phi)\,V = 0.4\,. \tag{31}$$

From eq. (27), it follows that

$$\frac{1}{\gamma}\frac{d\Phi}{d\tau} = 1 + \frac{W}{\gamma}\sin 2\Phi,$$

$\frac{W}{\gamma}\cos 2\Phi$ thus has the same form as the curve in Fig. 17 except that the origin is shifted to $(\frac{\pi}{4}, 1)$.

Eq. (31) is constructed in Fig. 18. The straight lines drawn from the origin represent the expression $0.2\,(2-\cos 2\Phi)V$ at different values $\gamma\tau$ as denoted by $0, \frac{\pi}{16}, \frac{\pi}{8}, \cdots$. Let the initial condition be: at $\tau=0$, $V=1$. A closed curve $0, 1, 2, \cdots 15$ is thus obtained which means that V is a periodic wave with period $16\gamma\Delta\tau = \pi$. The curve of V versus $\gamma\tau$ is plotted on the lower left side of Fig. 19. The relationship between $V(=\frac{1}{A^2})$ and A is shown on the upper left side. Through the V/A curve, V is turned into A as shown in the right side in the same figure.

By inspection of Fig. 17 and 19 we conclude that:
(a) A and $(1+\dot{\Phi})$, the amplitude and angular velocity respectively of oscillations in the circuit of Fig. 1 in Part I, are periodic with period $\frac{\pi}{\gamma}$.
(b) A and $(1+\dot{\Phi})$ are out of phase by 90^0, i.e., when the amplitude is a maximum, the frequency is a

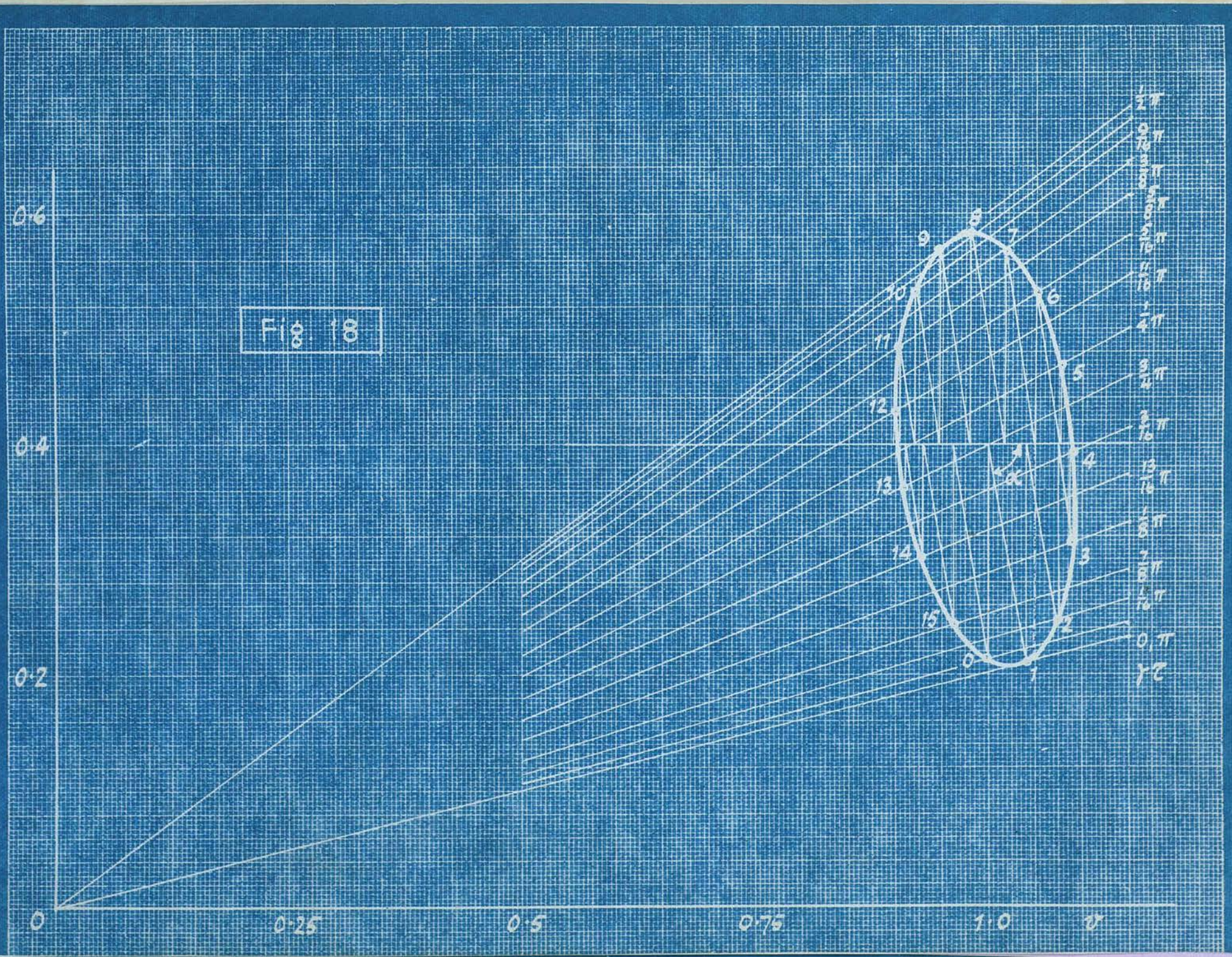
Fig. 18
0·6
0·4
0·2
0
0·25
0·5
0·75
1·0
α
0
1
2
3
4
5
6
7
8
9
10
11
12
13
14
15
1/2 π
9/16 π
5/8 π
1/2 π
7/16 π
1/4 π
3/16 π
1/8 π
1/16 π
0 π
γ

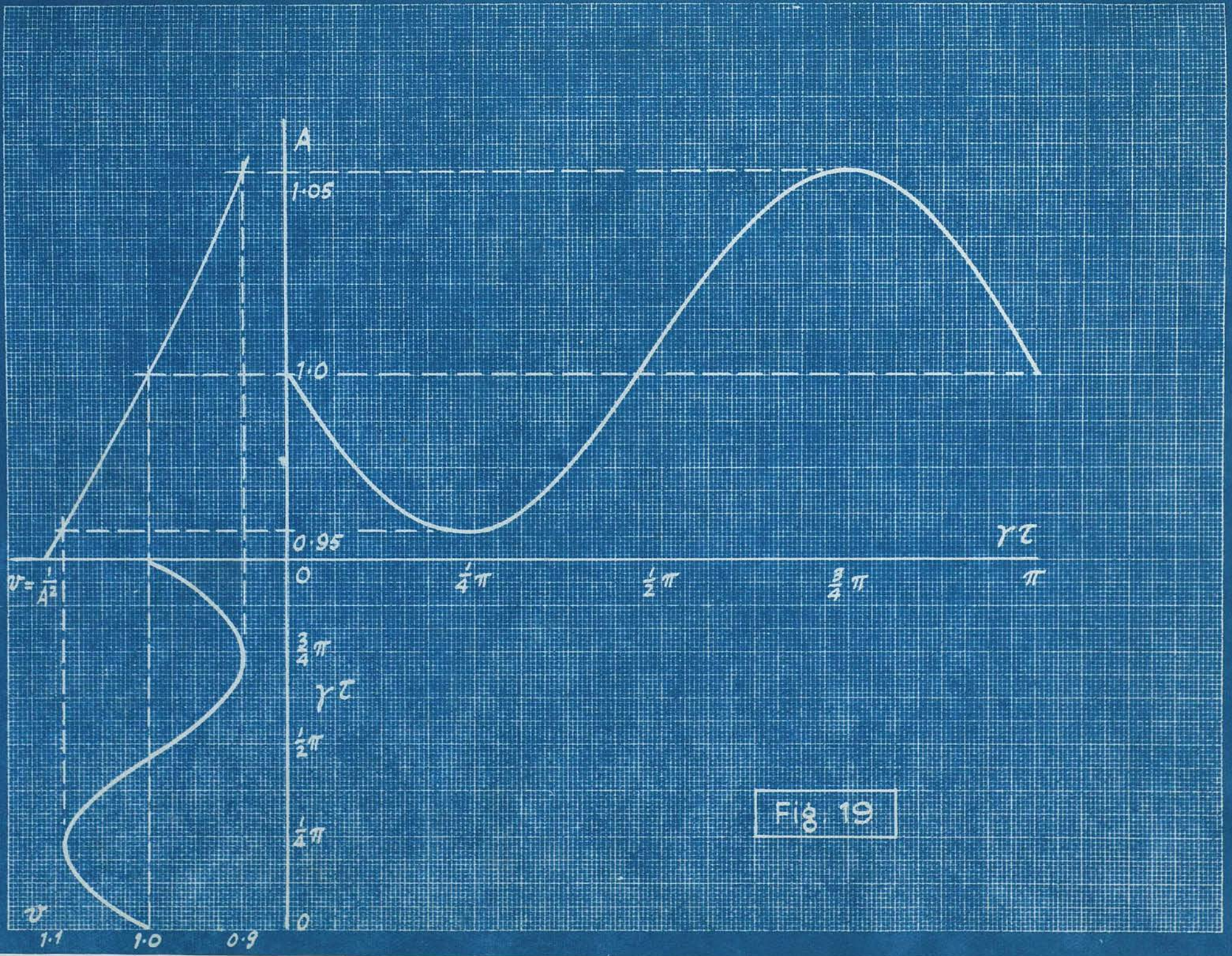

Fig. 19

minimum, and vice versa.

This agrees with that observed experimentally: see Section 3 of Part I.

Acknowledgments.

I wish to express my sincere thanks to Professor M.G. Say and Dr. C.B. Childs for their interest, encouragement and invaluable advice. My best thanks are also due to Mr. A.G. Thomson for his help during the preparation of the experimental work.

REFERENCES.

1. Lord Rayleigh: "On Maintained Oscillations." Phil. Mag., 15, 229, (1883).
   ---------- "On the Maintenance of Vibrations by Forces of Double Frequency, and on the Propagation of Waves through a Medium Endowed with a Periodic Structure." Phil. Mag., 24, 145, (1887).

2. C.V. Raman: "Experimental Investigations on the Maintenance of Vibrations." Proc. Indian Assoc. for Cultivation of Sc., Bull. 6, (1912).
   ---------- "Some Remarkable Cases of Resonance." Phys. Rev., 35, 449, (1912).
   ---------- "Maintenance of Vibration by Variable Spring." Phil. Mag., 24, 513, (1912).
   ---------- "On the Maintenance of Vibrations by Two Simple Harmonic Forces." Phys. Rev., 5,1,(1915).

3. H. Winter-Günther: "Selbsterregung von Systemen mit Periodiche veränderlichen Induktivitäten." Z. f. Hochfr., 37, 172, (1931).

4. W.L. Barrow: "On the Oscillations of a Circuit having a Periodically-Varying Capacitance." Proc. I.R.E., 22, 201, (1934).
   W.L. Barrow, D.B. Smith and F.W. Baumann: " A Further Study of Oscillatory Circuits Having Periodically Varying Parameters." J. Frank Inst., 221, 403, (1936).

REFERENCES (Contd.)

5. N. Minorsky: "Introduction to Non-Linear Mechanics." (Edwards, Ann Arbor, Mich. 1947).

6. N.W. McLachlan: "Theory and Application of Mathieu Functions." (Oxford. 1947).

7. K.J. Dejuhasz: "Graphical Analysis of Electric Circuits." J. Frank Inst., 228, 339, (1939).

8. A. Preisman: "Graphical Constructions for Vacuum Tube Circuits." McGraw Hill, (1943).

9. N. Levinson: "Transformation Theory of Non-Linear Differential Equations of the Second Order." Annals of Maths., 45, 723, (1944).

10. M.L. Cartwright: "Forced Oscillations in Nearly Sinusoidal Systems." J.I.E.E., 95 (III), 88, (1948).

11. E.L. Ince: "Integration of Ordinary Differential Equations." Oliver and Boyd, (1939).

12. A. Tustin: "A Method of Analyzing the Effect of Certain Kinds of Non-Linearity in Closed Cycle Control Systems." J.I.E.E., 94 (IIA), 152, (1947).
